INTRAVENOUS MICRODIALYSIS AND PHYSIOLOGICALLY-BASED PHARMACOKINETIC MODELING AS TOOLS TO EVALUATE PHARMACOKINETICS AND DRUG-DRUG INTERACTIONS

By

MANUELA DE LIMA TOCCAFONDO VIEIRA

A DISSERTATION PRESENTED TO THE GRADUATE SCHOOL
OF THE UNIVERSITY OF FLORIDA IN PARTIAL FULFILLMENT
OF THE REQUIREMENTS FOR THE DEGREE OF
DOCTOR OF PHILOSOPHY

UNIVERSITY OF FLORIDA

2011

To my Grandmother, Mother and Sister

ACKNOWLEDGEMENTS

I would like to express my appreciation and gratitude to my supervisor Dr. Hartmut Derendorf for his continuous support and intelligent guidance throughout my graduate program.

My gratitude is extended to my supervisory committee Dr. Veronika Butterweck, Dr Maria Grant, and Dr. Anthony Palmieri for their constructive guidance and availability.

I would like to thank the office staff of the Department of Pharmaceutics, Patricia Khan, Robin Keirnan-Sanchez and Sarah Foxx, for their kindly support on administrative matters, as well as faculty, post-doc fellows and graduate students for their friendship and support. A special gratefulness is extended to Daniela Conrado who helped me during the most challenging moments of my experiments. Her friendship, availability and remarkable knowledge when I needed the most will never be forgotten. I also want to express my appreciation to Dr. Rajendra P. Singh and Dr. Linung Zhuang for their assistance on my experiments.

I am also thankful to Dr. Shiew-Mei Huang and Dr. Ping Zhao, for their valuable guidance throughout my academic training, encouragement and appreciative support.

The CAPES/Fulbright program is acknowledged for funding my doctoral studies. Special thanks to the staff of the Institute of International Education, Joanne Forster and Anna Rendon, for the kindly support in administrative issues.

I also express my gratitude for all animals that participated in this research project.

Finally, I would like to thank my friends and family, especially my mother, brother and sister, for their love, encouragement and support always. I am also very thankful to my boyfriend, Christian, for his love, patience, encouragement and help during the course of my work.

TABLE OF CONTENTS

page

LIST OF TABLES

LIST OF FIGURES

Abstract of Dissertation Presented to the Graduate School
of the University of Florida in Partial Fulfillment of the
Requirements for the degree of Doctor of Philosophy

INTRAVENOUS MICRODIALYSIS AND PHYSIOLOGICALLY-BASED PHARMACOKINETIC MODELING AS TOOLS TO EVALUATE PHARMACOKINETICS AND DRUG-DRUG INTERACTIONS

By

Manuela de Lima Toccafondo Vieira

August 2011

Chair: Hartmut Derendorf
Major: Pharmaceutical Sciences

The purpose of this thesis was to evaluate the usefulness and accuracy of two distinct tools to support drug development: Intravenous Microdialysis (IV MD) and Physiologically-based Pharmacokinetic (PBPK) modeling.

The IV MD technique is proposed to be a promising *in vivo* tool for continuous free drug monitoring in (pre)clinical settings due to its various advantages compared to traditional blood sampling. The feasibility and accuracy of IV MD was evaluated by determining free concentrations of a lipophilic and highly protein-bound drug, triamcinolone acetonide (TA), under steady-state pharmacokinetics in anesthetized rodents. Microdialysis *in vivo* calibration was estimated by the retrodialysis method using budesonide as the calibrator compound. The mean steady-state total and unbound (microdialysate) concentrations were 3.64 ± 0.74 and 0.343 ± 0.072 µg/mL, respectively. The calculated unbound TA concentration in plasma corrected for protein binding was 0.378 ± 0.077 µg/mL, which is significantly not different to that determined by IV MD (α=0.05). The results demonstrated that IV MD is an accurate method to

determine unbound concentrations of TA following drug infusion at steady-state, thus a feasible approach for free drug monitoring.

PBPK modeling is proposed to be a valuable *in silico* tool for addressing linear and nonlinear pharmacokinetics and prediction of drug-drug interaction risk due to its advantageous integration of systemic properties and drug-dependent parameters to characterize pharmacokinetics (PK) of interacting drugs.

A PBPK model for telithromycin, a substrate and inhibitor of the enzyme cytochrome P450 3A4 (CYP3A4) with nonlinear PK, was constructed using either reversible or time-dependent inhibition (TDI) of CYP3A4. The model incorporating TDI of CYP3A4 suggested that rather than saturation of metabolic and efflux transport pathways, auto-inhibition of clearance via time-dependent CYP3A4 inhibition is the plausible mechanism for the observed time- and dose-dependent telithromycin PK. The TDI model successfully predicted the magnitude of drug-drug interaction perpetrated by telithromycin with midazolam (a probe CYP3A4 substrate): the predicted *vs*. observed geometric mean AUC ratios (+/- telithromycin) of midazolam after intravenous and oral administration were 3.26 *vs*. 2.20 and 6.72 *vs*. 6.11, respectively. In contrast, the PBPK model with reversible inhibition mechanism under-predicts the observed increase in midazolam exposure (geometric mean AUC ratios of 1.01 and 1.08 after intravenous and oral midazolam, respectively).

In conclusion, IV MD and PBPK modeling are useful and promising applications for evaluating pharmacokinetics and drug-drug interactions, thus aiding to guide successful drug development.

CHAPTER 1
INTRODUCTION

The long-term objective of the studies described here is to demonstrate the utility of intravenous microdialysis (IV MD) technique and physiologically-based pharmacokinetic (PBPK) modeling, specifically in the areas of preclinical and pediatric pharmacokinetics and drug-drug interactions.

Microdialysis [1-3] and PBPK [4,5] modeling are gaining appreciation in drug development process seen through increasing application of both techniques as a part of an overall preclinical and clinical pharmacology package.

Following the recognition of the utility of tissue microdialysis, IV MD may represent a promising tool for continuous free drug monitoring in (pre)clinical settings. When compared with traditional blood sampling, IV MD offers several advantages. First, continuous sampling is possible since the microdialysis process does not change the blood volume [6]. This not only allows pharmacokinetic studies in pediatric populations but also greatly reduces the number of experimental animals usually required for frequent PK sampling. Second, IV MD directly provides the unbound drug concentration which is generally considered pharmacologically more relevant [7]. Third, microdialysis sampling excludes proteins, therefore reducing enzymatic degradation of the drug and making sample preparation redundant [8]. However, the application of the microdialysis technique to lipophilic drugs seems to be problematic [9,10]. Based on these observations, the first aim of the proposed study was to evaluate the feasibility and accuracy of intravenous microdialysis technique to determine unbound concentration of lipophilic and highly protein-bound drugs using triamcinolone acetonide (TA) as a model compound.

Many of PBPK modeling and simulation applications in literature [11,12] and drug application submissions in the US regulatory agency [5] addressed questions related to drug-drug interactions (DDIs). The clinical consequences of DDIs range from lack of therapeutic efficacy to severe safety concerns. Thus, significant drug-drug interactions can lead to termination of a new drug development, withdrawal from the market, or strict restrictions of its use [13]. An understanding of the risk for DDIs by prediction models is an important component of the drug research and development processes. However, prediction of *in vivo* drug-drug interaction magnitude using enzymatic parameters generated *in vitro* remains challenging, due to the possibility of false-negative results from *in vitro* study not properly designed [14]. Based on these observations, the second aim of the proposed study is to evaluate the utility of PBPK modeling and simulation in predicting drug-drug interaction potential inferred from the assessment of a drug's nonlinear pharmacokinetics.

Specific Aims

Specific Aim 1

The first specific aim was designed to provide an assessment of the limitations and accuracy of the intravenous microdialysis technique using *in vitro* systems and rodent studies.

Specific Aim 1a: Bioanalytical assay development and validation

Develop and validate an efficient assay for simultaneous and selective analysis of TA and budesonide (microdialysis calibrator) in microdialysate and rat plasma samples using HPLC-PDA.

Specific Aim 1b: Triamcinolone acetonide microdialysis calibration

Determine the relative recovery of TA by a series of *in vitro* and *in vivo* microdialysis studies to evaluate the feasibility of using IV MD as a sampling technique to TA.

Specific Aim 1c: Investigation of budesonide as a microdialysis calibrator

Determine the relative recovery of budesonide by a series of *in vitro* and *in vivo* microdialysis studies and the factor by which it is related to TA recovery to verify the use of budesonide as a continuous internal recovery control.

Specific Aim 1d: Intravenous microdialysis study of TA

Perform an intravenous microdialysis study in rats to determine the accuracy of the sampling technique on the estimation of unbound triamcinolone acetonide levels compared to conventional blood sampling.

Specific Aim 2

The second specific aim was design to demonstrate the utility and predictive accuracy of PBPK modeling and simulation in mechanistically addressing telithromycin nonlinear pharmacokinetics and its drug-drug interaction potential.

Intravenous Microdialysis

Principles of Microdialysis

Microdialysis (MD) is a sampling technique to measure the protein-free fraction of endogenous and/or exogenous compounds in the blood [15,16] and extracellular fluid of several tissues (e.g. adipose tissue [17], muscle [18], brain [19], lung [20], bones [21,22] and liver [23,24].

The principles of microdialysis have been described in detail previously [2,6,25]. Briefly, a microdialysis probe, consisting of a small semi-permeable hollow fiber

membrane connected to outlet and inlet tubing, is inserted into a selected tissue or fluid-filled space. The MD probe is constantly perfused with a physiological solution (perfusate) at a low and constant flow rate (0.1-5μL/min). By means of diffusion according to their concentration gradient ($C_{sampling\ site}$) and size, solutes cross the semi-permeable membrane [26,27] and are taken with the perfusion flow [6]. The resulting concentration of the analyte in the solution leaving the probe ($C_{dialysate}$) will reflect the unbound diffusible level on the tissue [27]. After continuous sampling at regular intervals, microdialysate samples are analyzed.

Due to the continuous perfusion of the microdialysis probe, a complete equilibrium between the sampling site and the perfusion medium cannot be established; therefore, the concentrations in the dialysate samples are lower than those measured at the distant sampling site ($C_{sampling\ site} > C_{dialysate}$) [2]. In other words, to correlate concentrations measured in the dialysate with those present at the sampling site, a calibration factor, named recovery, is needed. The analyte's recovery can be determined at steady-state using the constant rate of analyte exchange across the microdialysis semipermeable membrane, namely extraction efficiency. The extraction efficiency is defined as the ratio between the loss/gain of analyte during its passage through the probe ($C_{perfusate} - C_{dialysate}$) and the difference in concentration between perfusate and the sampling target such as tissue fluid or *in vitro* medium ($C_{perfusate} - C_{sampling\ site}$), as shown in the equation [2,28]:

$$EE = \frac{(C_{perfusate} - C_{dialysate})}{(C_{perfusate} - C_{sampling\ site})}$$

At steady-state, the extraction efficiency of a microdialysis probe has the same value independent of the analyte concentration i.e. it does not matter whether the

analyte is enriched or depleted in the perfusate. Thus, microdialysis probes can be calibrated by either drug-containing perfusate or drug-containing sample solutions [2].

Several calibration methods are available to date: the low-flow-rate method, the no-net-flux method [29,30], the dynamic no-net-flux method [31] and the retrodialysis by drug or by calibrator methods [32]. The retrodialysis by drug is the most common calibration method for exogenous compounds in preclinical and clinical settings [2].

Several factors influence an analyte's recovery, including perfusion flow rate, probe's characteristics such as membrane composition and effective surface area, temperature [7], physicochemical properties of the analyte [33] and nature of the dialyzed tissue [34,35]. This latter factor precludes the use of *in vitro* calibration as a surrogate for *in vivo* recovery [2,34].

Microdialysis sampling has become an important technique allowing the *in vivo* measurement of endogenous and exogenous substances in the extracellular environment. As a practical, data rich, animal sparing *in vivo* method, MD is a useful tool that is increasingly applied in academia and drug research and development by the pharmaceutical industry [2]. Clinical microdialysis has also been shown as a ethically acceptable, safe and reproducible technique [2], especially in the fields of intensive care research [36-38], dermatology [1,39], clinical pharmacology [3,27], and metabolic and endocrinology research [24,40,41]. In addition, the MD technique also holds great promise for evaluation of pharmacokinetics and pharmacodynamics in laboratory animals and man as demonstrated in the areas of Central Nervous System research [42] and intravenous microdialysis [43].

Application of Intravenous Microdialysis

Initially determination of drug concentration by intravenous microdialysis does not seem of much interest as there is always the possibility to sample blood directly. However, intravenous microdialysis technique offers numerous advantages over conventional blood draw.

Since MD is a volume neutral technique, i.e. no net fluid (blood) loss, rich-data sampling from pediatric patients and small rodents is feasible. The limited total blood volume of children and small animals is one of the major problems in pharmacokinetic investigations in these populations. Blood loss from diagnostic sampling is reported to be the most common cause of anemia in hospitalized infants [44], therefore reducing or even avoiding blood sampling for drug analysis is clinically important. As for rodents, blood removal exceeding 20–25% of the total body volume usually produces signs of hypovolemia [45]. Consequently, a large number of small animals are used to obtain proper drug concentration-time profiles in pharmacokinetic studies. In addition, the physiological changes that result from blood sampling may alter drug pharmacokinetics. Intravenous microdialysis seems a promising approach to reduce disturbance of homeostasis associated with blood sampling, thus allowing pharmacokinetic and therapeutic monitoring in pediatric population and reducing the number of animals necessary for pharmacokinetic studies.

In addition, the continuous sampling of drug concentrations facilitated by the IV MD technique results in higher temporal resolution compared to blood sampling [6].

Furthermore, the MD semi-permeable membrane enables only the protein-free fraction of the drug to be diffused and thus, monitored. Since in general the unbound drug concentration is directly correlated to pharmacological effects, the assessment of

its concentration is more appropriate for PK/PD investigations [7] and free drug therapeutic monitoring [46].

The exclusion of proteins from the microdialysis samples allows little or no-sample preparation steps [8] whereas whole blood sample pre-treatment is usually time-consuming and tedious. Automated on-line analysis of microdialysate is therefore possible [47-50]. In addition, the risk of contamination of personnel is reduced. The exclusion of enzymes also diminishes the potential for sample degradation [48].

IV MD has been employed to study drug pharmacokinetic in rats [51-53]. Simultaneous microdialysis measurements in blood and other sampling sites (e.g. brain, liver) have been used to estimate the distribution and metabolism characteristics of a drug [7]. Interesting examples are the investigations of the disposition mechanism of metronidazole [47] and the metabolism of acetaminophen [54]. Intravenous microdialysis is also well suited for the determination of *in vivo* plasma protein binding of drugs such as ceftazidime [55] , methotrexate [56] and flurbiprofen [57] which displayed concentration dependent protein binding. Other preclinical studies have been conducted with the goal of further development of the technique [58-60], including development of new IV microdialysis probes for placement in the inferior vena cava [61] or carotid artery [62], and application of microdialysis calibrator [40].

The use of IV MD sampling in humans has also been demonstrated. A pilot study showed the utility of the technique to determine the pharmacokinetics of drugs, using sotalol as a model compound [16]. The application of the technique for monitoring endogenous parameters like drug induced alterations in serotonin plasma levels [63,64] or lactate, pyruvate and glucose plasma concentrations in healthy [65,66] and intensive

care patients has been demonstrated [67]. Levodopa and 3-O-methyldopa plasma levels were continuously monitored (2 to 6 hours) in Parkinson's disease patients to optimize management of levodopa therapy and to better characterize the pharmacokinetic profile of different formulations of the drug [15].

The majority of the preclinical and clinical studies employed the IV MD technique to monitor hydrophilic and/or low protein binding compounds. In fact, the use of microdialysis to measure lipophilic drugs seems to be one of the major limitations of the technique. Some reports of tissue microdialysis studies addressed this difficulty with the low recovery, deemed as the key factor restricting the accurate quantification [9,10,33,50].

As previously addressed, the physicochemical properties of the analyte, specially the partition coefficient which affects the permeability, have a significant influence on the diffusion process on the membrane and on the solubility in the hydrophilic perfusate medium; consequently, on the relative recovery [33]. Furthermore, the extent of protein binding is other factor that affects the microdialysis diffusion process quantitatively [9]. Higher protein binding results in lower unbound drug fraction that will diffuse and reduces the absolute amount of the drug that will be recovered.

In this context, the present project aims to investigate the feasibility of IV microdialysis to determine unbound concentrations of lipophilic and highly protein-bound drugs. Triamcinolone acetonide, a corticosteroid with moderate lipophilicity (Log $P_{o:w}$ of 2.5) (Chemspider database, Royal Society of Chemistry, Cambridge, UK) and high protein binding (90% in rat plasma [68] and 70-80% in human plasma [69,70]) was thus chosen as a model drug.

Another limitation of the MD technique that the proposed project aims to address is the time-dependence of the recovery. The reduction of probe efficiency during the course of IV MD experiments has been reported [58,60,71]. Accordingly, results and interpretations might be misleading. We will evaluate the continuous use of retrodialysis by a calibrator (microdialysis internal standard). This calibration method provides the advantage that changes in recovery during the experiment can be detected, as a change in the relative recovery of the analyte would always go along with a change in the loss of the calibrator [7]. In addition of providing more accurate data, the calibrator method should be a starting point to simplify microdialysis studies in animals and patients since this approach reduces the imposed calibration burden to a minimum.

Our research can provide a preliminary assessment for the application of the IV MD technique in clinical settings of therapeutic free drug monitoring in adults and pediatric patients. Direct measurement of free concentrations of strongly protein-bound drugs for therapeutic management is recommended in certain disease states and possible drug-drug interactions [46]. In addition, therapeutic drug monitoring in infants is more difficult to perform than in adults because of blood sample limitations [44] and the discomfort and invasiveness of the conventional sampling procedures [72].Thus, intravenous microdialysis may be a new and promising approach in this area given that it provides a continuous analysis of free drug levels without painful stress and disturbance of blood volume, drug concentration and binding equilibrium.

Consequently, preclinical evaluation of the intravenous microdialysis as a promising tool for sampling of lipophilic and highly protein-bound drugs will provide an

important foundation required to verify this technique suitable for therapeutic drug management and pharmacokinetic investigations, especially in pediatric population.

PBPK Modeling

Principles of PBPK Modeling

In classical pharmacokinetic modeling, the aim is to fit a mathematical function to the experimental data in order to determine pharmacokinetic parameters from the fitted curve. These parameters are then used to characterize the behavior of the compound and to make extrapolations to situations not yet investigated. PBPK-modeling, on the contrary, starts from the mathematical description of physiological processes and performs a genuine simulation of the pharmacokinetic behavior using this description [73].

The general concept of PBPK, introduced as early as 1937 by Teorell [74], is based on the recognition that the body handles a drug as an integrated system [75]. Accordingly, the whole body is divided into physiologically relevant compartments (main organs and tissues) which are mathematically connected by linear exchange reactions according to their physiology.

Figure 1 illustrates the human organism to be modeled and the division of its single organs, including the oral absorption components (the GI tract), systemic distribution components and elimination components (usually the liver and the kidneys). To depict the distribution of a drug in the body, the organs are connected via their arteries and veins to the arterial and venous blood pool. Inter-compartmental mass transport occurs via organ-specific blood flow rates with the mass transfer from the vascular space into the tissue interstitial space by passive permeation and partitioning between organ tissues and blood plasma; while the intracellular mass transfer occurs

via passive diffusion or active transport. Elimination processes are described as sink reactions or metabolic pathways in the eliminating organs [73].

From the previous description, we can delineate three major components of a PBPK model: model structure, drug-independent system properties and drug properties. The structural model includes all interdependent mass balance equations which are set up for each compartment to describe the fate of the compound within that organ/tissue. The system properties include the relevant physiological input parameters of the human body, such as organ mass or volume, body fluid dynamics (e.g., secretion of gastric acid and bile, blood flow, urine flow), and tissue composition (water, lipid and protein content), in particular drug receptors, drug-metabolizing enzymes, and membrane transporters [5,75,76].

The drug dependent components include physic-chemical properties (lipophilicity, molecular weight and acid dissociation constant), tissue affinity, plasma protein binding constant, membrane permeability, and enzymatic and transport activities [75]. The latter information includes the drug specific clearance, a required parameter in the PBPK model either from in vivo estimation or intrinsic clearances determined from in vitro experiments [73].

Application of PBPK Modeling

By integration of prior knowledge about the drug-dependent and the system dependent (the human organism) parameters, PBPK enables the study of the absorption, distribution, metabolism and excretion (ADME) processes at the cellular level. Accordingly, the drug's concentration time-profile in blood and tissues of interest can be predicted.

As previously outlined by Zhao et al [5], PBPK modeling and simulations generally include four basic steps: In step 1, drug-dependent parameters are incorporated into the PBPK model including the drug's clearance pathways. In step 2, the predicted concentration–time profiles are compared with those obtained from available in vivo human studies. In step 3, the PBPK model is refined according to the results from step 2. Finally, in step 4, the refined PBPK model is used for predicting PK profiles under various scenarios that have not been studied experimentally [5].

Therefore, PBPK modeling is a powerful tool to investigate the influence of drug specific properties as well as the effect of intrinsic (e.g. age, gender, genetics, organ dysfunction, disease state) and extrinsic factors (e.g. drug-drug interactions) on the ADME processes.

PBPK modeling and simulation has demonstrated its potential in the risk assessment of environmental toxins [77], and has being increasingly applied in the academia and drug research and development programs [76]. Several examples in the literature described the utility of PBPK modeling and simulation as tools for predicting human pharmacokinetics in critical areas of clinical pharmacology, including pediatrics [78-80],organ impairment [81], and drug–drug interaction [11,12]. The use of PBPK modeling and simulation to support regulatory review process also increased in the last decade with predictive potential of the technique been explored by both sponsors and FDA reviewers [5].

Particularly for evaluating drug-drug interaction risk of an investigational drug, PBPK may provide a more accurate prediction of the potential for drug–drug interactions than the traditionally used static approach (such as the use of [I]/Ki, where

[I] is the inhibitor concentration and Ki is the reversible inhibition constant) since PBPK-based prediction considers multiple factors and mechanisms that impact interactions [5]. For instance, PBPK model includes the fractional enzymatic metabolism of the victim drug and allows changes over time of the inhibitor concentration [82].

A critical component in the use of PBPK modeling and simulation is the availability of software tools that allows facile solution of the model equations [75]. The software systems vary from high-level programming or matrix computing (e.g. Matlab® ,The MathWorks Inc.) and biomathematical modeling (e.g ADAPT®, Biomedical Simulations Resource, University of Southern California) to custom-designed PBPK modeling and simulation such as SimCYP® (SimCYP Ltd) [83], GastroPlus® (Simulations Plus Inc) [84], and PK-Sim® (Bayer Technology Services GmbH) [73]. These latter proprietary PBPK software systems are highly sophisticated population-based PBPK modeling and simulations tools which continuously integrate the increasing knowledge of physiology, genetics and anthropometric properties (system-dependent parameters) to assess inter-individual variability on drug pharmacokinetics [85,86].

The present project aims to investigate the utility of PBPK modeling and simulation in predicting enzyme inhibition potential inferred from the assessment of a drug nonlinear pharmacokinetics.

Prediction of cytochrome P450 3A4 (CYP3A4) interaction potential are particularly significant as CYP3A4 is the most important enzyme in drug metabolism, thus, it is the most frequent target for pharmacokinetic drug-drug interactions (DDIs) [82].

DDIs occur when one drug alters the metabolism of a co-administered drug. The pharmacokinetic outcome is an increase or decrease in the systemic clearance and/or

bioavailability, and a corresponding change in the exposure of a co-administered drug. The clinical consequences of DDIs range from lack of therapeutic efficacy to severe drug adverse events. Because the impact of DDIs on patient health and safety, the knowledge of the risk for DDIs associated with a drug is an important component of drug research and development processes [82]. Significant drug-drug interactions may result in a possible termination of development, withdrawal from the market or strict restrictions on its use [87]

Telithromycin, a ketolide antibiotic, is a CYP3A4 substrate and inhibitor with dose- and time-dependent nonlinear pharmacokinetics [88,89]. Thus, telithromycin was chosen as an inhibitor model drug.

The study also aims to demonstrate the utility of the combination of the “bottom-up” and “top-down” approaches in the PBPK modeling by integrating available *in vitro* and *in silico* predicted drug interaction and enzyme/transporter kinetic data (“bottom-up”) with *in vivo* human pharmacokinetic and drug-drug interaction information (“top-down”) in the building of a drug PBPK model.

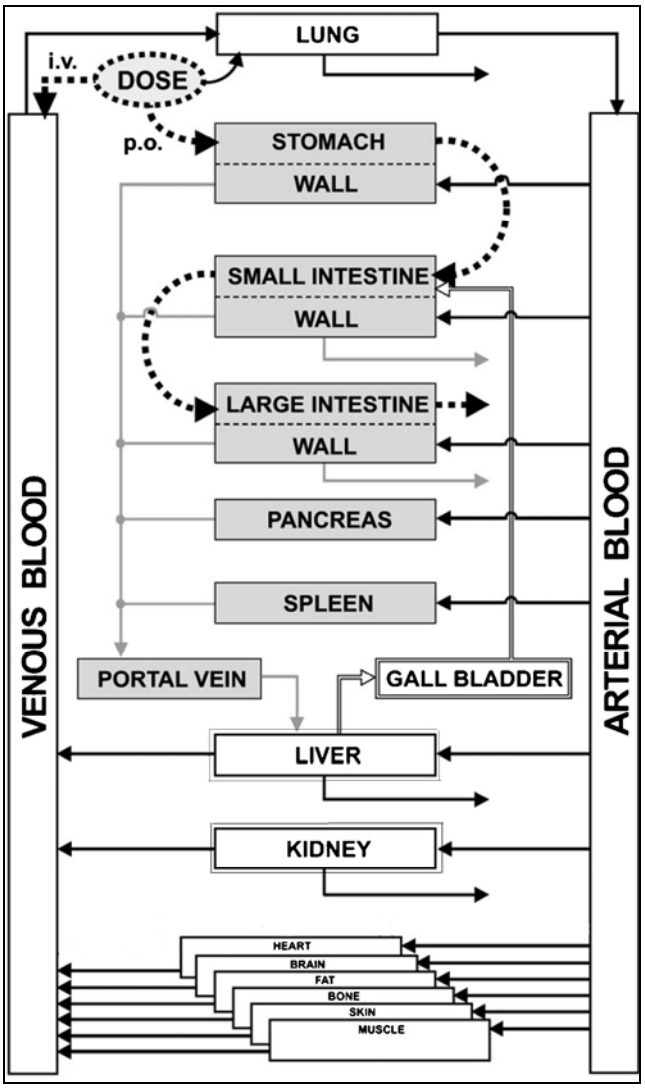

Figure 1-1. Schematic representation of the whole-body physiologically-based pharmacokinetic model. Modified from [73].

CHAPTER 2
DEVELOPMENT AND VALIDATION OF BIOANALYTICAL METHODS[1]

Background

Microdialysis studies rely on an efficient analytical method to determine free drug concentrations in microdialysate and at the same time, total concentration in plasma to assess the relationship between the unbound and bound levels. In addition, the assay must be sensitive to measure considerably low concentration of the analyte in small sample volumes since only a few microliters are obtained from microdialysis sampling. Another prerequisite of the method is the simultaneous quantification of the analyte and the calibration standard added to the microdialysis perfusion solution.

Some LC methods for determination of triamcinolone acetonide have been reported [70,90-93]. HPLC methods determined TA concentrations in human plasma after intravenous, intramuscular, oral or inhaled administration and were characterized by a laborious plasma extraction procedure and limited concentration ranges [70,90-92]. Also, these methods were not suitable for the purpose of the proposed PK study, since none of them simultaneously determines TA and budesonide (microdialysis calibration standard). An ultra sensitive reversed-phase capillary LC coupled to tandem mass spectrometry (*μ*LC/MS/MS) was able to quantified TA in porcine plasma following suprachoroidal administration; however, this approach required more sophisticated instrumentation [93]. Nevertheless, the main disadvantage of previously reported methods rests on the large plasma volume required for sample preparation, minimum of 750 μL, and/or the sample volume, minimum of 20 μL, subjected to the HPLC analysis.

[1]Reprinted with permission from Vieira M de LT, Singh RP, Derendorf H. Simultaneous HPLC analysis of triamcinolone acetonide and budesonide in microdialysate and rat plasma: Application to a pharmacokinetic study. J Chromatogr B Analyt Technol Biomed Sci 2010, 878: 2967-2973.

Specific Aim

The aim of this study was to develop and validate an efficient and sensitive assay for reliable quantification of TA and budesonide in microdialysate and rat plasma using common laboratory equipment (HPLC-PDA).

Materials

Chemicals and Reagents

• Blank male rat plasma	Lampire Biological Lab. (Pipersville, PA, USA)
• Budesonide	Purity ≥99%, Sigma (St. Louis, MO, USA)
• Fluticasone propionate	Purity ≥98%, Sigma (St. Louis, MO, USA)
• HPLC grade methanol	Fischer Scientific (Fair Lawn, NJ, USA)
• HPLC grade phosphoric acid	Fischer Scientific (Fair Lawn, NJ, USA)
• Lactated Ringer's Injection USP	Baxter Health Care (Deerfield, IL, USA)
• Triamcinolone acetonide	Purity ≥99%, Sigma (St. Louis, MO, USA)

Equipment and Disposables

• Balance	Mettler AE240, Toledo (Hightstown, NJ, USA)
• Cellulose membrane filter	0.45 µm poresize, Millipore (Bedford, MA,USA)
• Centrifuge	Fisher Scientific model Marathon 16KM (Pittsburg,PA, USA)
• Micropipettes	Eppendorf Research
• SPE cartridges	Bakerbond SPETM, C18 phase, 1mL capacity, sorbent, JT Baker (Deventer,Netherlands)
• SPE manifold	Vac Elut SPS 24, Varian (Palo Alto, CA,USA)
• Ultrasonic bath	Fisher Scientific model FS110H (Pittsburgh,PA,USA)
• Vortex	Kraft Apparatus Inc., Fisher Scientific model PV-5 (Pittsburgh,PA,USA)

Chromatographic Instrumentation

• Analytical column	Kromasil C18, 4.6 mm id, 25 cm, 5 µm particle, Hichrom (Reading, UK)

- Analytical software — Agilent ChemStation
- Autosampler — Agilent 1100 series , model G1329A
- Column oven — Agilent 1100 series, model G1316A
- Degasser — Agilent 1100 series, model G1379A
- Guard column — Kromasil C18, 3.2 mm id,10 cm, 5 µm particle, Hichrom (Reading, UK)
- HPLC system — Agilent 1100 Series (Waldbronn, Germany)
- Photodiode array (PDA) detector — Agilent 1100 series, model G1315B
- Quaternary pump — Agilent 1100 series, model G1311A
- Workstation — Hewllet-Packard Compaq p4

Methods

Chromatographic Conditions

Chromatographic separations were obtained using a Kromasil C18 analytical column which was protected by Kromasil C18 guard column. The column temperature was maintained at 25 °C and the detection wavelength was set at 254 nm. The isocratic mobile phase consisted of methanol: water in the ratio of 72:28 (v/v) at a flow rate of 0.8 mL/min was used to achieve desired chromatographic separation. The mobile phase was filtered through 0.45 µm cellulose membrane filter and degassed in an ultrasonic bath prior to use. The injection volume was 10 µL for microdialysates and 20 µL for extracted plasma samples. Samples were maintained at 4 °C in the autosampler prior to injection.

Before every run mobile phase was pumped through the system until a stabile base line was achieved. A blank injection of either lactated Ringer's solution for microdialysate samples or methanol for plasma samples was made at the start to

ensure system equilibration. A standard retention time and peak symmetry (between 0.8 and 1.2) were then verified. Blank lactated Ringer's solution or methanol injections were made periodically throughout run. At the end of the runs, the system was washed with mobile phase for at least 30 minutes. Mobile phase was not recycled.

Preparation of Stock and Working Solutions

Primary stock solutions of TA, fluticasone propionate (plasma internal standard, IS) and budesonide (microdialysis calibration standard) were prepared in methanol to yield for each solution concentrations of 1 mg/mL. These stock solutions were further diluted in methanol to get intermediate concentrations of 100 µg/mL for TA, 75 µg/mL for IS and 75 µg/mL for budesonide.

Working solutions of TA (1.5 - 750 µg/mL) and budesonide (7.5 - 150 µg/mL) required for spiking plasma and microdialysate calibration and quality control samples were subsequently diluted in methanol from primary and intermediate stock solutions. All methanolic solutions were stored at -20 °C, protected from the light, until use.

Preparation of Calibration Standards and Quality Control Samples

To obtain the desired concentration of TA for calibration and quality control (QC) samples, either blank rat plasma or Ringer's solution were spiked with 7% of TA working solutions of appropriate concentrations. Four levels of quality control samples at the lowest limit of quantification (LLOQ), low (LQC), medium (MQC) and high (HQC) end of the calibration curve were prepared for both matrices. Microdialysate calibration standards (0.1, 0.25, 0.5, 1, 2.5, 5 and 10 µg/mL) and QC samples (LLOQ= 0.1 µg/mL, LQC= 0.2 µg/mL, MQC= 2 µg/mL and HQC= 7 µg/mL) were prepared prior to each analytical run, whereas plasma calibration standards (0.5, 1, 2.5, 5, 10, 25 and 50

µg/mL) and QC samples (LLOQ= 0.5 µg/mL, LQC= 1 µg/mL, MQC= 20 µg/mL and HCQ= 40 µg/mL) were stored at -70 °C until analysis.

A 7% spiking with budesonide working solutions of appropriate concentrations were done in Ringer's solution to obtain the desired level of budesonide for calibration (0.5, 1, 2.5, 5, 10 µg/mL) and QC samples (LLOQ=0.5 µg/mL, MQC=2 µg/mL, HQC=7 µg/mL).

Plasma Sample Pre-treatment: SPE Procedure

Spiked plasma samples were completely thawed in a water bath at room temperature and vortex adequately. To 140 µL of the plasma sample, 10 µL of internal standards solution (75 µg/mL of fluticasone propionate containing 75 µg/mL of budesonide) were added to yield a concentration of 5 µg/mL. Samples were mixed 1:1 with 4% phosphoric acid solution to release protein-bound drug. After thorough mixing, samples were extracted using solid phase-extraction cartridges with C18 phase. The extraction was carried out on a SPE extraction manifold. Each cartridge was conditioned by 1 column volume of methanol followed by 1 column volume of water. The diluted plasma samples were loaded onto the conditioned SPE cartridges at a flow rate of 1mL/min. Washing was done with 600 µL of 2% phosphoric acid. Then, a low vacuum (2-5 mmHg) was applied for 2-5 minutes to remove the aqueous part. The analytes were eluted using 300 µL of methanol and a 20 µL aliquot of each sample was subjected to HPLC analysis.

Method Validation

Specificity

Six different sources of blank rat microdialysate and rat plasma were screened to investigate potential endogenous interferences in the retention times of TA, budesonide and fluticasone propionate (IS).

Linearity

The linearity range of the method for TA was evaluated by seven-point standard curves in the concentration range of 0.1-10 µg/mL for microdialysate and 0.5-50 µg/mL for plasma on three validation days. Budesonide calibration curves in microdialysate were prepared in the range of 0.5-10 µg/mL. Microdialysate calibration curves were constructed by plotting the analyte peak area *vs* concentration using $1/x^2$ linear regression; whereas for plasma calibration curves, the TA/IS (fluticasone propionate) peak area ratios *vs* TA concentrations were plotted using $1/x^2$ linear regression.

The linear model was accepted if the relative error (%RE, percent difference of the back-calculated concentration from the nominal concentration) were within 20% at the lower limit of quantification and within 15% at all other calibration levels. In addition, the similarity of slope and intercept (significance level of 0.05) among calibration curves (n=6, for each matrix) were verified.

The lower limit of quantification (LLOQ) was established as the lowest concentration used in the calibration curve for each matrix.

Accuracy and precision

The intra-day precision and accuracy of the method for quantifying TA were determined by analysis of four sets of plasma and six sets of microdialysate QC samples at the LLOQ, LQC, MQC and HQC levels in a single day. The inter-day

precision and accuracy were estimated by analysis of all QC samples over the three validation days. Accuracy and precision of the method for budesonide were determined by the analysis of six sets of microdialysis QC samples at the LLOQ, MQC and HQC. Accuracy was calculated as the mean relative error (RE) of the observed concentration ($_{Cobs}$) from the nominal concentration (C_{nom}) at each QC level according to the equation:

$$\%RE = \frac{(C_{obs}-C_{nom})}{C_{nom}} \times 100$$

Precision was expressed as percent of coefficient of variation and calculated as:

$$\%CV = \frac{\text{standard deviation of the mean}}{\text{Mean } C_{obs}} \times 100$$

Plasma extraction recovery

The extraction recovery from plasma were carried out in plasma QC samples at low, medium and high TA concentrations (1, 20 and 40 µg/mL) and at one concentration (5 µg/mL) of the IS (fluticasone propionate). The absolute percentage recovery was determined by comparing the mean peak area of four replicates of extracted samples with mean peak areas of un-extracted standards of equivalent concentration as follows:

$$\%AR = \frac{\text{peak area sample}}{\text{peak area standard}} \times 100$$

Stability

Stability tests were performed under settings that simulate the conditions likely to be encountered during sample collection, storage, preparation and analysis: microdialysate kept at room temperature (25 ± 2 °C) for 12h, process stability (autosampler at 4 °C for 24h), long-term stability of plasma at -70 °C for 2 months and plasma samples freeze-thaw stability (three cycles). Experiments were performed using three replicates of LQC, MQC and HQC samples of the corresponding matrix. Stability

was expressed as the mean percentage ratio of the observed concentration (C_{obs}) to the nominal concentration (C_{nom}) at each QC level according to the equation:

$$\%RE = \frac{C_{nom}}{C_{obs}} \times 100$$

Data analysis

Linear regression analyses were performed by GraphPad Prism version 4.00 for Windows (GraphPad Software, San Diego, CA, USA). The statistical analyses of calibration standards and quality controls were performed using EXCEL 2007 (Microsoft Corporation). Data are expressed as means ± standard deviation, unless otherwise stated.

Results and Discussion

Plasma Internal Standard Selection

Structural analogs of TA were screened to find suitable compounds for plasma internal standard. Fluticasone propionate was finally chosen as the internal standard for its better sensitivity and good correction as shown by the data.

Development of Chromatographic Method

Due to the relatively small number of samples but two different matrices (plasma and microdialysate) and two different analytes, it was not the goal to perform extensive method optimization but to provide sample analysis with adequate specificity, accuracy and precision. It was preferred to apply the same analysis technique for both matrices to allow a rapid switching from one assay to another.

Development of the Sample Pre-treatment Procedure

For microdialysate samples, due to the lack of proteins, no sample pre-treatment procedure was necessary. Thus samples were directly injected into the HPLC system.

However, the pre-analytical treatment of plasma samples was essential to obtain cleaner extracts. Different liquid-liquid and solid-phase extraction (SPE) procedures were tested. Liquid-liquid extraction using ethyl-acetate, dichloromethane and tert-butyl methyl ether as previously used by other investigators [90,91,94] were tested. However, our results showed relatively low recovery for TA, around 60%, poor reproducibility and specificity. Subsequently, SPE procedures were tested using octadecyl phase sorbent because of its extreme retentive nature for hydrophobic compounds. Initially, the pretreatment of the plasma samples with 4% phosphate acid aimed on the release of TA from plasma proteins. The optimization of the SPE procedure was done by varying the proportion of methanol in water used as washing solvent to minimize polar matrix interferences. The method proved to be unsuccessful as it did not improve the specificity of the method. However, an acidic condition washing (2% phosphoric acid) removed interfering endogenous substances without causing elution of the analytes. The volume of methanol as elution solvent was also optimized to improve the recovery of the analytes. A higher volume of eluate (300 µL instead of 150 µL) resulted in excellent recovery and minimal residual matrix. All these efforts helped us achieve an efficient SPE procedure with one wash and one elution step with no drying and reconstitution. Thus, this is a simple and economical plasma extraction procedure with increased sensitivity, specificity and throughput for determination of corticosteroids in small volume of plasma samples.

Method Validation

Specificity

The specificity is the ability of an analytical method to differentiate and quantify the analyte in the presence of potential interfering compounds.

Typical chromatograms obtained from blank rat microdialysate, blank rat plasma, the peak response of TA at the medium end of the calibration curve in plasma and artificial microdialysate (lactated Ringer's solution), and intravenous microdialysate and plasma samples obtained after constant-rate infusion of TA (23 mg/kg/h) to a rat are shown in Figures 2-1 and 2-2. TA, budesonide and IS (fluticasone propionate) were eluted at 6.8, 12.3 and 14.0 minutes, respectively. The results demonstrated there is no interference in the determination of the analytes, granting good method selectivity.

Linearity

The weighted linear regression (weighting factor: 1/concentration^2) analysis was used since this option provided an improvement in the residuals with a similar coefficient of determination (r^2) to the linear model. Calibration curves for TA in both matrices exhibited good coefficients of determination, $r^2 \geq 0.992$ for all microdialysate curves and $r^2 \geq 0.996$ for all plasma curves. Detailed results for linearity parameters for TA in microdialysate and plasma are listed in Table 2-1.

Slope and intercept among microdialysate calibration curves (n=6) were not significantly different ($\alpha=0.05$) allowing the construction of one common curve with slope of 15.49 (± 0.12) and intercept of -0.1046 (± 0.0297), r^2 =0.9959. Since differences among slopes and intercepts of plasma calibration curves (n=6) were not significant ($\alpha=0.05$), the pooled slope equals 0.2138 (± 0.0027) and intercept -0.0041(± 0.0031) with r^2 =0.9962. Good linearity values were also found for budesonide in microdialysate curves (Table 2-2). The common curve ($\alpha=0.05$) has a slope of 17.07 (± 0.22) and intercept of -4.053 (± 0.218) with r^2 =0.9932.

The lowest standard on the calibration curves for each matrix and analyte, TA and budesonide, were defined as the LLOQ since the analytes response were identifiable,

discrete (Figures 2-1 and 2-2), and reproducible with precision and accuracy less than ±20% (Tables 2-3 and 2-4).

The mean back-calculated concentrations of TA in microdialysate and plasma calibration standards with resulted accuracy (%RE) and precision (%CV) are listed in Table 2-3. The accuracy values of budesonide for various concentrations in microdialysate calibration standards ranged from -4.81% to 5.21% with precision between 1.74% and 5.51% (Table 2-4).

Accuracy and precision

The intra-day precision of TA QC samples for both matrices was less than 6.62%, and the accuracy ranged between -5.28% and 9.14%. The inter-day precision was less than 6.46%, and the accuracy values ranged between -3.19% and 6.30%. The mean observed value, coefficient of variation and relative errors of the microdialysate and plasma QC samples used on the three validation days are presented in Tables 2-5 and 2-6, respectively.

The intra-day accuracy of budesonide in microdialysate QC samples (n=6 at each concentration) ranged from -1.42% to 9.14% and precision values were between 1.80% and 4.50%. The inter-day accuracy values were 0.73% for LLOQ and 3.18% for MQC with CV of 3.39% and 4.89%, respectively.

The accuracy and precision values were well within acceptable limits stated for bioanalytical method validation: ±15% at low, medium and high range of concentrations and ± 20% at the LLOQ.

Extraction recovery

The extent of recovery of the TA and IS from plasma was reproducible and equivalent. The mean absolute recovery (n=4 at each concentration) at low, medium

and high QC samples were 109%, 103% and 99.6% with precision of 2.02%, 4.57% and 3.94%, respectively. The mean recovery of the IS was 95.7% with CV of 1.81%.

Stability

The results of stability test of TA in plasma and microdialysate QC samples are listed in Table 2-7. TA and budesonide in spiked microdialysate proved to be stable after sample preparation and storage in the sample tray of the autosampler at 4 °C for 24h and at room temperature for at least 12h. Average stability for budesonide at MQC was 99.2% with precision of 3.95% and 109% with precision of 6.57% under these respective conditions. The results of process stability of plasma QC samples demonstrated that the post-extraction solution is stable at 4 °C for at least 24h. Storing samples containing TA in plasma at -70 °C for 2 months or after three freeze-thaw cycles did not cause any degradation.

Overall, the results indicated reliable stability for TA and budesonide under the investigated conditions since the observed concentrations were all within 85-115% of the nominal concentrations.

In summary, a simple and specific HPLC-PDA method was developed for simultaneously quantifying TA and its microdialysis calibrator, budesonide, in microdialysate and rat plasma samples. Validation results showed that the method is highly reproducible for both matrices and meets the requirements for the pharmacokinetic investigations. The analytes are stable under the conditions which will be encountered during the proposed studies.

Table 2-1. Linear regression parameters for triamcinolone acetonide in plasma and microdialysate calibration standards

Curve	TA Plasma			TA Microdialysate		
	Intercept	Slope	r^2	Intercept	Slope	r^2
1	-0.0019	0.2156	0.9996	-0.0386	15.27	0.9916
2	-0.0047	0.2234	0.9997	-0.1201	15.15	0.9935
3	-0.0064	0.2163	0.9973	-0.1697	15.43	0.9952
4	-0.0083	0.2205	0.9961	-0.0262	15.34	0.9975
5	0.0003	0.2023	0.9979	-0.2037	16.10	0.9987
6	-0.0038	0.2053	0.9996	-0.0692	15.63	0.9992
Mean		0.2138			15.49	
SD		0.0083			0.36	
CV (%)		3.9			2.3	

Table 2-2. Linear regression parameters for budesonide in microdialysate calibration standards

Curve	Budesonide Microdialysate		
	Intercept	Slope	r^2
1	-4.388	17.22	0.9917
2	-3.807	16.91	0.9887
3	-4.458	17.89	0.9992
4	-3.821	17.03	0.9941
5	-4.210	17.08	0.9934
6	-3.634	16.33	0.9995
Mean		17.07	
SD		0.50	
CV (%)		3.0	

Table 2-3. Summary of observed TA concentration in microdialysate and plasma calibration standards

Microdialysate					Plasma				
Cnom	Mean Cobs	SD	%RE	%CV	Cnom	Mean Cobs	SD	%RE	%CV
0.1	0.100	0.004	0.36	3.52	0.5	0.485	0.015	-3.06	3.12
0.25	0.253	0.010	1.26	3.75	1	1.05	0.04	5.16	3.69
0.5	0.481	0.007	-3.75	1.41	2.5	2.65	0.20	6.15	7.51
1	0.987	0.031	-1.30	3.11	5	4.71	0.12	-5.76	2.59
2.5	2.45	0.11	-2.03	4.59	10	9.52	0.41	-4.84	4.35
5	5.01	0.18	0.14	3.49	25	25.1	1.1	0.34	4.19
10	10.5	0.2	5.35	1.59	50	50.9	2.6	1.86	5.12

Cnom= Nominal concentration (µg/mL) and Cobs= Observed concentration (µg/mL)
Mean values: n=6 at each concentration

Table 2-4. Summary of observed budesonide concentration in microdialysate calibration standards

Cnom	Mean Cobs	SD	%RE	%CV
0.5	0.503	0.008	0.60	1.59
1	1.00	0.05	0.58	4.53
2.5	2.38	0.13	-4.81	5.51
5	4.93	0.09	-1.46	1.74
10	10.5	0.4	5.21	3.96

Cnom= Nominal concentration (µg/mL) and Cobs= Observed concentration (µg/mL)
Mean values: n=6 at each concentration

Table 2-5. Intra- and inter-day accuracy (%RE) and precision (%CV) of observed TA concentrations in microdialysate quality controls

Cnom	Validation day	Mean Cobs	SD	%RE	%CV
0.1	1 (n=6)	0.103	0.004	2.72	4.00
	2 (n=6)	0.102	0.006	2.42	5.53
	3 (n=6)	0.106	0.005	6.44	5.02
	Inter-day (n=18)	0.104	0.005	3.84	4.72
0.2	1 (n=6)	0.211	0.014	5.51	6.65
	2 (n=6)	0.207	0.009	3.42	4.22
	3 (n=6)	0.201	0.005	0.67	2.45
	Inter-day (n=18)	0.206	0.011	3.21	5.26
2	1 (n=6)	2.06	0.02	2.98	1.15
	2 (n=6)	1.97	0.06	-1.74	3.10
	3 (n=6)	1.89	0.11	-5.67	5.59
	Inter-day (n=18)	1.97	0.11	-1.47	5.36
7	1 (n=6)	7.08	0.04	1.11	0.49
	2 (n=6)	6.75	0.12	-3.55	1.83
	3 (n=6)	7.27	0.36	3.80	4.90
	Inter-day (n=18)	7.03	0.24	0.41	3.35

Cnom= Nominal concentration (µg/mL) and Cobs= Observed concentration (µg/mL)

Table 2-6. Intra- and inter-day accuracy (%RE) and precision (%CV) of observed TA concentrations in plasma quality controls

Cnom	Validation day	Mean Cobs	SD	%RE%	%CV
0.5	1 (n=4)	0.510	0.034	2.03	6.59
	2 (n=4)	0.498	0.026	-0.43	5.20
	3 (n=4)	0.495	0.025	-0.91	4.99
	Inter-assay (n=12)	0.501	0.032	0.25	6.46
1	1 (n=4)	1.09	0.019	9.14	1.77
	2 (n=4)	1.05	0.051	4.46	4.92
	3 (n=4)	1.05	0.023	4.64	2.20
	Inter-assay (n=12)	1.06	0.056	6.30	5.29
20	1 (n=4)	19.3	0.915	-3.48	4.74
	2 (n=4)	19.4	1.060	-3.02	5.46
	3 (n=4)	19.4	0.425	-3.01	2.19
	Inter-assay (n=12)	19.4	1.004	-3.19	5.19
40	1 (n=4)	38.7	0.732	-3.34	1.89
	2 (n=4)	39.5	1.454	-1.31	3.68
	3 (n=4)	39.6	0.350	-1.08	0.89
	Inter-assay (n=12)	39.2	1.444	-1.94	3.68

Cnom= Nominal concentration (µg/mL) and Cobs= Observed concentration (µg/mL)

Table 2-7. Stability results of TA in rat plasma and microdialysate under various conditions

Storage Condition	LQC			MQC			HQC		
	Cobs (C_{nom})	% RE	% CV	Cobs (C_{nom})	% RE	% CV	Cobs (C_{nom})	% RE	% CV
Plasma									
3 freeze-thaw cycles	0.98 (1)	97.9	2.68	20.5 (20)	103	3.58	39.6 (40)	99.1	6.17
2 months at -70 °C	1.00 (1)	100	2.79	19.0 (20)	95.1	2.62	39.0 (40)	97.4	0.90
Process 4°C, 24h	1.02 (1)	102	2.78	19.2 (20)	96.0	0.75	40.6 (40)	102	3.03
Microdialysate									
Room temp. (25 °C), 12h	0.222 (0.2)	111	1.68	2.16 (2)	108	6.55	7.05 (7)	100	2.62
Process 4°C, 24h	0.202 (0.2)	101	1.84	1.96 (2)	97.9	4.07	7.04 (7)	100	1.72

Cobs= Observed concentration (µg/mL) and Cnom= Nominal concentration (µg/mL)
Mean values: n=3 at each concentration (µg/mL) for each storage condition

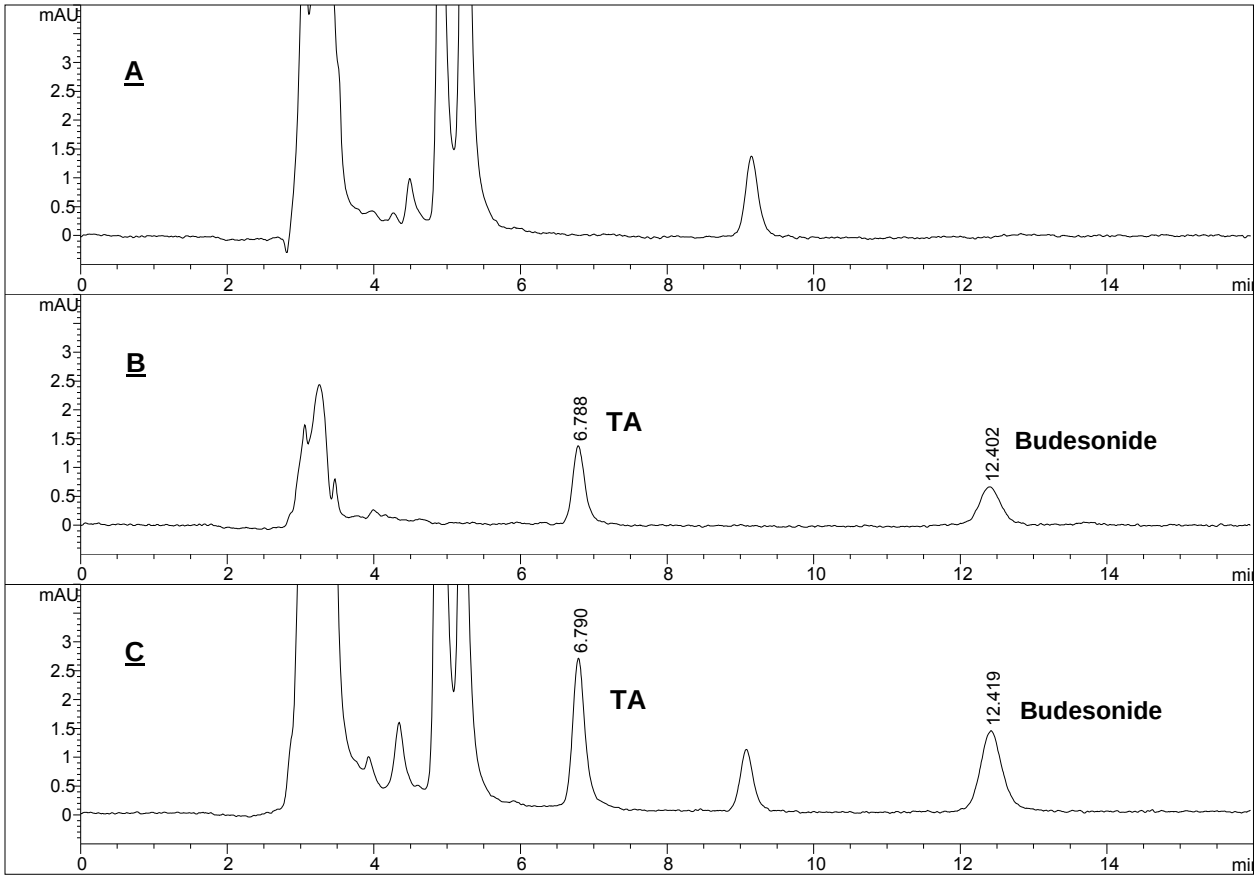

Figure 2-1. Representative microdialysis chromatograms. A) Blank intravenous microdialysate. B) Microdialysate calibration standard spiked with TA (1 µg/mL) and budesonide (1 µg/mL). C) Intravenous microdialysate sample containing TA (2.86 µg/mL) and budesonide (1.92 µg/mL) after drug infusion in a rat.

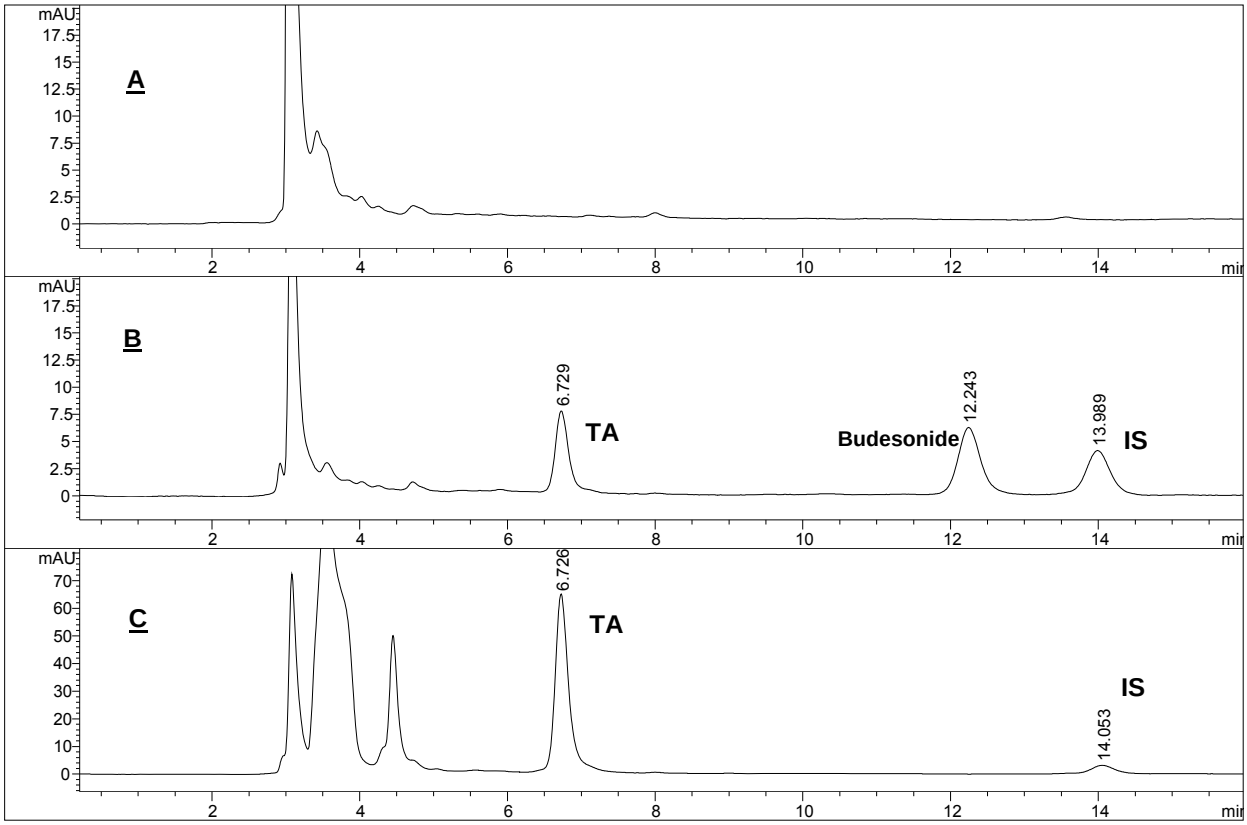

Figure 2-2. Representative plasma chromatograms. A) Blank rat plasma. B) Plasma calibration standard spiked with TA (5 µg/mL), budesonide (5 µg/mL) and IS (Fluticasone propionate, 5 µg/mL). C) Plasma sample containing TA (42.6 µg/mL) after drug infusion.

CHAPTER 3
TRIAMCINOLONE ACETONIDE MICRODIALYSIS CALIBRATION

Background

It is recommended to perform supportive *in vitro* MD experiments prior to animal use to obtain basic information on the feasibility of the method. The applicability of the MD technique can be limited by drug lipophilicity which can impair the diffusion through the microdialysis membrane and overall recovery [2,10,33]**.** Triamcinolone acetonide, our model compound has moderate lipophilicity (Log $P_{o:w}$ of 2.5) and is poorly soluble in water (21 µg/mL) (Chemspider database, Royal Society of Chemistry, Cambridge, UK).

One critical step to apply microdialysis is to determine the relative recovery of the analyte of interest. As MD probe is continuously perfused at a constant flow rate, complete equilibrium across the MD membrane cannot be established. Thus, the levels measured in the dialysate will always be lower than the actual levels in the investigated media ($C_{analyte\ sampling\ site} > C_{analyte\ dialysate}$). The factor by which the concentrations are interrelated during sampling ($C_{perfusate}=0$) is termed relative recovery [2]. The recovery value is determined *a priori* to calculate the actual concentration at the investigated media from the concentration in the dialysate as follows:

$$C_{analyte\ sampling\ site} = \frac{C_{analyte\ dialysate}}{Recovery}$$

A general measured of the degree of equilibration at a constant flow rate (or the steady-state rate of exchange across the MD membrane) is named extraction efficiency which has the same value for all drug concentrations in the perfusate ($C_{perfusate}$). Microdialysis probes can consequently be calibrated by either measuring the loss of analyte using drug-containing perfusate ($C_{perfusate} > 0$, Retrodialysis method) or the gain of the analyte using drug-containing sample solutions ($C_{perfusate}=0$, Extraction Efficiency method) [2].

The processes occurring during retrodialysis and extraction efficiency methods of microdialysis calibration are illustrated in Figure 3-1.

The *in vitro* recovery of TA was determined using the two calibration methods: the extraction efficiency (EE) and retrodialysis (RD). The *in vitro* studies were carried out to investigate the effects that drug characteristics may have on recovery, including the ability of the compound to diffuse through the MD membrane, whether the diffusion is symmetrical in both directions and independent of the drug concentrations.

However, the recovery obtained by the *in vitro* experiments do not replace the *in vivo* determinations [32,95]. The overall diffusion resistance of the *in vitro* medium might be much different from that one observed *in vivo* due to additional resistance derived from the interstitial space. Therefore, the *in vivo* recovery of the probes was determined by the most common method of *in vivo* calibration, retrodialysis by drug.

Specific Aim

The aim of this study was to determine the relative recovery of TA by a series of *in vitro* and *in vivo* studies to evaluate the feasibility of using microdialysis as a sampling technique for TA.

Materials

Chemicals and Reagents

- 0.9% Sodium Chloride Inj. USP — Baxter Health Care (Deerfield, IL, USA)
- 1000 UI/mL Heparin — Elkins-Sinn, Inc. (Cherry Hill, NJ, USA)
- Budesonide — Sigma (St. Louis, MO, USA)
- HPLC grade methanol — Fischer Scientific (Fair Lawn, NJ, USA)
- Isoflurane USP — Webster Veterinary (Charlotte, NC, USA)
- Lactated Ringer's Injection USP — Baxter (Deerfield, IL, USA)
- Triamcinolone acetonide — Sigma (St. Louis, MO, USA)

Equipment and Disposables

- Balance — Mettler AE240, Toledo (Hightstown, NJ, USA)

• Heated Stir Plate	Fisherbrand Isotemp
• Microfraction collector	CMA/142, CMA Microdialysis (Stockholm, Sweden)
• Micropipettes	Eppendorf Research
• Precision Infusion Pump	Harvard Apparatus Model 22, (South Natick, Mass., USA)
• Syringes	Becton Dickinson 309603 (Franklin Lakes,NJ, USA)
• Thermometer	Fisherbrand 76mm Immersion 14-997
• Tubing Adapter	CMA Microdialysis (Stockholm, Sweden)
• Vortex	Kraft Apparatus Inc., model PV-5, Fisher Scientific
• FEP tubing	ID 0.12mm, CMA Microdialysis (Stockholm, Sweden)
• Cellulose membrane filter	0.22 µm pore size, Millex® GV Millipore (Carrigtwohill, Co. Co Cork, Ireland)
• Microdialysis Probe	CMA/20 Elite, 14/10 PAES, cut-off 20kDa; membrane length 10 mm; CMA Microdialysis (Stockholm, Sweden)

Animals

Adult male Sprague-Dawley rats, weighting 250-300 grams, were purchased from Harlan Sprague-Dawley Inc. (Indianapolis, IN, USA). Animals were acclimatized to standard ACS housing in a 12-h light-dark cycle and constant temperature environment for a minimum of three days before being used. Animals had free access to food and water. The animal experimental procedures were approved by the Institutional Animal Care and Use Committee of University of Florida.

Methods

Preparation of Standard Solutions and Quality Control (QC) Samples

10 mg of TA were weighted and dissolved in 10 mL of methanol. The 1 mg/mL stock solution was diluted to a secondary stock of 100µg/mL in lactated Ringer's solution. Further dilutions were performed to obtain the seven standard solutions of TA at the concentrations of 10, 5, 2.5, 1, 0.5, 0.25 and 0.1µg/mL in lactated Ringer's solution. Four levels of QC samples at the lowest limit of quantification (LLOQ), low, medium and high end of the calibration curve (0.1, 0.25, 1 and 5 µg/mL) were also prepared.

Preparation of Calibration Solutions for Microdialysis

Stock solution of 1mg/mL of TA in methanol was prepared. Then a 100 µg/mL solution was obtained by dilution in lactated Ringer's solution. Further dilutions were performed to obtain the three calibration solutions of TA at the concentrations of 10, 5 and 1 µg/mL in lactated Ringer's solution. These concentrations were chosen based on the expected concentrations in the main preclinical study.

In vitro Microdialysis Calibration

Apparatus setup

During setup, a 5 mL syringe was filled either with blank lactated Ringer's solution (EE method) or analyte solution (RD method) and the enclosed air was cleared from the syringe. The syringe was placed on the precision pump, connected to the inlet of the probe and run at a flow rate of 1.5 µL/min for 30 minutes to allow for equilibration. The microdialysis probe was immersed in a 10 mL centrifuge tube containing approximately 8 mL of either blank lactated Ringer's solution (RD method) or analyte solution (EE method). The sampling solution was stirred at 300 rpm to guarantee equal

concentrations throughout the whole tube and temperature was controlled at 37 ± 1°C on a heated plate. The microdialysate samples were collected with the aid of the microfraction collector.

Extraction efficiency method (EE)

The MD probe was perfused with Blank lactated Ringer's solution at a constant flow rate of 1.5 µL/min and placed into the sampling tube containing TA solution, starting with the lowest concentration. Drug diffused from the sampling solution into the MD probe and was taken with the perfusion flow. The gain of the analyte through the membrane was then determined from the TA concentration in the microdialysate ($C_{dialysate}$). Three microdialysate samples were collected with 20 minutes intervals after the end of a 30 minutes equilibration period. To determine the actual TA concentration in the calibration solution to perform the calculations and to ensure that the concentration was consistent throughout the sampling period, two samples of the sampling solution were taken, one before the sampling period and one after ($C_{sampling\ sol}$). The same procedure was done for the remaining two concentrations, 5 and 10 µg/mL. The analyte concentrations in the samples were determined by a validated HPLC method. The experiments were performed using three different microdialysis probes. The percent recovery (%R) for the EE method was calculated as follows:

$$\%R = \frac{C_{dialysate}}{C_{sampling\ sol}} \times 100$$

Retrodialysis method (RD)

The MD probe was perfused with the analyte solution at a constant flow rate of 1.5µL/min. and placed into a calibration tube filled with blank lactated Ringer's solution. The drug diffused out of the probe into the calibration solution. The loss of the analyte

through the membrane was then determined from the TA concentration in the microdialysate ($C_{dialysate}$). Three microdialysate samples were collected with 20 minutes intervals after the end of a 30 minutes equilibration period. To obtain the actual concentration of the TA in the perfusion solution and to ensure that the concentration was consistent throughout the sampling period, two samples of the perfusate were taken, one before the sampling period and one after ($C_{perfusate}$). The lowest concentration, 1 µg/mL, was sampled first followed by the others with the exchange of calibration tube with fresh blank lactated Ringer's solution. Experiments were performed using three different probes. The percent recovery (%R) for the RD method was calculated as follows:

$$\%R = \frac{C_{perfusate} - C_{dialysate}}{C_{perfusate}} \times 100$$

Sample analysis

The concentration of TA in the *in vitro* microdialysate samples and calibration solutions were determined by the HPLC method described below. The HPLC system consisted of an Agilent 1100 series which included an autosampler (G1329A), a column oven (G1316A), a degasser (G1379A), a quaternary pump (G1311A) and a DAD detector (G1315B). Instrument control, data acquisition and processing were performed using ChemStation software. Chromatographic separations were obtained using LiChrospher® 100 RP-18 analytical column (5 µm particle size, Merck KGaA, Darmstadt, Germany) protected by a guard column (LiChroCART® Merck, KGaA, Darmstadt, Germany). The column temperature was maintained at 25 °C and the detection wavelength was set at 254 nm. The isocratic mobile phase consisted of methanol and water in the ratio of 70:30 (v/v) at a flow rate of 0.8 mL/min. A volume of

10 µL of each microdialysate sample and calibration solutions was directly injected into the column without previous preparation. Samples were maintained at 4 °C in the autosampler prior to injection.

In vivo Microdialysis Calibration

Animal preparation

In vivo microdialysis calibration was performed with the animals under anesthesia. Isoflurane was employed as an inhalation anesthetic as previously described [96,97]. Experimental procedures were in accordance with the criteria of the Canadian Council of Animal Care [98]. Animals were anesthetized by using Isotec-4 isoflurane vaporizer (SurgiVet/ Smiths Medical, Waukesha, WI). The rat was placed in an induction chamber which is supplied with an air-isoflurane (4%) mixture at a flow rate of 500 mL/min. After complete induction (2-3 minutes), the animal was transferred to the nonrebreathing circuit (face mask).The surgical level of anesthesia was confirmed by the absence of reflexes using noxious stimuli. Isoflurane anesthesia was maintained at 2.5-3% during acute surgical procedures and at 1.5–2% during prolonged experimental observations. Anesthetic depth and animal general well being were monitored by observing the rat's respiratory pattern, tissue perfusion, internal temperature and response to stimulation by pinching the toe pads. Animal body temperature was maintained at 99.5-101°F by a heating pad. To maintain the body fluid balance, sterile isotonic saline were administered at a constant rate of 0.5 mL/h through a catheter inserted on the tail ventral artery. The surgery site (pectoral area) was shaved and disinfected by swiping the area with 70% isopropyl alcohol. The rat was placed in the dorsal position with the tail towards the experimenter.

Probe insertion

A vertical incision was made in the skin over the pectoral muscle on the right side of the midline to expose the pectoral muscle and the jugular vein above it. A needle placed into a split introducer was inserted through the pectoral muscle into the right jugular vein. By removing the needle, the blood seeped back through the split tube. Rapidly, the microdialysis probe was inserted through the split introducer. The probe was secured by suturing its wings to the pectoral muscle using surgical silk, and the split introducer was then removed. The skin incision was closed by a suture. During surgery the inlet tubing of the probe was connected to a precision infusion pump and perfused with 10 IU heparin in lactated Ringer's solution at flow rate of 1.5 µL/min. After probe insertion the flow rate was increased to 8 µL/min for 5 minutes in order to remove air bubbles. The outlet tubing of the probe was checked to ensure the liquid was flowing.

***In vivo* retrodialysis method**

After 5 minutes, the perfusate was changed to the calibration solution of triamcinolone acetonide (5 µg/mL) in lactated Ringer's with the flow rate reduced to 1.5 µL/min. The probe was perfused for 60 minutes to equilibrate the system. Following this stabilization period, microdialysate samples were collected by the microfraction collector at 20 minutes intervals for 1-6 hours. Samples were stored at 4 °C until HPLC analysis was performed (within 24 hours). At the beginning and the end of the experiment, TA concentration in the perfusate was determined. The retrodialysis recovery of TA was calculated according to the equation:

$$\%R = \frac{C_{perfusate} - C_{dialysate}}{C_{perfusate}} \times 100$$

where %R is the percent recovery, $C_{perfusate}$ is the average TA concentration in the perfusate before and after the experiment, and $C_{dialysate}$ is the TA concentration in the microdialysate sample.

Sample analysis

The concentration of TA in *in vivo* microdialysate samples and calibration solutions in lactated Ringer's solution were determined using the HPLC method described in Chapter 2.

Data Analysis

Linear regression and statistical analyses were performed using GraphPad Prism version 4.00 for Windows (GraphPad Software, San Diego, CA, USA).The significance level was set at 0.05. Data are expressed as means ± standard deviation.

Results and Discussion

HPLC Method Validation

A seven-point linear calibration curve for TA was obtained in the range of 0.1-10 µg/mL. The analysis was performed with weighted linear regression ($1/Y^2$). The slope for the standards was 16.14 (± 0.28) and the intercept was 0.2671 (± 0.0717) with r^2 value of 0.9969. The method was validated by performing three calibration curves on each of the three consecutive days and by analyzing quality control samples (LLOQ= 0.1 µg/mL, LQC= 0.25 µg/mL, MQC= 1 µg/mL, and HQC= 5 µg/mL, n=6 at each concentration per day). The intra- and inter-day precision (%CV) values were smaller than 6.09% and 8.85%, respectively. The inter-day accuracy ranged from -4.34% to 11.5%. The results are listed in Table 3-1. The retention time of TA was approximately 5.3 minutes. The analytical method was specific, accurate and precise supporting the analysis of the *in vitro* microdialysis samples.

After the *in vitro* studies deemed TA suitable for use with microdialysis sampling, another HPLC-PDA method was developed and validated to determine TA in both microdialysate and rat plasma samples.

In vitro Microdialysis Calibration

The temporal resolution of microdialysis is determined by the perfusion rate and sensitivity of the analytical assay. Since there is a minimum sample volume requirement for the assay technique, a higher flow rate would provide shorter sampling intervals. However, the recovery is reduced because there is not enough time for equilibration between the solution inside the probe and the surrounding media to occur. Thus, the analyte concentration in the microdialysate is decreased. Therefore, a compromise has to be made between flow rate and sample volume. A flow rate of 1.5 µL/min and a sampling time of 20 minutes would provide 30 µL of sample. A volume of 10 µL was directly injected into the HPLC column without previous preparation.

Prior to animal studies, diffusion characteristics of TA through the semi-permeable membrane of the microdialysis probe were investigated *in vitro*.

In the present study two concentration-ranging *in vitro* microdialysis methods were used, extraction efficiency (EE) and retrodialysis (RD). Both methods are acceptable to characterize the diffusion process of the analyte through the MD membrane since the general assumption for the all calibration methods is that the recovery is the same regardless of whether the solute exchange occurs through either loss or gain. The mean *in vitro* recovery of triamcinolone acetonide by the RD and EE methods were 65.5% ± 5.3% and 66.8% ± 8.5%, respectively (see Table 3-2 for results).

Linear regression analysis was performed using the recoveries from either RD or EE methods versus TA concentration on the perfusate or medium, respectively (Figure

3-2). The mean regression line for the RD and EE methods were y= (-0.056 ± 0.314)x + (65.9 ± 2.15) and y= (-0.800 ± 0.425)x + (71.1 ± 2.75) (x=TA concentration, y= recovery), respectively. The slope and intercept between the calibration methods were not significantly different (α=0.05) allowing the conclusion that the efficiency of diffusion is quantitatively the same in both directions through the membrane and the recovery is independent of the drug concentration. Therefore, the retrodialysis method seems adequate to be used as a MD probe calibration method for TA in the *in vivo* experiment and a linear recovery (constant value) during the drug concentration-time profile determination is to be expected.

Our results are in agreement to reports in the literature which observed that MD relative recovery is concentration independent [99].

Furthermore, *in vitro* experiments demonstrated that no relevant adsorption processes to MD probe membrane or tubing took place.

There is not a minimum recovery requirement to perform microdialysis technique. However, percent recoveries inferior to 10% could result in analyte levels in the microdialysate samples to low to be accurately quantified [10]. As previously demonstrated [59], a relative recovery superior to 20% is recommended for more reliable estimation of the unbound drug concentrations. Low relative recovery (<20%) has been reported for moderate and highly lipophilic drugs such as bethametasone propionate [33], caspofungin [100], and variconazole [99] which may be attributed to the low solubility of the compounds in the perfusate solution and/or unspecific binding to the MD probe device.

In general, it is worthwhile to aim at higher recoveries in microdialysis studies and be aware that the recoveries obtained *in vitro* may overestimate those observed *in vivo* [71]. The *in vitro* experiments were done as a preliminary study to an *in vivo* calibration.

In vivo Microdialysis Calibration

An accurate measure of recovery requires that the calibration is done *in vivo*. The retrodialysis method was a very simple and convenient method for recovery determination *in vivo.* The obtained *in vivo* recovery of TA by retrodialysis will be used next to back-calculate the actual plasma unbound concentrations from IV microdialysate samples (Chapter 5).

The average recovery of TA obtained from four different animals for up to 6 hours of sample collection using the retrodialysis method was 59.9 ± 6.1% (range from 44.1% to 70.0%) as shown in Table 3-3. The *in vivo* RD recovery of TA was in the same range observed on the preliminary *in vitro* experiments, 65.5 ± 5.3% (58.7-80.8%) and 66.8 ± 8.5% (48.9-80.1%) (mean ± SD, with range between parentheses), for the retrodialysis and extraction efficiency methods, respectively.

To confirm the integrity of the probes used the *in vivo* calibration and assess the difference in relative recovery by retrodialysis *in vitro* and *in vivo*, *in vitro* retrodialysis were conducted after the animal experiment. Those additional *in vitro* studies were performed following the same procedures described in the retrodialysis method section of this chapter, but with an increase of the sample collection time for up to 6 hours.

The average *in vitro* retrodialysis recovery of TA for probes 1-4 was 65.5 ± 3.2% (Table 3-4). The average value is greatly comparable to the average *in vivo* recovery using the same probes, 59.9 ± 6.1%, and to the *in vitro* recoveries of 65.5 ± 5.3% and

66.8 ± 8.5% obtained by the RD and EE methods, respectively, using a different set of probes. These results also allowed the conclusion that the probes 1-4 were fully functional and with no loss of integrity after the *in vivo* calibration studies.

Both, the difference in recovery between individual probes and fluctuation within each probe contribute to the variability found in the average recovery value on both *in vivo* (Tables 3-3) and *in vitro* (Table 3-4) scenarios. The coefficient of variation within each probe is depicted in the data. Overall, a smaller coefficient of variation was found for the *in vitro* recovery than for the recovery of TA determined *in vivo* by the retrodialysis method.

The recoveries over time for all four probes under *in vivo* and *in vitro* conditions are illustrated in Figures 3-3 and 3-4. A slightly fluctuation in recovery over 180 minutes sample collection was observed both *in vivo* and *in vitro* (Figure 3-3); whereas a moderate fluctuation was observed under longer time frame (Figure 3-4). The largest fluctuation *in vivo* was displayed during the 360 minutes sampling using probe 3 in the present experiment. To evaluate the dependence of recovery on time, the mean recovery value by retrodialysis obtained in the first half of microdialysis collection time (0-180min) was compared to the mean value obtained in the second half of the experiment (200-360 min) under *in vivo* and *in vitro* conditions. For both probes 3 and 4, the *in vitro* recoveries determined within the first time frame of the experiment were not statistically different ($\alpha = 0.05$) to those obtained later; whereas, the *in vivo* recoveries obtained in the second half of the experiment were significantly lower than the ones determined in the first half. The results are illustrated in Figure 3-5. Within six hours, the

recovery in blood gradually decreased by 17% for probe 3. A similar phenomenon has been observed by other investigators [58,60,71,101,102].

Based in our current results of the comparison of *in vivo* and *in vivo* recoveries over time, we may infer that changes in probe clearance over time are likely related to the probe microenvironment rather than to the loss of probe integrity. The reduction in probe membrane clearance may be attributed to fiber clotting, plasma protein and/or cell deposition on the surface on the membrane. In addition, the convective blood flow around the probe implanted in the jugular vein may be small and variable, thus alterations in blood flow due to local vasoconstriction or long last narcosis results in fluctuations and decline in the probe recovery [57]. Some authors also found that the magnitude of the reduction in recovery is dependent on the particular tissue. For example, Sjoberg *et al* observed a gradual decrease in recovery over five hours of microdialysis sample collection in the blood but not in brain [102]. Acknowledgement of a possible time-dependent recovery is suggested for an adequate evaluation of the accuracy of the intravenous microdialysis technique.

In conclusion, this study demonstrated that TA has the ability to freely cross the microdialysis membrane with percent recoveries well over 10%. In our current study, the *in vitro* recoveries of TA were independent of drug concentrations and direction across the membrane. The *in vivo* recovery of TA by retrodialysis was in the same range that the one obtained in *in vitro* conditions; however a time-dependency of *in vivo* recovery was observed. The experimental results indicated that triamcinolone acetonide is a suitable drug to be evaluated by microdialysis, despite its moderate lipophilicity.

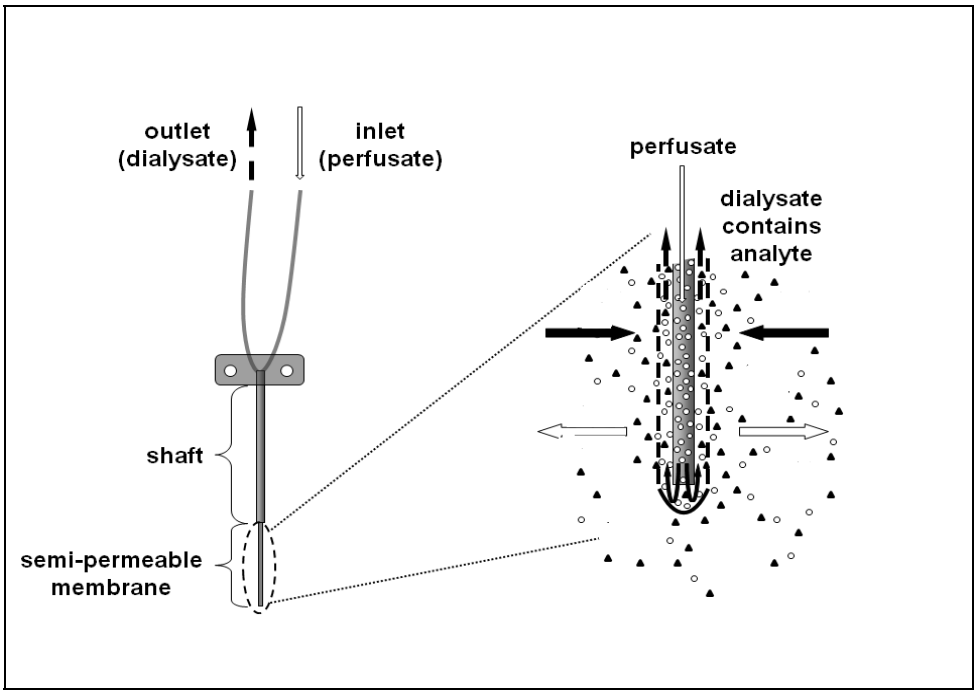

Figure 3-1. Schematic figure of a flexible microdialysis probe of concentric design. The magnified membrane region illustrates the diffusion of an analyte of interest from the perfusate (○) into the medium during retrodialysis (white arrow) or the diffusion of the analyte from the sampling solution (▲) into the probe and taken with the perfusate during extraction efficiency (dark arrow) methods of probe calibration (Source: http://en.wikipedia.org/wiki/File:Schematic_illustration_of_a_microdialysis_probe.png, accessed May 15, 2011).

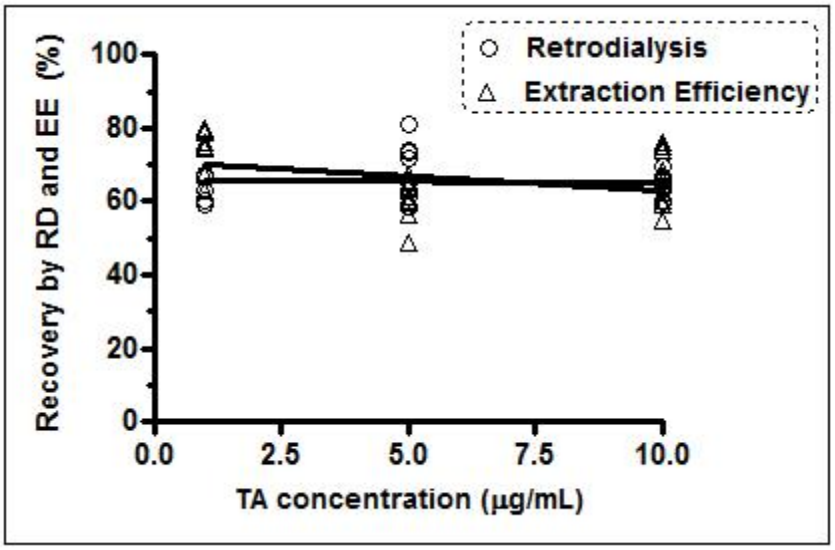

Figure 3-2. Dependence of relative recovery on concentration of TA in perfusate or medium during retrodialysis or extraction efficiency methods. Flow rate of 1.5 µL/min. Linear regression lines: y_{RD}= -0.056x + 65.9 and y_{EE}= -0.800*x* + 71.1.Three replicates for 3 different probes are shown.

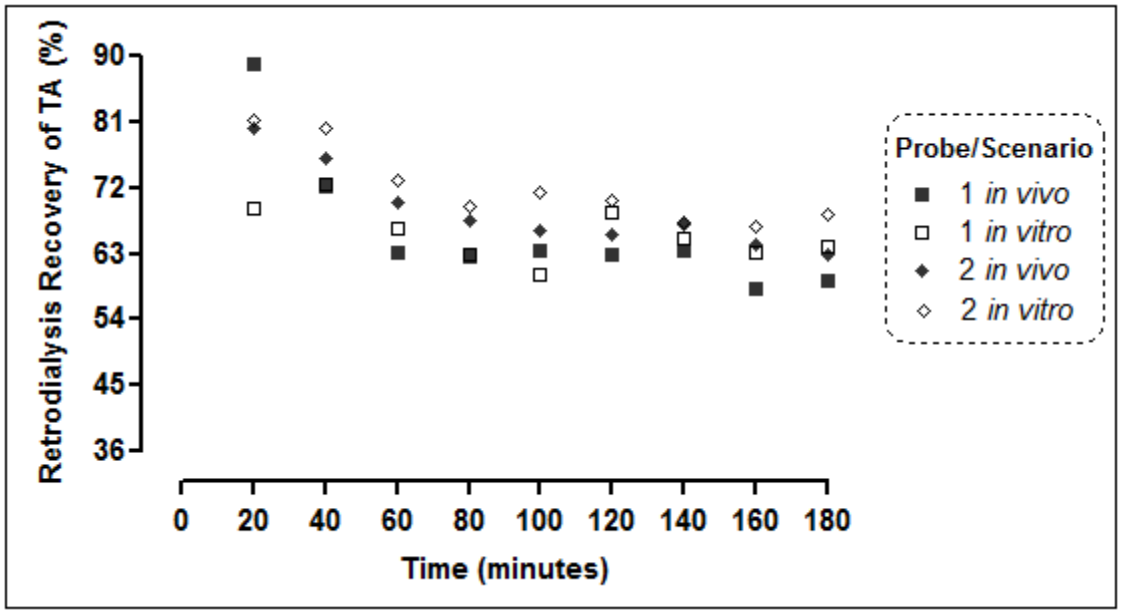

Figure 3-3. The *in vivo* and *in vitro* probe recoveries of TA for probes 1 and 2 by retrodialysis over time.

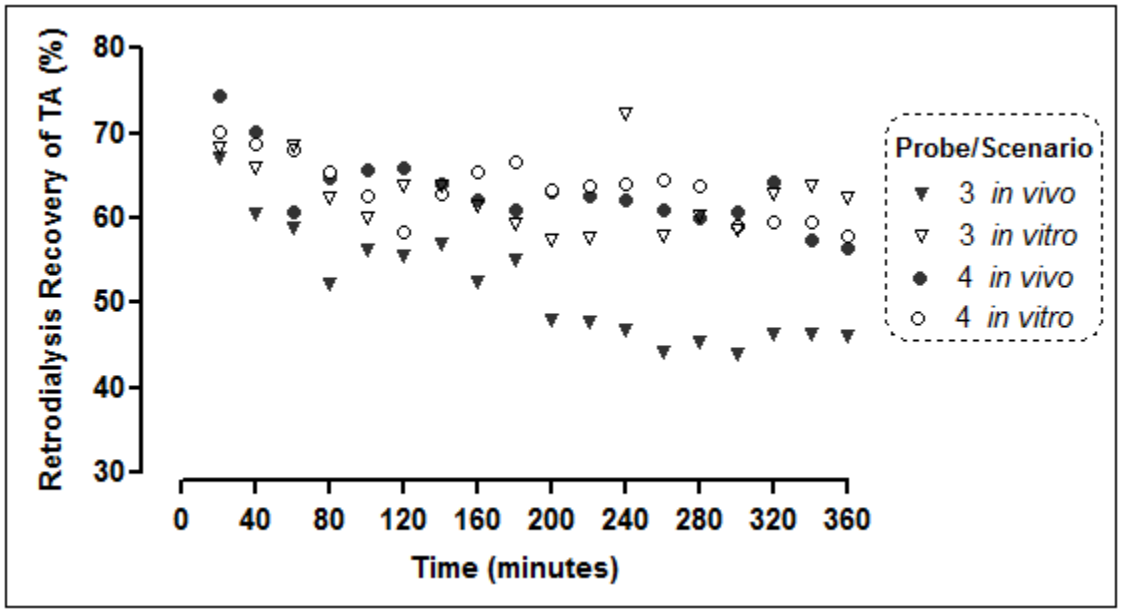

Figure 3-4. The *in vivo* and *in vitro* probe recoveries of TA for probes 3 and 4 by retrodialysis over time.

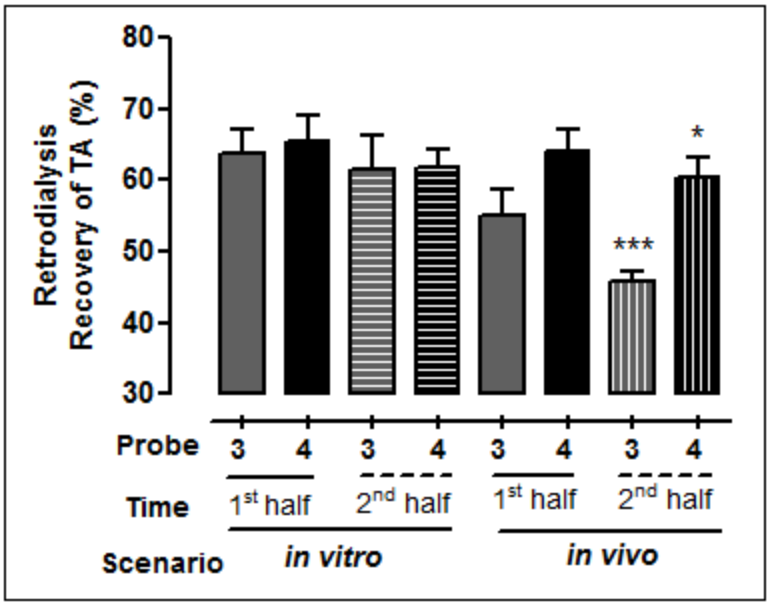

Figure 3-5. Dependence of the *in vivo* and *in vitro* recoveries of TA on time (1st half= 0-180 min and 2nd half= 181-360 min) for the microdialysis probes 3 and 4 using the retrodialysis method. Means ± SD of 9 determinations are shown. *P<0.05; ***P<0.001.

Table 3-1. Intra-day and inter-day accuracy (%RE) and precision (%CV) of observed TA concentrations in microdialysate quality controls during the three day-validation

Cnom	Validation day	Mean Cobs	SD	%RE	%CV
0.1	Intra-day (n=6)	0.096	0.005	-4.28	6.09
	Inter-day (n=18)	0.096	0.008	-4.33	8.85
0.25	Intra-day (n=6)	0.271	0.008	8.71	2.90
	Inter-day (n=18)	0.278	0.010	11.51	3.49
1	Intra-day (n=6)	1.01	0.06	0.97	5.84
	Inter-day (n=18)	1.00	0.05	0.78	4.90
5	Intra-day (n=6)	4.95	0.13	-1.05	2.53
	Inter-day (n=18)	4.97	0.18	-0.58	3.66

Cnom= Nominal concentration (µg/mL) and Cobs= Observed concentration (µg/mL)

Table 3-2. Comparison of the *in vitro* microdialysis recoveries (%R) of TA by the retrodialysis and extraction efficiency methods

Cnom (µg/mL)	Retrodialysis				Extraction Efficiency			
	Mean %R	SD	%CV	Range	Mean %R	SD	%CV	Range
1	63.8	3.7	5.75	59.0- 67.1	74.3	5.8	7.76	62.9- 80.1
5	68.1	7.2	10.5	58.7- 80.8	59.8	5.1	8.47	48.9- 67.1
10	64.3	3.2	5.06	59.5- 69.7	66.3	7.7	11.5	54.9- 76.2
Overall	65.5	5.3	8.14	58.7- 80.8	66.8	8.5	12.8	48.9- 80.1

Cnom=Nominal concentration

Table 3-3. *In vivo* microdialysis recovery (%R) of TA by the retrodialysis method

Probe	*In vivo* Retrodialysis of TA				
	n	Mean %R	SD	%CV	Range [Min-Max]
1	9	62.3	2.3	3.75	58.2 - 65.3
2	9	64.0	5.1	8.01	53.1 - 69.9
3	17	50.8	5.5	10.8	44.1 - 60.5
4	17	62.4	3.3	5.24	70.0 - 56.4
Overall		59.9	6.1	10.2	44.1 - 70.0

Table 3-4. *In vitro* microdialysis recovery (%R) of TA by the retrodialysis method

Probe	*In vitro* Retrodialysis of TA				
	n	Mean %R	SD	%CV	Range [Min-Max]
1	12	65.0	4.2	6.50	57.0 - 72.6
2	12	70.8	5.1	7.21	66.3 - 81.4
3	18	62.6	4.1	6.59	57.5 - 72.4
4	18	63.6	3.6	5.68	57.9 - 67.0
Overall		65.5	3.2	4.88	55.5 - 81.4

CHAPTER 4
INVESTIGATION OF BUDESONIDE AS A MICRODIALYSIS CALIBRATOR

Background

The shortcoming of retrodialysis for probe calibration is that variations of the recovery during the experiment are not monitored. Changes in the probe membrane and/or its microenvironment may occur during the study resulting in reduction of probe efficiency with time. In fact, several intravenous MD preclinical studies reported reduction of probe efficiency with time [58,60,71,101,102]. Possible causes are alterations in blood flow due to local vasoconstriction and/or mechanical disturbances which can reduce membrane permeability like molecules and/or cell deposition on the surface of the membrane [60,71]. This drawback can be overcome by using a continuous internal recovery control as first introduced for brain microdialysis [32] and further applied in blood microdialysis studies [16,59,103].

The microdialysis calibration standard is added to the perfusate during the experimental period and it is assumed that the relative recovery by loss of the calibrator into the investigated media is representative for the recovery by gain of the analyte from the media during the experiment [26]. An illustration of the retrodialysis by calibrator process is presented in Figure 4-1.

The ideal retrodialysis calibrator in microdialysis is the compound of interest itself. However, individual recovery estimates cannot be made with the drug of interest present in the perfusion solution when that drug is also administered systemically. A radiolabeled or deuterated analog of the drug may be a suitable choice for calibrator; however its availability is limited and requires also a more refined analytical detector such as mass spectrometer. Therefore, a compound similar to the drug of interest in

terms of its molecular size, degree of ionization and lipophilicity may serve as a calibrator [32,59].

To improve the accuracy of the estimated TA concentrations, we proposed to use the retrodialysis by calibrator method to monitor the recovery continuously and to correct for changes in TA recovery during the experimental period.

Budesonide, a corticosteroid with physicochemical properties (MW 430.54 g/mol, Log $P_{o:w}$ of 2.9, neutral at pH 7.4, protein binding 92% in rat) similar to our investigated compound TA (MW 434.50 g/mol, Log $P_{o:w}$ of 2.5, neutral at pH 7.4, protein binding 90% in rat) (Chemspider database, Royal Society of Chemistry, Cambridge, UK) was then chosen as a calibrator.

Specific Aim

The aim of this study was to verify the use of budesonide as a microdialysis calibrator for triamcinolone acetonide. The microdialysis probe recovery of budesonide was estimated *in vitro* as well as *in vivo* and correlated to TA.

Materials

Chemicals and Reagents

• 0.9% Sodium Chloride Inj. USP	Baxter Health Care (Deerfield, IL, USA)
• 1000 UI/mL Heparin	Elkins-Sinn, Inc. (Cherry Hill, NJ, USA)
• Budesonide	Sigma (St. Louis, MO, USA)
• HPLC grade methanol	Fischer Scientific (Fair Lawn, NJ, USA)
• Isoflurane USP	Webster Veterinary (Charlotte, NC, USA)
• Lactated Ringer's Injection USP	Baxter Health Care (Deerfield, IL, USA)
• Triamcinolone acetonide	Sigma (St. Louis, MO, USA)

Equipment and Disposables

• Balance	Mettler AE240, Toledo (Hightstown, NJ, USA)
• Cellulose membrane filter	0.22 µm pore size, Millex® GV Millipore (Carrigtwohill, Co. Co Cork, Ireland)

- FEP tubing — ID 0.12mm, CMA Microdialysis (Stockholm, Sweden)
- Heated stir plate — Fisherbrand Isotemp
- IV catheters — Monoject Angel Wing Butterfly, Becton Dickinson (Franklin Lakes,NJ, USA)
- Microdialysis probe — CMA/20 Elite, 14/10 PAES, cut-off 20kDa; membrane length 10 mm; CMA Microdialysis (Stockholm, Sweden)
- Microfraction collector — CMA/142, CMA Microdialysis (Stockholm, Sweden)
- Precision infusion pump — Harvard Apparatus Model 22, (South Natick, Mass., USA)
- Small animals surgery tools — Surgical Grade Stainless Steel, various suppliers
- Syringes — Becton Dickinson 5 mL (Franklin Lakes,NJ, USA)
- Thermometer — Fisherbrand 76mm Immersion 14-997
- Tubing adapter — CMA Microdialysis (Stockholm, Sweden)
- Vortex — Kraft Apparatus Inc., model PV-5, Fisher Scientific

Animals

Adult male Sprague-Dawley rats, weighting 250-300 grams, were purchased from Harlan Sprague-Dawley Inc. (Indianapolis, IN, USA). Animals were acclimatized to standard ACS housing in a 12-h light-dark cycle and constant temperature environment for a minimum of three days before being used. Animals had free access to food and water. The animal experimental procedures were approved by the Institutional Animal Care and Use Committee of University of Florida.

Methods

Preparation of Calibration Solutions for Microdialysis

Stock solutions of 1 mg/mL of TA and budesonide in methanol were prepared. From the stock solutions, 100 µg/mL solutions of each analyte were obtained by dilution in lactated Ringer's solution. Further dilutions in lactated Ringer's solution were performed to obtain the calibration solutions of TA in the concentrations of 1, 5 and 10 µg/mL and budesonide, 10 µg/mL. A lactated Ringer's solution containing both TA (5 µg/mL) and budesonide (10 µg/mL) was also prepared.

In vitro Microdialysis

Apparatus setup

During setup, a 5 mL syringe was filled with perfusate (analyte solution) and the enclosed air was cleared from the syringe. The syringe was placed on the precision pump, connected to the inlet of the probe and run at a flow rate of 1.5 µL/min for 30 minutes to allow for equilibration. The microdialysis probe was immersed in a 10mL centrifuge tube containing approximately 8 mL of either blank lactated Ringer's solution or analyte solution, depending on the experimental design. The sampling solution was stirred at 300 rpm to guarantee equal concentrations throughout the whole tube and temperature was controlled at 37 ± 1°C on a heated plate. The microdialysate samples were collected with the aid of an automated microfraction collector.

Extraction efficiency of TA and retrodialysis of budesonide at a constant flow rate

The *in vitro* microdialysis probe recovery of budesonide was determined by retrodialysis (RD), while triamcinolone acetonide recovery was estimated by the extraction efficient (EE) method of probe calibration in a dose-range fashion. The

scenario of recovery by loss of calibrator and by gain of drug emulates the condition of the main IV microdialysis study (Chapter 5).

MD probe was perfused with budesonide solution (10 µg/mL) at a constant flow rate of 1.5 µL/min and placed into the sampling tube containing TA solution, starting with the lowest concentration (1 µg/mL). TA diffused from the sampling solution into the MD probe and was taken with the perfusion flow. Budesonide diffused out of the probe into the solution. The gain of TA and the loss of budesonide through the membrane were then determined from the respective concentrations of each analyte in the microdialysate samples ($C_{TA\ dialysate}$ and $C_{bud\ dialysate}$). Three microdialysate samples were collected with 20 minutes intervals after the end of a 30 minutes equilibration period. To determine the actual TA and budesonide concentrations in the sampling ($C_{TA\ sampling\ sol}$) and perfusion ($C_{bud\ perfusate}$) solutions respectively, two samples of the each solution were taken, one before the sampling period and one after. The same procedure was done for the remaining two sampling solutions of TA, 5 and 10 µg/mL. The concentrations of the analytes in the samples were determined by a validated HPLC method. The experiments were performed using two different microdialysis probes. The percent recovery (%R) for each analyte was calculated as follows:

$$\%R_{TA} = \frac{C_{TA\ dialysate}}{C_{TA\ sampling\ sol}} \times 100$$

$$\%R_{Budesonide} = \frac{(C_{bud\_perfusate} - C_{bud\ dialysate})}{C_{bud\ perfusate}} \times 100$$

Extraction efficiency of TA and retrodialysis of budesonide at different flow rates

The MD probe was placed into the sampling tube containing TA solution (10 µg/mL). Then, the probe was perfused with budesonide solution (10 µg/mL) at each of 4 flow rates (1.5, 2, 2.5 and 3 µL/min). The gain of TA and the loss of budesonide through

the membrane were then determined from the respective concentrations of each analyte in the microdialysate samples ($C_{TA\ dialysate}$ and $C_{bud\ dialysate}$). Time was allowed for system equilibration when the flow rate was changed. At each flow rate, three microdialysate samples of 30 µL volume were collected using different sampling intervals (20, 15, 12 or 10 minutes for the respective ascending flow rates). To determine the actual TA and budesonide concentrations in the sampling ($C_{TA\ sampling\ sol}$) and perfusion ($C_{bud\ perfusate}$) solutions respectively, two samples of the each solution were taken, one before the sampling period and one after. The lowest flow rate, 1.5 µL/min, was evaluated first followed by the others with the exchange of sampling tube with fresh TA solution. The concentrations of the analytes in the samples were determined by a validated HPLC method. The experiments were performed using two different microdialysis probes. The percent recovery (%R) for each analyte at each flow rate was calculated as follows:

$$\%R_{TA} = \frac{C_{TA\ dialysate}}{C_{sampling\ sol}} \times 100$$

$$\%R_{budesonide} = \frac{(C_{perfusate} - C_{bud\ dialysate})}{C_{perfusate}} \times 100$$

In vitro retrodialysis of TA and budesonide

The MD probe was perfused with a solution of TA (5 µg/mL) and budesonide (10 µg/mL) in lactated Ringer's at a constant flow rate of 1.5 µL/min. The probe was placed into a tube filled with blank lactated Ringer's solution. Both analytes diffused out of the probe into the blank solution. The loss of the each analyte through the membrane was then determined from the $C_{dialysate}$. After the end of a 30 minutes equilibration period, microdialysate samples were collected with 20 minutes intervals during 3-6 hours. The actual concentration of the TA and budesonide in the perfusion solution were

determined by sampling the perfusate before and after the sampling period ($C_{TA\ perfusate}$ and $C_{bud\ perfusate}$). Experiments were performed using four different probes. The percent recovery (%R) for each analyte was calculated as follows:

$$\%R_{TA} = \frac{(C_{TA\_perfusate} - C_{TA\_dialysate})}{C_{TA\ perfusate}} \times 100$$

$$\%R_{budesonide} = \frac{(C_{bud\_perfusate} - C_{bud\_dialysate})}{C_{bud\ perfusate}} \times 100$$

Where %R is the percent recovery, $C_{perfusate}$ is the average analyte concentration in the perfusate before and after the experiment, and $C_{dialysate}$ is the analyte concentration in the microdialysate sample.

In vivo Microdialysis Calibration

In vivo retrodialysis of TA and budesonide

In vivo calibration was performed according to the procedure described in the section *in vivo* Microdialysis of Chapter 3. Briefly, the animals (n=5) were anesthetized with isoflurane and placed in a heating pad in the dorsal position. A microdialysis probe was placed into the right jugular vein with the aid of a needle and guide cannula. The probe was perfused with 10 UI heparin solution in Ringer's at 8 µL/min for 5 minutes.

After 5 minutes, the perfusate was changed to the calibration solution of triamcinolone acetonide (5 µg/mL) and budesonide (10 µg/mL) in lactated Ringer's. The flow rate was reduced to 1.5 µL/min. Following 1 hour equilibration, microdialysate samples were collected by the microfraction collector at 20 minutes intervals for 1-6 hours. At the beginning and end of the experiment, TA and budesonide concentration in the perfusate ($C_{perfusate}$) were determined by a validated HPLC method. The percent recovery (%R) for each analyte was calculated according to the equations:

$$\%R_{TA} = \frac{(C_{TA\ perfusate} - C_{TA\ dialysate})}{C_{TA\ perfusate}} \times 100$$

$$\%R_{budesonide} = \frac{(C_{Bud\ perfusate} - C_{Bud\ dialysate})}{C_{Bud\ perfusate}} \times 100$$

Where %R is the percent recovery, $C_{perfusate}$ is the average analyte concentration in the perfusate before and after the experiment, and $C_{dialysate}$ is the analyte concentration in the microdialysate sample.

Sample Analysis

TA and budesonide concentration in microdialysate samples and calibration solutions in lactated Ringer's solution were determined using the HPLC method described in Chapter 2.

Data Analysis

Linear regression and statistical analyses were performed using GraphPad Prism version 4.00 for Windows (GraphPad Software, San Diego, CA, USA). Group comparisons were made using analysis of variance. The significance level was set at 0.05.

Results and Discussion

In the present study the relative recovery of TA and budesonide and its correlation were estimated in a series of *in vitro* and *in vivo* microdialysis studies. In the first set of *in vitro* experiments, the *in vitro* relative recovery of TA was determined by the extraction efficient method (EE), while budesonide by the retrodialysis (RD) to mimic the proposed *in vivo* condition of the main study. The mean (percent of coefficient of variation) recovery of TA determined by EE was 66.3 (CV= 10.2%) while the average recovery of budesonide by retrodialysis was 77.4 (CV= 7.3%). The calculated ratio of TA:budesonide recovery is 0.86 (CV= 9.3%) (Table 4-1). Although both recoveries

differed significantly ($P < 0.05$), this, however, is not a hinder to the practical implementation of the proposed microdialysis calibration seeing that a steady correlation between the recovery of drug and calibrator is observed. This assumption is based on the recommendations for application of endogenous compounds (e.g. urea) as microdialysis calibrators [104,105].

Further analysis and experiments were performed to verify the stability of the recovery ratio of TA:budesonide ($RR_{TA:bud}$). Dependence of the $RR_{TA:bud}$ on the drug concentration is displayed in Figure 4-2. Linear regression analysis of *in vitro* $RR_{TA:bud}$ versus TA concentration in the surrounding medium yielded a regression line with a slope of -0.0018 (± 0.0082) and an intercept of 0.8495 (± 0.0534).The slope did not differ significantly from zero (95% CI: -0.1029 to 0.1064, α=0.05) allowing the conclusion that the recovery ratio is concentration independent over the range investigated. Concentration independence in pilot *in vitro* studies would indicate that the calibrator would correct the recovery of TA from the extracellular space *in vivo* in a linear fashion with a constant factor.

To investigate the stability of the correlation of the recoveries of TA and budesonide under influential factors that affect recovery, *in vitro* recoveries of both analytes were determined under different flow rates. Relative recoveries by gain (by EE method) and by loss (by RD method) are influenced by the perfusion fluid flow rate used with the inverse effect of flow rate on the relative recoveries, for both hydrophilic and lipophilic drugs [7,26,106]. Figure 4-3 A illustrates the relationship between recovery and flow rate. As flow rates were increased from 1.5 to 3 µL/min, the relative recovery by loss of calibrator budesonide reduced from approximately 78% to 53%. Likewise, the

recovery by gain of TA were decreased from around 66% to 41% over the ascending flow rate range (Table 4-2). A linear regression analysis was conducted (natural logarithm transformation of the recovery values versus flow rate) to verify the assumption of constant ratio under a recovery changing factor (Figure 4-3 B). Mean regression function of TA was $y = (0.3323 \pm 0.0645)x - (0.0420 \pm 0.1496)$, $r^2 = 0.9299$ (x= flow rate, y= TA recovery), while mean regression function of budesonide was $y = (0.2645 \pm 0.0320)x - (0.1342 \pm 0.0743)$, $r^2 = 0.9715$ (x= flow rate, y= budesonide recovery). The slopes were not significantly different ($\alpha = 0.05$) suggesting that the recovery of both compounds are affected in the same magnitude, hence the correlation of TA and budesonide recoveries (i.e. $RR_{TA:bud}$) would remain constant under circumstances that would affect the recovery of both TA and budesonide.

In the third set of *in vitro* experiments, the microdialysis probe recovery of budesonide and TA were determined by the retrodialysis method under constant flow rate (1.5 µL/min) for up to 6 hours to verify the steadiness of the $RR_{TA:bud}$ over time. The mean (± standard deviation) relative recovery of TA was 65.5 ± 3.2%, while the average recovery of budesonide was 78.6 ± 3.4% with a mean calculated $RR_{TA:bud}$ of 0.83 ±0.03. Results of four different probes are listed at Table 4-3. The recovery ratios of TA:budesonide obtained under recovery by loss of TA or recovery by gain of TA were not significantly different ($\alpha = 0.05$; $RR_{TA:bud}$ of 0.83 *vs* 0.86, respectively). Hence, the steadiness of correlation of the relative recoveries of TA and budesonide in *in vitro* settings was demonstrated.

It is recommended [107,108] that by proper calibration, intraindividual coefficients of variation for microdialysis measurements should range around 20%. Mean ratio of

recovery TA to budesonide ± 20% was defined as quality criterion for the interindividual and intraindividual precision of the retrodialysis by calibrator technique. Practicability of budesonide as a microdialysis calibrator could be assumed if 90% of all determined ratios were within this interval as previous suggested [108]. Figure 4-4 displays the individual recovery ratios of TA to budesonide for four different probes obtained by *in vitro* retrodialysis for up to 6 hours. The correlation of TA to budesonide recovery was satisfactorily constant over time with all intra- and inter-probe $RR_{TA:bud}$ well within ± 20% interval defined as quality criterion. The coefficient of variation of the recovery ratio of TA to budesonide within probes and overall are presented in Table 4-3.

As it is often the case, MD probe relative recovery determined in *in vitro* medium may not be a good surrogate for the *in vivo* recovery due to the complexity of the *in vivo* sampling matrix [32]. Thus, the recoveries of the analyte and the calibrator, and their correlation (Recovery Ratio analyte:calibrator), were subsequently determined in rodents. For five animals, the mean retrodialysis recoveries of TA and the calibrator budesonide were 59.0% (CV= 9.5%) and 84.9% (CV= 5.4%), respectively, with a mean *in vivo* ratio of recovery of TA to budesonide ($RR_{TA:bud}$) of 0.70. The overall $RR_{TA:bud}$ variability of five different probes was 9.0% (Table 4-4). Additionally, all intraindividual and interindividual $RR_{TA:bud}$ fell within the 20% precision interval, defined as quality criterion of recovery ratio. The individual recovery ratios of five probes over 1 to 6 hours dialysate collection are presented in Figure 4-5. The intraindividual RR_{TAbud} was fairly constant over time converse to the relative recovery of TA, as previous observed in our current investigation.

To improve the accuracy in the estimated concentrations by microdialysis, a recovery of the calibrator of 20% or higher is preferable for more reliable estimation [59]. In the current study, the *in vivo* recovery of the proposed calibrator, budesonide, far exceeded the 20% recovery threshold (overall retrodialysis recovery of 85% with CV of 5.4%).

In summary, we here presented a valuable characterization of the retrodialysis by calibrator technique under *in vitro* and *in vivo* conditions. Together, the data suggested that budesonide may be considered an appropriate calibrator for TA. Although the estimated recovery of the calibrator and the recovery of the test drug, TA, are significantly different in both *in vitro* and *in vivo* conditions, the average ratio of the recoveries were fairly constant under diverse tested scenarios, including over time *in vivo*.

In the subsequent experimental evaluation of the IV MD technique (Chapter 5), the *in vivo* probe recovery was monitored continuously using the retrodialysis by calibrator method.

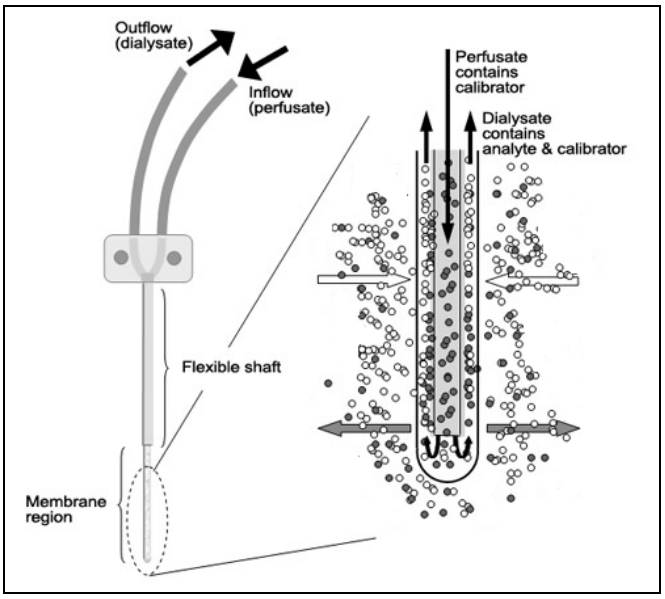

Figure 4-1. Schematic illustration of a flexible microdialysis probe of concentric design. The magnified membrane region illustrates net diffusion of an analyte of interest (○) into the probe (white arrow), and the diffusion of the calibrator (●) which has been added to the perfusate, from the probe to the sampling site (dark arrow). (Source: http://en.wikipedia.org/wiki/File:Schematic_illustration_of_a_microdialysis_probe.png, accessed May 15, 2011).

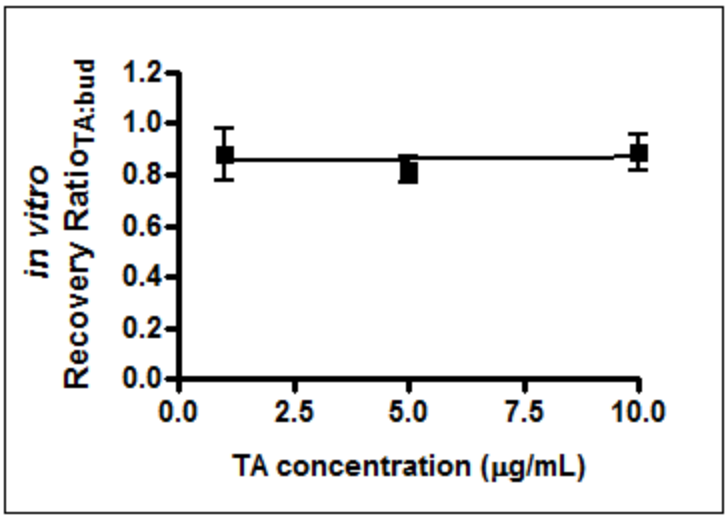

Figure 4-2. Dependence of relative recovery ratio TA to budesonide on concentration of TA in medium under constant flow rate (1.5 µL/min). Linear regression line: $y = -0.0018x + 0.8495$ (95% CI slope: -0.103 to 0.106). Means ± SD of 6 determinations of two probes are shown.

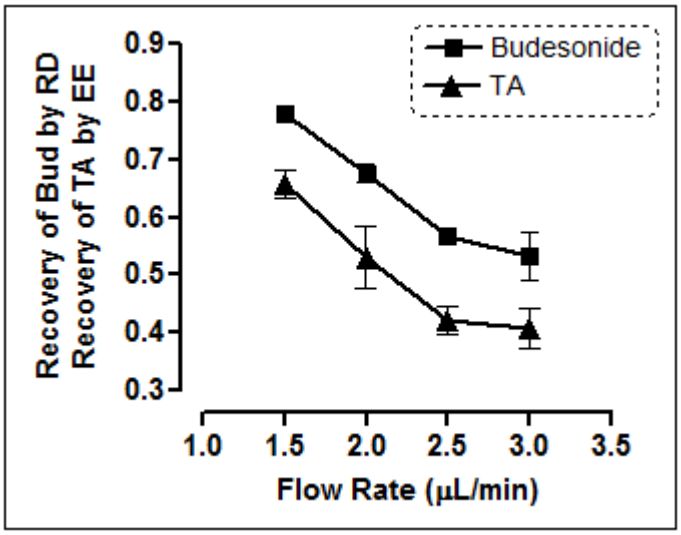

A

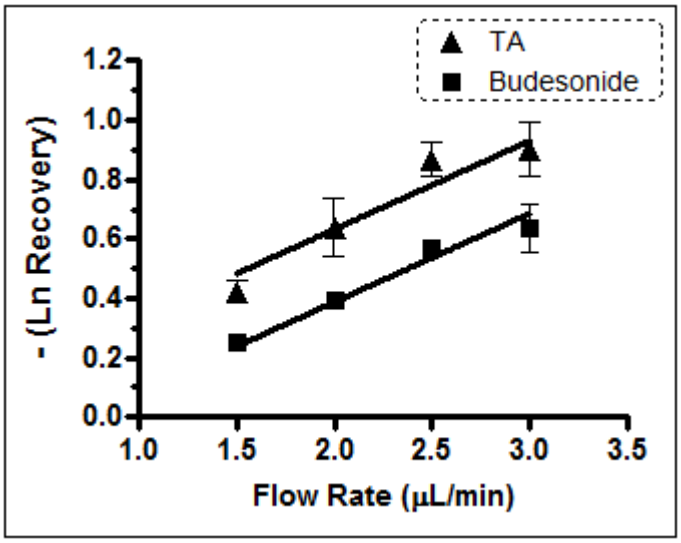

B

Figure 4-3. The effect of flow rate on recovery by gain of TA and by loss of budesonide during extraction efficient (EE) and retrodialysis (RD) calibration *in vitro*, respectively. A) Dependence of relative recovery on flow rate of perfusate. B) Linear relationship between the logarithmic transformation of recovery and flow rate. Linear regression lines: y_{TA}= 0.3323*x* - 0.0420 and $y_{budesonide}$= 0.2645*x* -0.1342. Means ± SD of 6 determinations of two probes are shown.

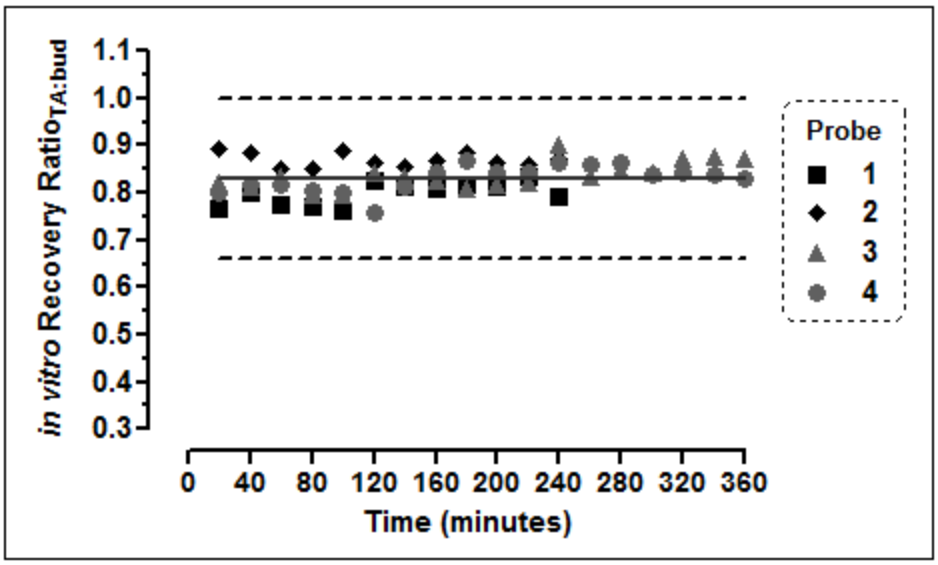

Figure 4-4. Individual recovery ratios of TA to budesonide for four probes obtained by *in vitro* retrodialysis over time. Line: Mean $RR_{TA:bud}$ =0.83; dotted lines: mean ratio ± 20%.

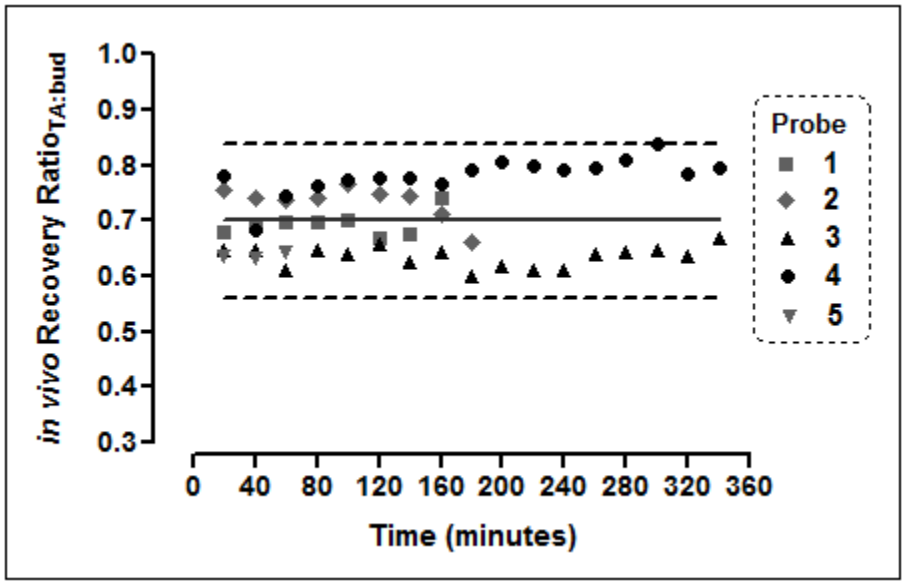

Figure 4-5. Individual recovery ratios of TA to budesonide for five probes obtained by *in vivo* retrodialysis over time. Line: Mean $RR_{TA:bud}$ =0.70; dotted lines: mean ratio ± 20%.

Table 4-1. Comparison of the *in vitro* recovery of TA versus budesonide at a constant flow rate (1.5 µL/min)

TA Cnom (µg/mL)	Extraction efficiency of TA			Retrodialysis of budesonide			Recovery Ratio TA:budesonide		
	Mean Recovery (%)	SD	%CV	Mean Recovery (%)	SD	%CV	Mean	SD	%CV
1	70.6	4.9	6.94	81.1	4.4	5.43	0.88	0.07	11.5
5	61.6	6.3	10.2	75.6	7.3	9.66	0.82	0.05	6.10
10	66.8	6.5	9.73	75.4	3.0	3.98	0.87	0.10	11.5
Overall	66.3	6.8	10.2	77.4	5.6	7.24	0.86	0.08	9.30

Cnom= Nominal concentration
Mean values: n=6 at each concentration using two different probes

Table 4-2. Comparison of the *in vitro* recovery of TA versus budesonide at different flow rates

Flow Rate (µL/min)	Extraction efficiency of TA			Retrodialysis of budesonide			Recovery Ratio TA:budesonide		
	Mean Recovery (%)	SD	%CV	Mean Recovery (%)	SD	%CV	Mean	SD	%CV
1.5	65.7	2.5	3.77	77.8	1.4	1.77	0.84	0.04	4.88
2	53.1	5.4	10.2	67.7	1.5	2.16	0.78	0.07	8.29
2.5	42.2	2.5	5.84	56.6	1.1	2.00	0.74	0.04	5.12
3	40.8	3.5	8.52	53.2	4.2	7.93	0.77	0.09	12.7
Overall							0.80	0.07	9.06

Mean values: n=6 recovery determinations at each flow rate using two different probes

Table 4-3. Comparison of *in vitro* recovery of TA versus budesonide by retrodialysis

Probe	Retrodialysis of TA			Retrodialysis of budesonide			Recovery Ratio TA:budesonide		
	Mean Recovery (%)	SD	% CV	Mean Recovery (%)	SD	%CV	Mean	SD	%CV
1 (n=12)	65.0	4.2	6.46	81.5	5.4	6.63	0.80	0.03	3.75
2 (n=12)	70.8	5.1	7.20	81.4	5.2	6.39	0.87	0.02	2.30
3 (n=18)	62.6	4.1	6.54	74.8	4.5	6.01	0.84	0.03	3.57
4 (n=18)	63.6	3.6	5.66	76.6	5.0	6.53	0.83	0.03	3.61
Overall	65.5	3.2	4.89	78.6	3.4	4.33	0.83	0.03	3.61

n= microdialysate fractions collected for recovery determinations.

Table 4-4. Comparison of *in vivo* recovery of TA versus budesonide by retrodialysis

Probe	Retrodialysis of TA			Retrodialysis of budesonide			Recovery Ratio TA:budesonide		
	Mean Recovery (%)	SD	%CV	Mean Recovery (%)	SD	%CV	Mean	SD	%CV
1 (n=9)	62.3	2.3	3.69	89.7	2.0	2.23	0.69	0.02	2.90
2 (n=9)	64.0	5.1	7.97	87.0	4.1	4.71	0.73	0.03	4.11
3 (n=18)	50.8	5.5	10.8	79.9	8.0	10.0	0.64	0.02	3.13
4 (n=18)	62.4	3.3	5.29	80.1	5.6	6.99	0.78	0.03	3.85
5 (n=3)	55.8	1.4	2.51	87.6	3.0	3.42	0.64	0.01	1.56
Overall	59.0	5.6	9.49	84.9	4.6	5.41	0.70	0.06	8.57

n= microdialysate fractions collected for recovery determinations.

CHAPTER 5
INTRAVENOUS MICRODIALYSIS STUDY OF TA

Background

When compared to traditional blood sampling methods, IV MD provides a powerful tool to continuously monitor the extracellular free drug concentration in the blood. The advantageous no net-fluid loss of the IV MD technique results in rich data collection while sparing the animals. In addition, it does not alter the drug's PK due to physiological changes that result from blood sampling [6]. Several reports have been published describing the successful application of IV MD sampling in rodents and man and at the same time addressing the current limitations of the technique, such as a possible time-dependent change in recovery [58,71]. While most IV MD studies used hydrophilic and low-protein binding drugs, in this work we aim to evaluate the application of the technique for a moderately lipophilic and high-protein binding compound.

The present intravenous microdialysis study will be conducted to measure the protein-unbound TA concentrations in the blood, following continuous intravenous drug infusion in rats. The free drug levels will be compared to total plasma concentrations obtained by traditional blood sampling. To account for changes in the relative recovery, continuous use of retrodialysis by the calibrator budesonide was introduced. Since microdialysis samples the unbound fraction, the extent of binding of the drug to plasma proteins must be known to compare the microdialysis results to those from blood. The extent of binding of TA to rat plasma proteins will be determined by the gold-standard method, ultrafiltration.

Specific Aim

The aim of this study is to evaluate the accuracy of the IV MD sampling technique on the estimation of unbound triamcinolone acetonide levels compared to the total concentrations, corrected for protein binding, obtained by conventional sampling. The performance of two calibration methods, retrodialysis by drug or by calibrator was also assessed.

Materials

Chemicals and Reagents

• 0.9% Sodium chloride inj. USP	Baxter Health Care (Deerfield, IL, USA)
• 1000 UI/mL Heparin	Elkins-Sinn, Inc. (Cherry Hill, NJ, USA)
• Blank male rat plasma	Lampire Biological Lab. (Pipersville, PA, USA)
• Budesonide	Sigma (St. Louis, MO, USA)
• HPLC grade methanol	Fischer Scientific (Fair Lawn, NJ, USA)
• Isoflurane USP	Webster Veterinary (Charlotte, NC, USA)
• Lactated Ringer's injection USP	Baxter (Deerfield, IL, USA)
• Triamcinolone acetonide	Purity ≥99%, Sigma (St. Louis, MO, USA)
• Volon® A soluble injection	Triamcinolone acetonide dihydrogenphosphate dipotassium salt, Dermapharm, Germany)

Equipment and Disposables

• Balance	Mettler AE240, Toledo (Hightstown, NJ, USA)
• Cellulose membrane filter	0.22 µm pore size, Millex® GV Millipore (Carrigtwohill, Co. Co Cork, Ireland)
• Centrifugal filter device	Ultrafree®-MC, 30,000 NMWL, Millipore Amicon (Bedford, MA, USA)
• Centrifuge	Fisher Scientific model Marathon 16KM (Pittsburgh, PA, USA)

• FEP tubing	ID 0.12 mm, CMA Microdialysis (Stockholm, Sweden)
• IV catheters	Monoject Angel Wing Butterfly, Becton Dickinson (Franklin Lakes,NJ, USA)
• Microdialysis probe	CMA/20 Elite, 14/10 PAES, cut-off 20kDa; membrane length 10 mm; CMA Microdialysis (Stockholm, Sweden)
• Microfraction collector	CMA/142, CMA Microdialysis (Stockholm, Sweden)
• Precision infusion pump	Harvard Apparatus Model 22, (South Natick, Mass., USA)
• Small animals surgery tools	Surgical grade stainless steel, various suppliers
• Syringes	Becton Dickinson 1, 5 and 10 mL (Franklin Lakes,NJ, USA)
• Thermometer	Fisherbrand 76 mm Immersion 14-997
• Tubing adapter	CMA Microdialysis (Stockholm, Sweden)
• Ultrasonic bath	Fisher Scientific model FS110H (Pittsburgh, PA, USA)
• Vortex	Kraft Apparatus Inc., model PV-5, Fisher Scientific

Animals

Adult male Sprague-Dawley rats, weighting 250-300 grams, were purchased from Harlan Sprague-Dawley Inc. (Indianapolis, IN, USA). Animals were housed to 12-h light-dark cycle and at constant temperature for a minimum of three days before being used with free access to food and water. In the experiment, the rats were weighted before the surgical procedure for dose adjustment based on weight. The animals were numbered in the sequence of the experiments without identifying devices (non-survival surgical

experiment). The experimental procedures were approved by the Institutional Animal Care and Use Committee of University of Florida.

Methods

Ultrafiltration

Preparation of stock and working solutions

Primary stock solutions of TA (1 mg/mL) and fluticasone propionate (plasma internal standard, IS) (1 mg/mL) were prepared in methanol. Each stock solution was further diluted in methanol to get intermediate concentrations of 100 µg/mL for TA and 75 µg/mL for IS.

Working solutions of TA (1.5- 150 µg/mL) required for spiking plasma and lactated Ringer's solution were subsequently diluted in methanol from primary and intermediate stock solutions. All methanolic solutions were stored at -20 °C, protected from the light, until use.

Preparation of samples

Pooled blank rat plasma was spiked with TA standard solutions of different concentrations to obtain total concentrations of 2.5, 5 and 10 µg/mL to cover the expected concentration range in the *in vivo* experiments. The same concentrations were also prepared in lactated Ringer's solution.

Blank plasma ultrafiltrate was obtained by centrifugation of pooled blank rat plasma in ultrafiltration units at 4000 rpm for 15 min. The procedure was performed with multiple samples to generate enough matrix volume. The calibration standards and quality controls were prepared in ultrafiltrate, lactated Ringer's solution and plasma, respectively. Calibration curves were constructed over the appropriate analytical range for each matrix.

Sample processing

A 0.6 mL sample volume at each concentration was incubated at 37°C for 30 minutes to allow for equilibration. A 140 µL aliquot of plasma was then taken to assess total TA concentration ($C_{plasma\ total}$). The remaining volume was transferred to an ultrafiltration device and centrifuged at 4000 rpm for 2 minutes. Less than 10% of the total volume was filtered to prevent disturbance of the protein binding equilibrium. Experiments were performed in triplicate for each concentration.

Samples of TA in lactated Ringer's solution, at the concentrations of 2.5, 5 and 10 µg/mL were submitted to the steps described above to assess the binding of the analyte to the membrane of the ultrafiltration device.

Sample analysis

The ultrafiltrate samples and plasma samples after 30 minutes incubation were analyzed by the HPLC method described in Chapter 2. The concentrations of ultrafiltrate samples ($C_{ultrafiltrate}$) represent the unbound concentrations of TA in plasma. The concentrations of plasma samples represent the total plasma concentrations ($C_{plasma\ total}$). The concentrations in the ultrafiltrate from lactated Ringer's solution were compared to the concentrations on the initial solutions and expressed in terms of percent recovery.

The calibration standards and quality controls were prepared in ultrafiltrate, lactated Ringer's solution and plasma, respectively. All samples were analyzed by the HPLC method described in Chapter 2. Briefly, the plasma samples were pre-treated by solid-phase extraction before injection and the ultrafiltrate samples were directly injected into the analytical column of the HPLC system for analysis.

Data analysis

As the total drug concentration equals the sum of the concentrations bound and unbound, the unbound fraction (f_u) of TA in rat plasma is calculated as:

$$f_u = \frac{C_{ultrafiltrate}}{C_{plasma\ total}}$$

***In vivo* Microdialysis Recovery**

Microdialysis probe recovery *in vivo* was estimated in each animal by retrodialysis during all experimental procedure, utilizing budesonide as a retrodialysis calibrator.

In vivo calibration was performed according to the procedure described in details in the section *in vivo* Microdialysis of Chapter 3. Briefly, the animals (n=5) were anesthetized with the inhalation anesthetic isoflurane and placed in a heating pad in the dorsal position. A microdialysis probe was placed into the right jugular vein with the aid of a needle and guide cannula. The probe was perfused with 10 UI heparin solution in Ringer's at 8 µL/min for 5 minutes.

After 5 minutes, the perfusate was changed to the calibration solution of budesonide (10 µg/mL) in lactated Ringer's. The flow rate was reduced to 1.5 µL/min. Blanks were collected for at least 1 hour following insertion of the probe. After equilibration, microdialysate samples were collected using a microfraction collector at 20 minutes intervals for the whole experimental period (3 hours). At the beginning and end of the experiment, budesonide concentration in the perfusate ($C_{perfusate}$) was determined by a validated HPLC method. The percent relative recovery (%R) of budesonide for each dialysate fraction ($C_{bud\ dialysate\ i}$) was calculated as follows:

$$\%R_{budesonide\ i} = \frac{(C_{bud\ perfusate} - C_{bud\ dialysate\ i})}{C_{bud\ perfusate}} \times 100$$

where %R budesonide is budesonide probe recovery for the *i*th collection determined by retrodialysis, $C_{bud\ perfusate}$ is the average budesonide concentration in the perfusate before and after the experiment, and $C_{bud\ dialysate}$ is budesonide concentration in the dialysate for the *i*th collection.

Intravenous Microdialysis of TA

One hour following the surgical implantation of the microdialysis probe in the animal's right jugular vein and equilibration of the calibrator recovery, the phosphate salt of TA was administered as an intravenous bolus of 5 mg/kg followed by a 2.3 mg/kg/h continuous infusion at a rate of 1 mL/h via an i.v. catheter placed in the caudal ventral artery. The loading bolus dose (D) was determined by the product of the aimed total plasma concentration at steady-state (C_{ss}= 3 mg/L) and the volume of distribution of TA in rats after i.v. administration (V= 1.67 L/kg) as previously reported [109]

$$D= C_{ss} \times V$$

The continuous infusion rate (R_0) was calculated based on reported total body clearance after i.v. administration in rats (CL_{iv}) of 0.7 L/h/kg [109] as follows:

$$R_0= C_{ss} \times CL_{iv}$$

Intravenous microdialysis sampling was carried out for 3 hours after drug administration. Microdialysate samples ($C_{dialysate}$) were continuously collected every 20 minutes with the aid of an automated microfraction collector. Samples were stored at 4 °C and analyzed within 24 hours.

Venous blood samples were drawn at baseline (time zero) and after dose administration at the midpoint of the microdialysis sampling interval with correction for the microdialysis probe and outlet tubing dead volume in order to make dialysis samples and blood samples comparable in time [110]. Blood samples (300 µL) were collected in

tubes containing heparin via the lateral caudal veins and centrifuged at 3000 rpm for 8 minutes to separate plasma. Then, plasma samples were stored at -70 °C until assay.

Sample Analysis

TA and budesonide concentration in microdialysate samples and calibration solutions in lactated Ringer's solution were determined directly using the HPLC method described in Chapter 2. TA concentration in plasma samples were determined after plasma extraction and HPLC analysis using the methods described in Chapter 2. The concentration-response calibration curve for each matrix was obtained following each experiment.

Data Analysis

TA total plasma concentration-time profiles were fitted to a biexponential equation for intravenous data [70,92] by nonlinear regression using the program Scientist (Micromath, Salt Lake City, UT, USA). Measured concentrations of TA were fitted to the following equation:

$$C_t = A\, e^{(-\alpha t)} + B\, e^{(-\beta t)}$$

where C_t is the total TA plasma concentration, A and B are hybrid constants, α and β are the first-order rate constants of distribution and elimination, respectively.

The following pharmacokinetic parameters were then obtained from the best-fit coefficients and exponents: the intercompartmental rate constants k_{12} and k_{21}, the elimination rate constant from the central compartment (k_{10}), the terminal distribution and elimination half-lives ($t½_{\alpha}$ and $t½_{\beta}$, respectively), and the volume of distribution at steady-state (Vd_{ss}), using the respective equations:

$$k_{21} = \frac{A\,\beta + B\,\alpha}{A + B}$$

$$k_{10} = \frac{\alpha \times \beta}{k_{21}}$$

$$k_{12} = \alpha + \beta - k_{10} - k_{21}$$

$$t_{1/2\alpha} = \frac{0.693}{\alpha}$$

$$t_{1/2\beta} = \frac{0.693}{\beta}$$

$$Vd_{ss} = \frac{(1 + k_{12})}{k_{21}} \times \frac{D}{(A+B)}$$

The total body clearance of TA (CL) was calculated based on plasma level data:

$$CL = \frac{R_0}{C_{ss}}$$

where R_0 is the infusion rate and C_{ss} is the model predicted steady-state plasma concentration.

TA phosphate is almost completely and rapidly converted into TA [111], therefore this conversion could be neglected in the pharmacokinetic analysis as had been described before [70,92].

The unbound TA concentrations in plasma (C_u) determined by microdialysis were calculated using the microdialysis probe recovery for each collection interval using budesonide retrodialysis and the factor by each *in vivo* recovery of TA and budesonide are related as follows:

$$C_u = \frac{(C_{\text{TA dialysate } i} \times RR_{\text{TA:Bud}}) \times 100}{\%R_{\text{budesonide } i}}$$

where C_u is the calculated unbound TA concentration, $C_{\text{TA dialysate}\_i}$ is TA concentration in the dialysate for *i*th collection, $\%R_{\text{budesonide } i}$ is budesonide probe recovery for *i*th collection by retrodialysis, and $RR_{\text{TA:Bud}}$ is the recovery ratio of TA:Bud *in vivo.*

TA unbound plasma concentrations at steady-state obtained by IV MD were compared with plasma levels, corrected for protein binding, using a paired *t*-test.

Statistical analyses were performed by GraphPad Prism version 4.00 for Windows (GraphPad Software, San Diego, CA, USA) with the significance level set at 0.05. Unless otherwise stated, all data are expressed as means ± standard deviation.

Results and Discussion

Determination of Unbound Fraction of TA by Ultrafiltration

The results of protein binding of TA in presence of different drug concentrations in rat plasma are summarized in Table 5-1. The overall mean of unbound fraction of TA in rat plasma was 0.104 ± 0.011. The average plasma protein binding of TA was then calculated to be 89.6 ± 1.1%, which is consistent with values previously reported of 81% [112] and 90.1% [68]. The estimate values of protein binding remained relatively constant over plasma triamcinolone acetonide concentration range of 2.5-10 μg/mL, suggesting linear protein binding.

Nonspecific adsorption of TA to the ultrafiltration device was determined by ultrafiltration of TA in lactated Ringer's solution. The concentrations in the ultrafiltrate samples were compared to the concentrations on the initial solutions tested. The mean recovery was 98.7 ± 3.8% confirming no loss due to nonspecific binding.

Our results are in agreement with a previous study where TA protein binding in human plasma was independent of the tested concentration range and the drug showed no binding to the ultrafiltration device [69,70].

The mean free fraction value of 0.104 was used in subsequent comparisons of microdialysis and rat plasma samples.

In vivo Microdialysis Recovery

In the present study, the retrodialysis by calibrator is suggested to determine the unbound concentrations of TA. The *in vivo* probe recovery is monitored continuously during the time-frame of the experiment by the relative recovery of the calibrator, budesonide. The overall mean budesonide recovery determined by retrodialysis in rats during the 3-hour IV MD study of TA was 80.0 ± 4.0 (CV= 5.02%). This value was consistent with the one obtained during the validation phase *in vivo* study (Chapter 4), overall mean recovery of 84.9 ± 4.6 (CV= 5.40%).Table 5-2 lists the individual budesonide recovery of five rats treated with TA. In general, the intra- and inter-animal precisions of recovery were satisfactorily high as all coefficient of variation values were less than 10%. The highest variability in recovery was encountered for animal R8, probably as a consequence of the gradual decrease of probe recovery overtime. Budesonide recovery decreased from around 87% to 68% in the time-frame of the experiment (22% reduction). Likewise, animal R10 had approximately 15% time-dependent reduction in probe recovery in the 3-hour IV MD sampling. No considerable changes in *in vivo* probe recovery were observed for the remaining animals/probes. Nevertheless, the observed reduction of probe efficiency may not be of relevance in the current IV MD study as intra-probe variations of 20% are accepted under *in vivo* conditions [107].Yet, the calibrator is valuable as a quality control during the experiment.

Budesonide recovery determined by retrodialysis during the course of the IV MD experiment was used to back-estimate the recovery of TA. The overall mean TA recovery using retrodialysis by calibrator was 55.5 ± 2.8 (CV= 5.02%). The individual TA recoveries for each animal are listed in Table 5-2.

The performance of two retrodialysis methods, retrodialysis by drug and retrodialysis by calibrator, in estimating unbound plasma concentrations of TA from IV MD data was subsequent evaluated. The concentration-time profiles of TA were calculated from the microdialysate concentrations corrected (I) by the mean *in vivo* recovery of TA ($\%R_{TA}$= 59.0%) estimated by retrodialysis in Chapter 2 or (II) by the recovery of budesonide at each collection interval adjusted by the *in vivo* recovery ratio TA:budesonide ($RR_{TA:bud}$= 0.7).

Intravenous Microdialysis of TA

Total and unbound plasma concentration-time profiles of TA after constant rate infusion (5 mg/kg i.v. bolus + 2.3 mg/kg/h infusion) are shown in Figure 5-1. The mean total plasma concentration over a period of 180 min was 3.64 ± 0.74 µg/mL, and the measured microdialysate concentrations corrected for recovery by retrodialysis by calibrator was 0.343 ± 0.072 µg/mL. The total plasma concentrations were analyzed by a two-compartment body model with the pharmacokinetic model adequately fitted the concentration-time profile. Figure 5-2 shows two representative examples of individual curve fits. The evaluation of goodness of fit was done by the respective model selection criteria (MSC) and the coefficient of determination (CD). The MSC is a modified Akaike information criterion that allows comparison of the appropriateness of a model: the greater the value of the MSC, the better the fit. The results of the individual pharmacokinetic parameter estimates are shown in Table 5-3. TA has a considerable fast distribution of 13.7 min and a fairly short half-life of 76 min as determined by the compartmental analysis. These values are in agreement with literature where a distribution half-life of around 5 min [70] and elimination half-life of 115 [70] and 180 min [113] were reported after intravenous administration of TA phosphate in humans. The

model estimated mean clearance value of 10.8 mL/min/kg is also comparable to value of 11.2 mL/min/kg previously observed in rats after i.v administration [109].

As can be seen from Figure 5-1, the first TA concentration determined from microdialysis sampling was lower than expected after an i.v. bolus dose and infusion, as observed with the plasma total concentration. Similarly, other investigators also observed lower IV microdialysate concentration, corrected for the recovery, compared to the total plasma level at the first sampling point after a 5-min intravenous administration of theophylline in rats, during IV MD [60]. In fact, this behavior may be likely following i.v administration of drugs with fast distribution pharmacokinetics, such as TA and theophylline, as previously stated in a review of the microdialysis technique [53]. This possible drawback of IV MD sampling to characterize the systemic pharmacokinetics of a drug is related to the fact that the first analyte concentration is obtained at the midpoint of the first collection interval. Thus, if the intravenous pharmacokinetics of a drug with a rapid distribution into the peripheral tissues is studied, the first analyte concentration may only be obtained at 10 min (in case of a 20-min collection interval) following administration which may not give a very accurate description of the early distribution phase of the substance [53].

Since the purpose of the study was to evaluate the accuracy of the IV MD technique by comparison of the unbound concentrations obtained by microdialysis with the plasma levels from conventional blood sampling corrected for protein binding, concentration-time profiles at steady-state were investigated. Furthermore, under steady-state conditions, fluctuations in probe recovery can be better monitored and the performance of two alternative methods of *in vivo* MD calibration can also be compared.

The average unbound steady-state concentrations determined by intravenous microdialysis corrected for retrodialysis by drug and retrodialysis by calibrator were 0.310 ± 0.084 and 0.343 ± 0.072 μg/mL, respectively. The calculated unbound TA concentration in plasma corrected for protein binding was 0.378 ± 0.077 μg/mL, which is not significantly different to those determined by microdialysis sampling (α=0.05). The individual plasma concentrations of TA at steady-state are listed in Table 5-4.

The systemic clearance of TA was calculated based on plasma level as the ratio of the infusion rate (R_0) to the observed mean steady-state concentration (C_{ss}). The mean CL obtained from total plasma levels was 10.9 ± 2.2 mL/min/kg which was comparable to the model fitted CL (10.8 ± 2.0 mL/min/kg, Table 5-3). The mean CL values calculated from steady-state microdialysate concentrations, corrected for recovery using retrodialysis by drug or retrodialysis by calibrator, were found to be 13.9 ± 3.9 and12.0 ± 2.6 mL/min/kg, respectively. Both CL values were not significantly different (α=0.05) from the one obtained from conventional blood sampling.

The use of the retrodialysis by calibrator calibration method gave fairly comparable corrected unbound concentrations as the use of retrodialysis by drug. Therefore, an experimental design with calibrator is valuable for monitoring and if necessary compensating for changes in probe recovery over time. The errors introduced by an unaccounted fluctuation of the drug recovery propagate to some extent to overall variability in the estimated unbound concentrations, and ultimately pharmacokinetic parameters. In our current study, the coefficient of variation of the estimated CL from microdialysis sampling corrected by recovery by calibrator was 22%, whereas corrected by recovery by drug was 28%. If the recovery of the calibrator shows no significant trend

during the experiment, the estimated drug recovery using the retrodialysis by drug calibration method seems sufficient to use for the estimation of reliable unbound concentrations.

In conclusion, intravenous microdialysis is an accurate method to determine unbound concentrations of TA following drug infusion at steady-state. The microdialysis recovery of TA can be monitored using either retrodialysis by drug or retrodialysis by the calibrator budesonide. Intravenous microdialysis sampling appears to be a feasible approach for free drug monitoring of lipophilic and highly protein-bound drugs.

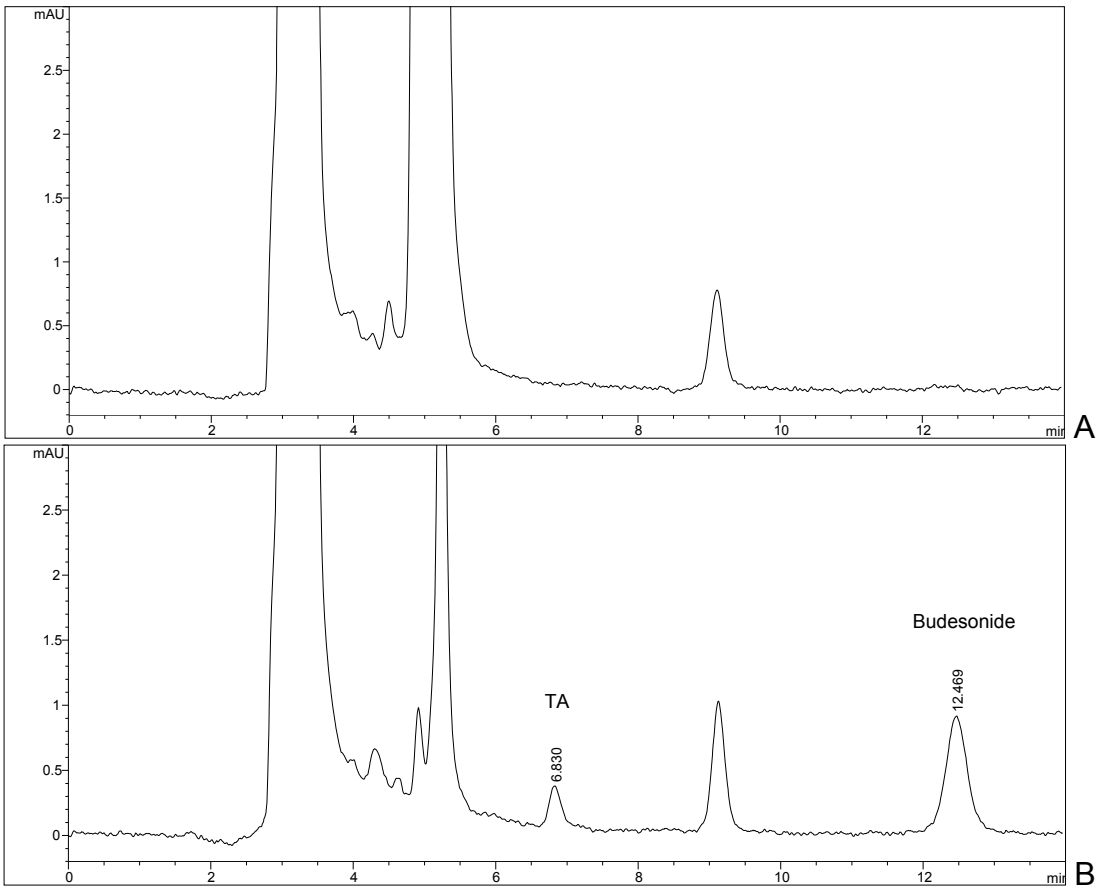

Figure 5-1. Representative chromatograms of IV MD samples. A) Blank microdialysate prior to dosing. B) Microdialysate sample containing the drug TA (0.24 µg/mL) and the calibrator budesonide (2.1 µg/mL) after i.v. infusion at steady state.

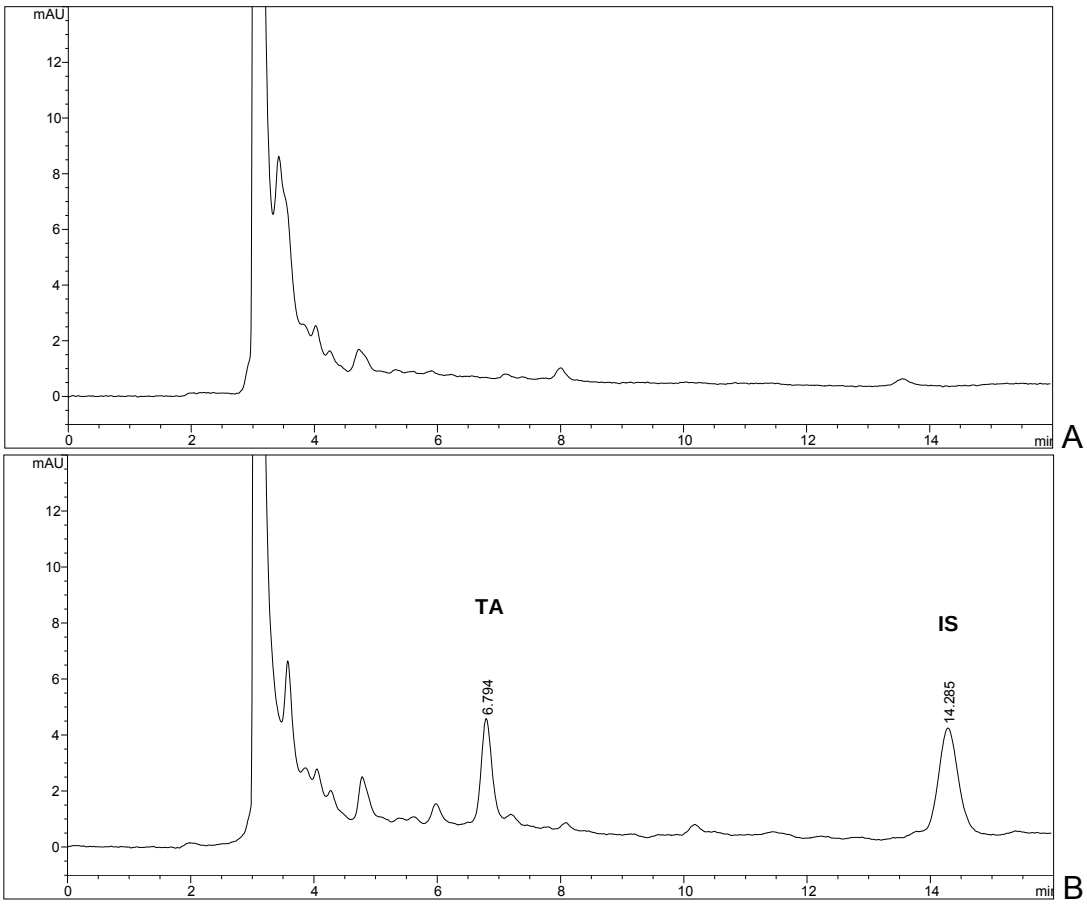

Figure 5-2. Representative chromatograms of rat plasma samples. A) Blank plasma prior to dosing. B) Plasma sample containing the drug TA (3.2 µg/mL) and the plasma internal standard (IS) after i.v infusion at steady state.

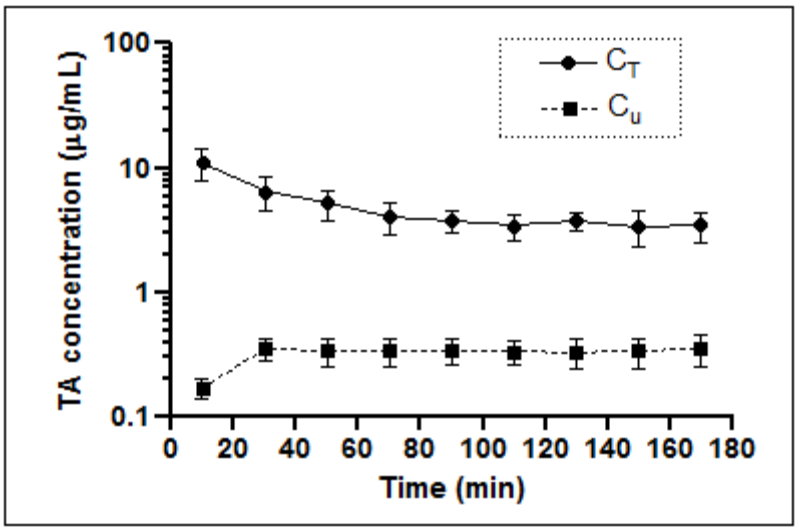

Figure 5-3. Plasma concentration time-profiles of TA in rats (n=5) after constant rate infusion (5 mg/kg bolus + 2.3 mg/kg/h). Means ± SD of total plasma concentration (C_T, ●) obtained by conventional blood sampling and unbound concentration (C_u, ■) obtained by IV MD technique corrected for recovery using the retrodialysis by calibrator method are shown.

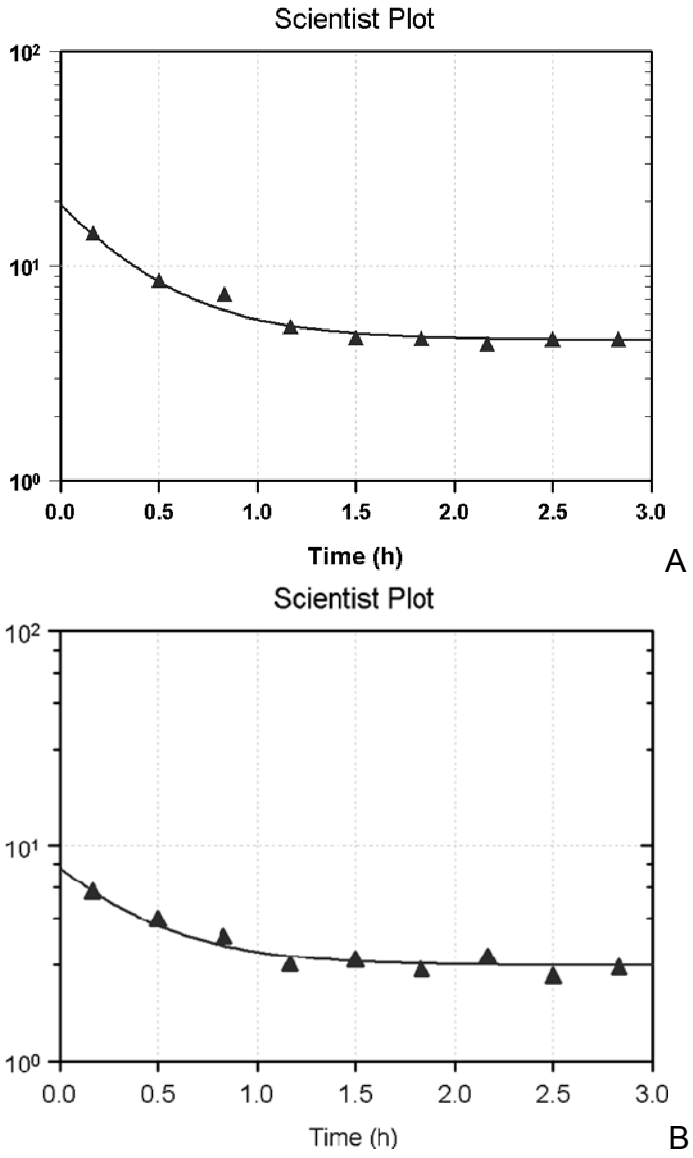

Figure 5-4. Concentration-time profiles of TA for two representative animals after constant rate infusion (5 mg/kg bolus + 2.3 mg/kg/h). A) Compartmental fitting of total plasma (▲) profile of animal R6 (coefficient of determination of 0.999 and MSC of 6.82). B) Compartmental fitting of total plasma (▲) profile of animal R10 (coefficient of determination of 0.958 and MSC of 2.28).

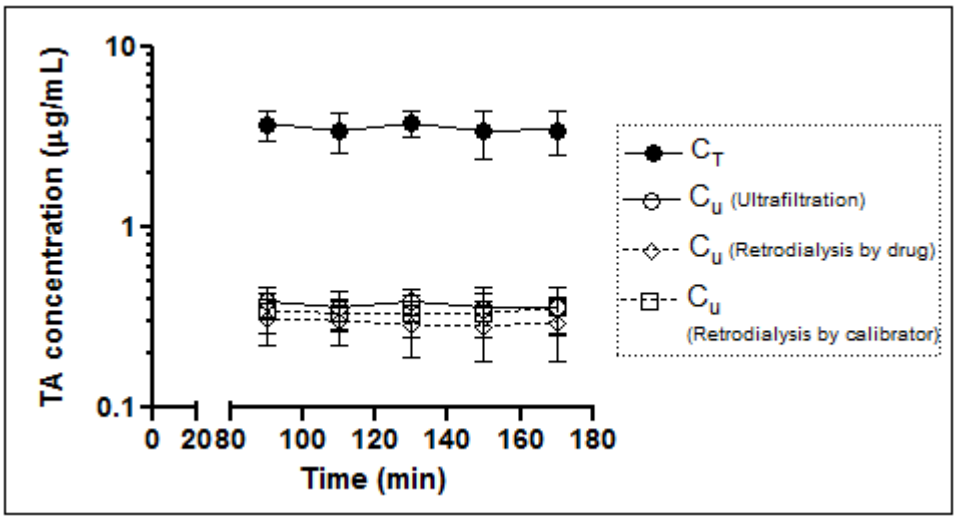

Figure 5-5. Steady-state plasma concentration time-profiles of TA in rats (n=5) after constant rate infusion (5 mg/kg bolus + 2.3 mg/kg/h). Means ± SD of total plasma concentration (C_T, ●) obtained by conventional sampling and unbound concentrations determined by ultrafiltration (C_u, ○), and obtained by IV MD sampling, corrected for recovery using the retrodialysis by drug (C_u, ◇) or retrodialysis by calibrator (C_u, □) methods are shown.

Table 5-1. Triamcinolone acetonide unbound fraction in rat plasma determined by ultrafiltration

Replicates/ Concentration (µg/mL)	2.5	5	10
1	0.092	0.114	0.104
2	0.103	0.116	0.096
3	0.094	0.122	0.099
Mean	0.096	0.117	0.099
SD	0.006	0.004	0.004

Table 5-2. *In vivo* recovery of budesonide and TA

Animal	Determined Recovery of budesonide by retrodialysis			Estimated Recovery of TA by retrodialysis by calibrator			Recovery
	Mean	SD	Range	Mean	SD	Range	%CV
R5	82.9	2.1	85.8-79.4	57.5	1.5	59.5-55.3	2.56
R6	83.2	2.8	86.9-80.5	57.7	2.0	61.4-56.5	3.39
R8	73.3	6.7	86.9-68.0	50.8	4.7	60.2-46.3	9.15
R9	80.3	1.3	81.8-78.6	55.7	0.9	54.8-56.8	1.59
R10	80.1	4.7	87.7-74.1	55.6	3.3	60.8-51.4	5.91
Overall	80.0	4.0	87.7-68.0	55.5	2.8	61.4-46.3	5.02

Mean of n= 9 dialysate fractions for each animal

Table 5-3. Individual pharmacokinetic parameter estimates of TA in rats after i.v. constant rate infusion

Parameter/ Animal	R5	R6	R8	R9	R10	Mean	SD
C_{ss} (µg/mL)	4.21	4.57	3.35	3.39	2.81	3.67	0.711
Vd_{ss} (mL/kg)	496	422	493	524	971	581	221
CL(mL/min/kg)	9.10	8.38	11.5	11.3	13.7	10.8	2.09
K_{21} (min^{-1})	0.008	0.013	0.015	0.017	0.015	0.014	0.003
K_{12} (min^{-1})	0.009	0.008	0.010	0.019	0.011	0.012	0.004
t ½ α (min)	14.1	15.2	13.4	9.54	16.3	13.7	2.59
t ½ β (min)	106.8	70.2	61.2	63.0	78.6	76.0	18.6

$C_{ss:}$ total plasma concentration at steady state; Vd_{ss}: volume of distribution at steady-state; CL: systemic clearance; K_{12} and K_{21}: intercompartmental rate constants; $t_{½α}$: distribution half-life; $t_{½β}$:elimination half-life.

Table 5-4. Individual steady-state plasma concentrations of TA, total ($C_{ss,T}$) and unbound ($C_{ss,u}$) determined by utrafiltration or IV MD corrected by the two methods of probe calibration, in rats after i.v. constant rate infusion

Animal	$C_{ss,\ T}$		$C_{ss,\ u}$ (corrected for f_u by ultrafiltration)		$C_{ss,\ u}$ IV MD (retrodialysis by drug)		$C_{ss,\ u}$ IV MD (retrodialysis by calibrator)	
	Mean	SD	Mean	SD	Mean	SD	Mean	SD
R5	4.29	0.11	0.446	0.012	0.357	0.022	0.388	0.014
R6	4.55	0.11	0.473	0.012	0.410	0.014	0.437	0.018
R8	3.22	0.12	0.335	0.013	0.221	0.025	0.301	0.048
R9	3.32	0.04	0.344	0.004	0.317	0.022	0.347	0.030
R10	2.81	0.23	0.292	0.024	0.221	0.012	0.251	0.008
Overall	3.64	0.75	0.378	0.077	0.310	0.084	0.343	0.072

Mean of n=5 determinations at steady-state

CHAPTER 6
UTILITY OF PBPK MODELING IN ADDRESSING NONLINEAR PHARMACOKINETICS AND DRUG INHIBITION MECHANISMS OF TELITHROMYCIN

Background

Telithromycin, an antibacterial agent of the ketolide class, is a CYP3A inhibitor *in vitro*. Inhibition *in vivo* has been demonstrated with a number of substrates cleared by CYP3A4. For example, telithromycin increased the area under the concentration-time curve (AUC) of CYP3A probe drugs simvastatin, midazolam and cisapride by 9-, 6-, and 2-fold, respectively [88]. According to the draft FDA drug-drug interaction guidance [114-116] telithromycin can be categorized as a strong CYP3A inhibitor *in vivo*. *In vitro* studies reported telithromycin inhibition of CYP3A4 activity via an apparent competitive mechanism with a reversible inhibition constant K_i of 58 μM [117,118]. In addition, there is no report to-date on the use of human *in vitro* data in predictive models to assess the interaction magnitude produced by telithromycin.

Telithromycin is also a substrate of CYP3A4 (Figure 6-1). Human absorption, distribution, metabolism and excretion (ADME) studies showed that the metabolic, renal and biliary/intestinal excretion clearance account for approximately 65%, 23% and 12% of the total drug clearance, respectively, after 400 mg i.v. infusion over 1.5 hr [88]. Based on *in vitro* data, it is estimated that around 50% of telithromycin metabolism is mediated by CYP3A4 and the remainder is CYP-independent [119]. Telithromycin is a substrate of the efflux transporter P-glycoprotein (P-gp) as well, as demonstrated in an *in vitro* Caco-2 cell transport study [120].

After an oral dosing of 800 mg telithromycin, the absorption into gut wall is estimated to be higher than 90% with an absolute bioavailability of 57% that considers impact of first-pass gut and liver metabolism [121]. Food does not affect its

bioavailability [122]. In addition, telithromycin displays nonlinear pharmacokinetics: doubling from 400 to 800 mg q.d. and from 800 to 1600 mg q.d. in both single- and multiple-dosing scenarios resulted in an increase of approximately 3-fold in exposure (a larger than dose proportional increase in AUC) [89]. Also, accumulation of telithromycin was observed after multiple doses with $AUC_{24,SS}$ (area under the plasma concentration-time curve from 0 to 24 hours at steady-state) exceeding the projections from single-dose kinetics ($AUC_{24,SD}$) by 1.4-fold (Accumulation ratio (R_{ac})= $AUC_{24,SS}/AUC_{24,SD}$) (Table 6-1) with an increase in the main (initial) elimination half-life by 20-30%. The R_{ac} value was independent of dose [89]. Independent compartmental PK analysis and simulations (WinNonlin Enterprise version 5.2, Pharsight, Sunnyvalle, CA) confirmed that accumulation was not to be expected after once-daily seven days of 800 mg dosing (R_{ac}=1.01). The deviation from dose proportionality and time- dependent kinetics of telithromycin have been attributed to a reduction in the metabolic clearance with increasing doses while the renal clearance remained unchanged [88,89] . The nonlinearity of telithromycin pharmacokinetics may be attributed to either saturation (metabolic enzymes and/or efflux transporters) and/or time-dependent enzyme inhibition.

Physiologically-based pharmacokinetic (PBPK) models have been increasingly applied in the drug research and development program as tools for predicting human pharmacokinetics and drug-drug interaction risks associated with the investigational drug [123]. By integrating system properties and drug-dependent parameters, a PBPK model has the advantage of evaluating the effect of multiple mechanisms that determine pharmacokinetics of an investigational drug.

Specific Aim

The purpose of this study is to apply PBPK modeling and simulation to predict the enzyme inhibition potential derived from the nonlinear pharmacokinetics of telithromycin. Specifically, a series of PBPK model for telithromycin were sequentially constructed using available *in vitro* metabolism and interaction data, and results from clinical pharmacokinetic studies to describe the nonlinear kinetics resulting from time-dependent inhibition (TDI) mechanism of CYP3A4. The model was used to predict the magnitude of drug-drug interaction of telithromycin with the CYP3A4 probe substrate, midazolam.

Methods

In the present study, PBPK modeling and simulations were carried out using the software SimCYP® Population-Based ADME Simulator (V10.10, SimCYP Ltd, Sheffield, UK) to take advantage of the sophistication of this particular software, such as the use of the dynamic estimates of *in vivo* concentrations of the precipitant drug, the accountability for inter-individual variability among the population and, in particular the CYP3A4 substrate midazolam PBPK compound profile.

Initial Model

A PBPK model for telithromycin both as a substrate and interacting drug of CYP3A4 was constructed within the software SimCYP®. Drug-dependent component comprises parameters necessary to describe the absorption, distribution, metabolism and excretion (ADME) (Figure 6-1) and the drug-drug interaction mechanisms. Data describing the physicochemical properties (molecular weight and pKa) and plasma protein binding of telithromycin (unbound plasma fraction, *f*u) were obtained from the literature (Table 6-2). The logarithm of the octanol-water partition coefficient (Log P)

value was obtained from the Chemspider database (Royal Society of Chemistry, Cambridge, UK). Human blood-to-plasma partition ratio (B/P) value was estimated (Parameter Estimation function within SimCYP®) using the mean plasma concentration-time data after intravenous administration (400 mg, 2.5 h infusion time) in healthy volunteers [121]. Initial estimate of B/P value is based on rodent data [124].

The volume of distribution at steady-state (V_{ss}) and values for the tissue-to-plasma partitioning of telithromycin into adipose, bone, brain, gut, heart, kidney, liver, lung, muscle, skin, and spleen were calculated *in silico* from the drug physicochemical properties, *f*u and the composition of the tissues using the equations developed by Rodgers and coworkers [125-127]. The Advanced Dissolution, Absorption and Metabolism (ADAM) model was used to predict the fraction absorbed (*f*a) and first order absorption rate constant (ka) from *in vitro* permeability data in Caco-2 cells (Table 6-2). Description of the differential equations and the parameter relationships within the software are described in details elsewhere [128-130]. Besides CYP3A4, telithromycin is also a substrate of the efflux transporter, P-glycoprotein (P-gp). The kinetic constants (K_m and V_{max}) of P-gp-mediated efflux of telithromycin *in vitro* were obtained from the literature [120]. Telithromycin clearance (CL) is comprised of hepatic, biliary and renal contributions (CL_H, CL_{Bile}, CL_R) as outlined in Figure 6-1. Hepatic intrinsic clearance ($CL_{u,int,H}$) at the enzyme level was back-calculated from systemic clearance values obtained from intravenous data [121] by retrograde calculation. The method employs the re-arranged well-stirred model equation [131] as follows:

$$CLu_{\text{int},H} = \frac{CL_{H,B} \times Q_{H,B}}{fu_B(Q_{H,B} - CL_H)}$$

where $Q_{H,B}$ is the hepatic blood flow (84.8 L/h), fu_B=fu/(B/P) is the fraction unbound in the blood (values were 0.3 and 0.7 for fu and B/P, respectively), and $CL_{H,B}$= CL_H/(B/P) is the hepatic metabolic clearance in blood (53.6 L/h) derived from $CL_{iv,B}$ (82.4 L/h) after subtraction of $CL_{R,B}$ and $CL_{Bile,B}$ (Table 6-1) . As net unbound hepatic intrinsic clearance ($CLu_{int,H}$) is the sum of all intrinsic clearances by all enzymatic and transporter pathways, the $CLu_{int,H}$ of CYP3A4 was calculated from the fractional metabolism of CYP3A (50% CL_H) reported from *in vitro* and *in vivo* results from a human mass balance study using an oral solution of telithromycin 800 mg [88]. The remaining hepatic metabolism (50% of CL_H) was assigned to the non-CYP pathway. An array of scaling factors for hepatocellularity was used, including different amount of microsomal protein per gram of liver, specific enzyme abundance, relative enzyme activity, and liver weight [83]. The maximum rate of metabolism of the enzyme CYP3A4 ($V_{max,CYP3A4}$) was calculated as follows:

$$V_{\max,CYP3A4} = CLu_{\text{int},CYP3A4} \times K_{m,CYP3A4}$$

assuming the same $K_{m,CYP3A4}$ as the reported $K_{i,CYP3A4}$ from *in vitro* inhibition study [118]. The value was corrected for the unbound fraction of the drug in microsomal incubation (fu_{mic}= 0.447) predicted *in silico* from compound lipophilicity and assumed microsomal protein concentration of 1 mg/mL. Defining clearance based on V_{max} and K_m enables us to evaluate potential dose-dependent non-linearity and saturation of clearance for larger doses as well as for multiple administrations.

The transporter-mediated intestinal/biliary excretion was incorporated in the model using the published Michaelis-Menten constant (K_m) for P-gp [120] and by retrograde calculation of maximum rate of transport (J_{max}, in pmol/min/million cells) from the *in vivo*

biliary clearance of 6.9 L/h (assuming average liver weight of 1600 g and 117.5 million cells/g liver)[132]. The initial model also incorporated a reversible $K_{i,CYP3A4}$ (25 μM after correction for nonspecific binding) allowing the simultaneous inhibition of CYP3A4. The roles of potential saturation of intestinal and hepatic CYP3A4 and/or P-gp on the drug nonlinearity were evaluated by simulations using the initial model.

Modified Model

Model building is a continuous exercise as more data are incorporated and further information on verifying the performance are obtained by contrasting the simulation outcome and observed data. Following the confirmation of negligible contribution of saturation in CYP3A4 and P-gp on the nonlinear PK observed *in vivo* (see Results section in relation to outcome of initial model), the model was further developed to investigate the contribution of auto-inhibition via time-dependent CYP3A4 inhibition mechanism to nonlinear pharmacokinetics of telithromycin (Table 6-1). The kinetic parameters describing TDI process are the inactivation rate constant k_{inact} (maximal inactivation rate at saturating concentration of the inhibitor), the potency of the inactivation (K_I, inhibitor concentration causing half- maximal inactivation) and the turnover rate of the enzyme *in vivo*, k_{deg} (first-order rate constant for degradation). Details of the enzyme mechanism-based inhibition process can be found in a previous report [133]. In the modified model, a much higher CYP3A4 contribution on the metabolic pathway of telithromycin should be considered to overcome the inactivation of this enzyme over the time course of drug administration following single dose. In other words, the observed contribution of 50% for metabolic elimination by CYP3A4 could be considered a time-averaged value where initial contribution was high, but it reduced as the active enzymes level went down due to TDI. Thus, to assign higher CYP3A4

metabolism, the V_{max} of CYP3A4 within the initial model (7.3 pmol/min/pmol of isoform) was increased by 2.66-, 4.00-, 4.66- or 5.33- folds, assuming that a higher intrinsic value of V_{max} becomes an apparent V_{max} in the presence of TDI. Under each new value of V_{max} (2.66-, 4.00-, 4.66 or 5.33-fold initial value), sensitivity analyses were conducted to determine the effect of a range of k_{inact} (range 1-10 hr^{-1}) and K_I (1-25 μM) values on the apparent oral clearance (Dose/AUC_{0-24h}) of a single oral dose of telithromycin (400, 800, or 1600 mg q.d. were tested). Three dimensional (3D) plots were generated for each V_{max} value with the concurring TDI over the 400-1600 mg SD range. Figure 6-2 shows two representative 3D plots of 2.66- and 4.66-fold increase in V_{max} of CYP3A4 within the range of K_I and k_{inact} values. As can be seen from the 3D plots, the increase in V_{max} with concurrent TDI led to an increase in Dose/AUC_{0-24h} in a dose-dependent manner. The pharmacokinetic profiles of telithromycin after seven days of therapy (400, 800 or 1600 mg q.d.) were simulated using different combinations of V_{max} and TDI parameter (K_I and k_{inact}) values to evaluate their effect on the clearance at steady-state (Dose/$AUC_{144-168h}$). The most plausible combinations of the three parameters (V_{max}, K_I and k_{inact} of CYP3A4) and resulting apparent oral clearance values predicted from simulations under ascending single and multiple doses were compared to the observed clearance reported in the NDA review [119] (Table 6-3). The values of K_I of 6 μM, k_{inact} of 10 h^{-1} and Vmax of 35 μM (4.66-fold of initial value from initial model) were selected as the most representative for the dose- and time-dependent PK of telithromycin. Simulations were performed using the software default values (V10.10) of the intrinsic turnover of CYP3A4, k_{deg} of 0.019 and 0.030 h^{-1} for liver [134] and gut [135], respectively.

Both the initial and the modified models were qualified by visually comparing simulated telithromycin plasma concentration-time profiles with mean plasma profiles and pharmacokinetic parameters from six clinical studies [89,136-140]. Mean plasma profile data from literature were digitized using GetData® Digitizer (Version 2.24). A detailed description of telithromycin PBPK model and parameters are illustrated in Figure 6-1 and listed in Table 6-2.

Simulations

Pharmacokinetic simulations were conducted using various clinical study conditions (10 trials of 10 subjects each, unless specified otherwise). Mean and distribution of demographic covariates (e.g. age, gender, body weight, body surface area, organ weight, and tissue composition) and drug parameters were generated using Monte-Carlo approach, under predefined study designs, within the PBPK software.

The effects of telithromycin on a concomitantly administered CYP3A4 substrate midazolam were evaluated using midazolam drug-dependent parameters compiled in the compound library of the PBPK software. DDI simulations were performed using both the initial and modified telithromycin models to compare the magnitude of drug-drug interaction via the reversible (competitive) and time-dependent mechanism of CYP3A4 inhibition.

The reported inhibition constant $K_{i\ CYP3A4}$ of 58 μM was evaluated after correction for the nonspecific microsomal binding. Two extremes of microsomal protein concentration in the *in vitro* incubations, representing the most likely and the unlikely scenarios, respectively, are 1 or 10 mg/mL microsomal protein. The *in silico* estimates of the unbound fraction of telithromycin (fu_{mic}) were 0.447 and 0.075, resulting in "unbound" K_i values of 25 and 4.3 μM, respectively. Both values were tested as

reversible inhibition inputs. The CYP3A4 TDI parameters incorporated in the modified telithromycin model were K_I of 6 μM and k_{inact} of 10 h^{-1} (Table 6-1).

Extra DDI simulations were performed using modified telithromycin PBPK model (with TDI mechanism) and midazolam model modified by adjusting the contribution of the CYP3A4 metabolism (fm_{CYP3A4}). CYP3A4 was assumed to be the only CYP3A isoform to accommodate the inhibition of this enzyme by telithromycin during PBPK simulation. As the SimCYP® default fm_{CYP3A4} for midazolam is 0.96, two other fm_{CYP3A4} values, 0.86 and 0.94, were tested in TDI prediction model. The fm_{CYP3A4} values of 0.86 and 0.94 were estimated from ketoconazole interaction after i.v. and oral administration of midazolam, respectively (University of Washington Metabolism and Transport Drug Interaction Database, Version 4.0).

All drug-drug interaction simulations were conducted using time-based simulations according to the trial design reported, including the dose regimen, number of subjects, age range and gender ratio in virtual healthy volunteer populations [119]. In this study, a single intravenous infusion (i.v.) or oral (p.o.) dose of midazolam was administered to male healthy volunteers (n=12) on day 5 after oral administration of telithromycin (800 mg q.d. for 6 days). Each trial was simulated 10 times to assess inter-study variability. Geometric mean of the ratios (both with and without an enzyme inhibitor under reversible or time-dependent mechanisms) of midazolam PK parameters were calculated and compared with the observed values.

Results

Prediction of Nonlinear Pharmacokinetics of Telithromycin

Using the initial PBPK model, the simulated pharmacokinetic profile was compared to observed data from healthy subjects after a single intravenous infusion (400 mg for

2.5 h) (Figure 6-3A) or single 800 mg oral dose (Figure 6-3B). The simulated intravenous pharmacokinetic profile reasonably described the observed data regarding the distribution and elimination phases (dotted line). The model also satisfactorily predicted the concentration-time profiles after single oral administration, suggesting the robustness of the model to reflect absorption characteristics of telithromycin.

To delineate the contribution of the P-gp efflux on the drug bioavailability and nonlinearity, simulations were performed under the conditions with and without the apical intestinal transporter in the initial model. Table 6-4 shows a comparison of the predicted parameters, C_{max}, AUC, fraction absorbed in the small intestine (*f*a jejunum), and apparent oral clearance (CL/F) across the doses of 400, 800 and 1600 mg SD under these different scenarios. The intestinal P-gp efflux pump showed minimal impact on the oral absorption of the drug as a consequence of the intrinsic high passive permeability of telithromycin (Papp: 21 x 10^{-6} cm/s) [120], its high oral dose level (gastro-intestinal luminal fluid concentration > 1 mM) and its apparent high affinity for P-gp (K_m of 9.8 μM) with low maximum rate of transport (Jmax value of 5 pmol/min) [120]. Figure 6-4A shows the transient saturation of the efflux clearance of P-gp in the apical membrane of the jejunum when a low dose was administered. Thus, the efflux transport would not likely contribute to the observed deviation of dose-proportionality.

The potential saturation of CYP3A4 elimination pathway was tested. Since the kinetic values of the enzymatic metabolism of telithromycin by CYP3A4 were unavailable, we assumed similar affinity for the enzyme as reported for the inhibition constant ($K_{m,\ CYP3A4}$ of 25 μM after correction for nonspecific microsomal binding). The initial model predicted apparent oral clearance of the doses 400, 800 and 1600 mg after

single dose administration were 116, 115 and 113 L/h, respectively; while after seven once-daily doses were 105, 104 and 102 L/h, respectively. The maximum predicted accumulation ratio (R_{ac} = $AUC_{24,ss}/AUC_{24}$) of 1.1 and AUC/dose ratio of 1.0 (across three doses) did not translate to the mean observed R_{ac} of 1.4 and AUC/dose ratio of 1.6 (Table 6-1), respectively [89]. The intestinal and hepatic intrinsic clearances of CYP3A4 showed transient saturation already at the lowest dose (400 mg, Figure 6-4B). Due to the uncertainty of the $K_{m,CYP3A4}$ value, the enzyme saturation was further tested using a much higher affinity for the enzyme by a 100-fold reduction of this value. The new $K_{m,CYP3A4}$ led to an additional reduction of the apparent oral clearance, 91, 84 and 80 L/h after single doses and 85, 79 and 74 L/h after multiple doses of 400, 800 and 1600 mg q.d., respectively. However the predicted decrease was modest and the decrease seems proportional with the ascending doses. Thus, the proposed CYP3A4 enzymatic saturation did not appear to be a plausible mechanism to the observed deviation from dose-proportionality and time-dependent kinetics of telithromycin (Table 6-1).

Based on the greater apparent oral clearance (Table 6-1) observed at 400 mg single dose as compared to higher doses, it was reasonably assumed in fact a higher intrinsic clearance of CYP3A4, and exposure/dose nonlinearity was caused by auto-inhibition of CYP3A4. The initial model was modified by optimizing CYP3A4 metabolism and auto-inhibition via time-dependent CYP3A4 inhibition. Sensitivity analyses were conducted to simultaneously evaluate the impact of the changes in the intrinsic clearance of CYP3A4 (ascending values of initial V_{max}), and in the parameters of TDI, K_I and k_{inact}, on telithromycin PK nonlinearity (Figure 6-2). The performance of the modified

model by incorporating the time-dependent CYP3A4 inhibition in predicting the steady-state kinetics of telithromycin after ascending doses compared to the initial model is illustrated in Figure 6-5. Previously published data [89] of once-daily administration at all three dose levels were collected to aid model modification. The corresponding pharmacokinetic profiles (solid line) using modified (with TDI) model are in fair agreement with the observed pharmacokinetic profile of telithromycin on day 1 and day 7; whereas the initial model (dotted line) under-predicts the dose-and time- dependent kinetics at all dose levels. Although the modified model still over-predict telithromycin exposure (higher predicted AUC compared to observed AUC) after multiple doses of 400 mg, optimizing CYP3A4 metabolism and incorporating TDI mechanism could reasonably reconcile the higher apparent oral clearance of the single-dose of 400 mg, as well as the dose- and time- dependency of clearance. The clinically observed, greater than expected accumulation was accurately estimated by the modified model (observed versus simulated mean R_{ac} of 1.4- and 1.4-fold, respectively). Likewise, the estimated mean deviation from dose-proportionality, AUC/dose ratio of 1.3, is in good agreement with the mean clinical value of 1.6 (81% accuracy) (Table 6-1). Figure 6-6 illustrates a comparison of the observed and simulated AUC as a function of dose by the initial and modified models. The initial model prediction of exposure/dose parallels the linear dose dependency; whereas the modified TDI model was in close agreement with the observed deviation from dose-proportionality. The significant difference of the amount of unchanged drug excreted renally (as % dose) across doses was also predicted by the modified model (Table 6-1). The effect of auto-inhibition via TDI on the clearance and oral bioavailability of telithromycin at steady-state was satisfactorily

estimated according to Figure 6-7, which shows the comparison between simulated PK profile of the therapeutic dose of 800 mg after seven doses and clinical data from six different trials. Therefore, the time-dependent CYP3A4inhibition was deemed plausible in explaining the pharmacokinetic nonlinearity of telithromycin.

Prediction of the Magnitude of Drug-Drug Interaction

To further verify the telithromycin PBPK model that predicts its nonlinear PK, the magnitude exposure change for the CYP3A4 substrate midazolam (fm_{CYP3A4} of 0.96) upon co-administration of telithromycin was simulated using both the initial and modified telithromycin models.

The prediction of the drug-drug interaction by telithromycin using the reported reversible K_i (within initial model) was unsuccessful. Namely, using the "most likely unbound" K_i of 25 μM as an input interaction parameter, the simulated midazolam AUC ratios (AUCR= $AUC_{inhibited}/AUC_{control}$) were 1.00 and 1.08 after single infusion (i.v.), and single oral (p.o.) midazolam, respectively. Similarly, AUCR values predicted using the "unlikely unbound" K_i of 4.3 μM were 1.04 and 1.33 after i.v and p.o. dosing of midazolam, respectively. In comparison, the observed AUCR values were 2.2 and 6.1 after i.v. and p.o. midazolam, respectively.

Conversely, the modified telithromycin model incorporating time-dependent inhibition of CYP3A4 reasonably predicted the observed increase in midazolam exposure produced by telithromycin interaction. Table 6-5 summarizes the predicted and observed ratio increases in maximum plasma concentration (C_{max}), $AUC_{(0,\infty)}$ and hepatic and intestinal availability (F_H and F_G) after i.v. and p.o. midazolam concomitantly with telithromycin (800 mg q.d., 6 days). The modified model predicted the inhibition of CYP3A4 dependent metabolism of midazolam by telithromycin both at intestinal and

hepatic levels: a predicted geometric mean AUC ratios of midazolam (GMR) of 3.2 after i.v. dosing of midazolam (decrease in CL_H), and a predicted GMR of 6.7 after p.o. dosing of midazolam (decrease in CL_H and increase in F_G and F_H). These values are in good agreement with observed GMRs (2.2 and 6.1 after i.v. and p.o., respectively). The predicted GMR for each of the 10 simulated trials ranged from 2.2-4.9 and 4.1-9.1 after i.v. and p.o. midazolam, respectively (Figure 6-8).

The outcome of DDI simulations depends both on the information related to victim drug as well as those of perpetrator. Hence, additional DDI simulations were conducted with a modified midazolam PBPK model by adjusting the contribution of the CYP3A4 metabolism from the SimCYP compound profile (fm_{CYP3A4} of 0.96). The fm_{CYP3A4} values of 0.86 and 0.93 were tested. This exercise was to assess similar DDI potential by telithromycin under varying importance of CYP3A4 for the victim drug since the accuracy of this parameter has a significant impact on drug-drug interactions involving strong inhibitors [141]. The AUC GMR obtained with i.v. midazolam were 2.52 (range from 2.2 to 2.9 among 10 simulated trials) and 3.23 (range 2.79-3.85) for fm_{CYP3A4} values of 0.86 and 0.93, respectively; while the AUC GMR after oral midazolam were 5.54 (range 4.29-7.30) and 7.12 (range 6.23-8.78) for fm_{CYP3A4} values of 0.86 and 0.93, respectively. The predicted increases in exposure were similar to the ones obtained under the scenario of 96% contribution of CYP3A4 on midazolam metabolism (SimCYP compound profile) and observed values, as described above and listed in Table 6-5.

Discussion

The utility of the PBPK modeling and simulation to predict the pharmacokinetic consequences of CYP3A4 inactivation by telithromycin by integrating *in vitro* and *in vivo* pharmacokinetics and interaction data has been demonstrated in this report. The

metabolic and efflux transporter saturation as mechanistic hypotheses for the observed time- and dose-dependent telithromycin pharmacokinetics were tested to be implausible. On the contrary, the time-dependent inhibition of CYP3A4 reasonably predicted the changes in CL/F at ascending single and multiple-doses. The modified model incorporating time-dependent CYP3A4 inhibition was further used to successfully predict the magnitude of interaction with midazolam (a probe CYP3A4 substrate, Table 6-5), suggesting that inactivation of CYP3A4 rather than reversible inhibition of the enzyme largely explains the interaction mechanism.

In vitro-to-*in vivo* extrapolation (IVIVE) models such as PBPK have been applied in the prediction and evaluation of drug-drug interactions via competitive and/or mechanism-based inhibition [142-144]. However, the successful predictability of PBPK is dependent on the knowledge of the drug-dependent parameter values for the structural model and drug interaction data. Hence the models are not fixed and they develop as more information is gathered and integrated to the system. Once reliable *in vitro* and *in vivo* absorption, distribution, metabolism, elimination (ADME) data are obtained during various stages of drug development, PBPK may reasonably predict the full disposition-time profile [145], the complexities of oral drug absorption and elimination [128,129,146], and the interindividual variability in clearance by incorporating age-dependent and genetic variations in enzyme abundance and activity [147].

In spite of the sparse availability of *in vitro* metabolism data of telithromycin, our investigation demonstrated the utility of PBPK modeling and simulation in informing mechanisms of drug nonlinear pharmacokinetics based on *in vivo* data. The current model indicates that rather than saturation of metabolic and transporter pathways, the

time-dependent inhibition of the metabolic clearance could be responsible for the pharmacokinetic nonlinearity. The modified telithromycin PBPK model with TDI parameters (K_I and k_{inact} , obtained using multiple sensitivity analyses) and the $K_{deg,CYP3A}$ of 0.019 h^{-1} (default value of SimCYP, V10.10) sufficiently predicted the pharmacokinetic nonlinearity of telithromycin; whereas the initial model incorporating only modest saturation of CYP3A4 and intestinal P-gp did not recover the changes in the apparent oral clearance of telithromycin (Figure 6-5 and 6-6).

The accurate prediction of an *in vivo* enzyme inhibition using a PBPK model may be restricted by the difficulties in determining the inhibition mechanism and obtaining accurate inhibition parameters *in vitro* (e.g., K_i for reversible and/or and k_{inact} /K_I for TDI) [148,149]. If the *in vitro* TDI experiment, usually used to distinguish between reversible inhibition and mechanism-based inactivation and to screen out compounds with this type of CYP inactivation property, is not properly designed, it can result in false positive results due to reversible inhibition from a metabolite(s) generated *in situ,* or false negative results from inadequate resolution of the method to separate potent reversible inhibitors from potent time-dependent inhibitors [14]. Our investigation demonstrated the stepwise nature of building PBPK models and utility of simulation in informing the potential clinical DDI using available *in vivo* pharmacokinetic data when *in vitro* interaction data are ambiguous. The telithromycin inhibition mechanism for CYP3A was further supported by the *in vivo* drug interaction data.

According to the draft drug-drug interaction guidance [115], the ratio of the total maximum plasma concentration of inhibitor ([I]) over reversible K_i *in vitro* of more than 0.1 would suggest the need for further *in viv*o drug interaction evaluation [150]. For

telithromycin, the [I]/ $K_{i, CYP3A4}$ at 800 mg once daily dosing regimen was calculated to be 0.11 - 0.66. The initial PBPK model of telithromycin considering reversible inhibition predicted less than 22% increase in midazolam exposure. Based on the analysis of pharmacokinetic nonlinearity, the modified model incorporating TDI mechanism suggested the clinical drug-drug interaction potential of telithromycin as a strong CYP3A4 inhibitor by increasing AUC of the sensitive CYP3A4 substrate midazolam by more than 500% (predicted GMR of AUC is 6.72, Table 6-5), which was confirmed by the observed GMR of midazolam AUC of 6.11 [88,151].

Paroxetine is another example of a substrate and inhibitor for the same CYP (CYP2D6), which displays nonlinear pharmacokinetics attributed to metabolic saturation [152]. Paroxetine significantly inhibits CYP2D6 *in vivo*, yet IVIVE using *in vitro* reversible inhibition data suggested marginal CYP2D6 inhibition. Recent *in vitro* data provided evidence for TDI of CYP2D6 by paroxetine [153]. Accordingly, IVIVE of the *in vitro* TDI data, using a scaling mathematical model, accurately predicted the fold-increases in several CYP2D6 victim drugs AUC by paroxetine and the 5- fold drug accumulation at steady-state [123]. The third example is clarithromycin whose nonlinear pharmacokinetics can also be explained by auto-inactivation of CYP3A4-mediated clearance. Application of a semi-PBPK model incorporating CYP3A4 TDI mechanism accurately predicted the nonlinear PK of clarithromycin and the clinical observed interaction magnitude with midazolam [154].

Systems approaches such as PBPK modeling and simulation consider the pharmacokinetic properties of the substrate and interacting drugs, which may be useful to fully understand the mechanisms and time courses of drug interactions observed in

clinical studies. Furthermore, the prediction method provide important information for making informed decisions to minimize the potential disadvantages of new drug candidates (e.g. restriction to a specific population in the label, discontinuation of further development) and ultimately it may help design proper *in vivo* interaction studies, including dose selection, the timing of dosage of interacting drugs.

Although TDI mechanism is clearly superior to the reversible inhibition mechanism in explaining telithromyicin's time- and dose- dependent pharmacokinetics, and predicting midazolam interaction studies *in vivo*, the modified TDI model is yet not perfect. For example, it is recognized that the modified model slightly over-predicted both telithromycin exposure after multiple doses of 400 mg q.d (Table 6-1), and AUCR of midazolam after i.v. dosing (Table 6-5). Nonetheless, these demonstrate the great utility of a PBPK model in revealing knowledge gaps and informing further studies if necessary.

In summary, this study demonstrates the utility and predictive accuracy of PBPK modeling and simulation to address telithromycin pharmacokinetic nonlinearity and CYP3A4 interaction potential on midazolam *in vivo*. The integration of *in vivo* human pharmacokinetic data and *in vitro* and *in silico* data using PBPK approach in this study exemplifies the combination of "top-down" and "bottom-up" approaches, which may be especially helpful when there is scarcity or uncertainty in metabolic and drug interaction data during early stage of drug development. Any discrepancy observed between simulations and experiments suggests knowledge gaps on processes that have not been considered during simulation and indicates additional studies needed to bridge the gap.

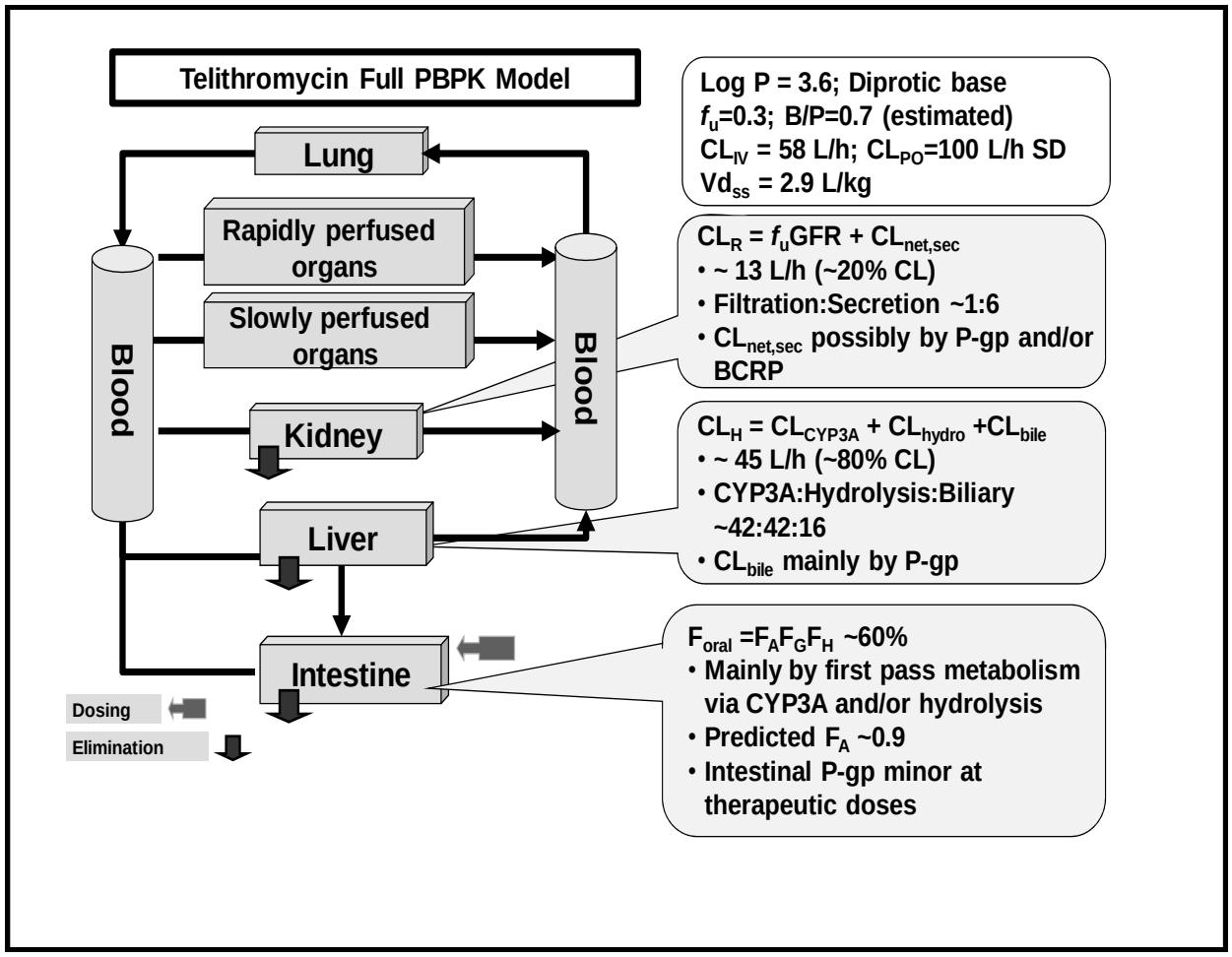

Figure 6-1. Schematic representation of telithromycin PBPK model. Abbreviations: B/P: blood-to-plasma ratio; CL_{iv}: systemic clearance after intravenous administration; CL_{po}: apparent oral clearance; F: bioavailability (subscripts "A, G and H", denote absorption, gut, hepatic, respectively); f_u: plasma unbound fraction; GFR: glomerular filtration rate; Vd_{ss}: volume of distribution at steady state.

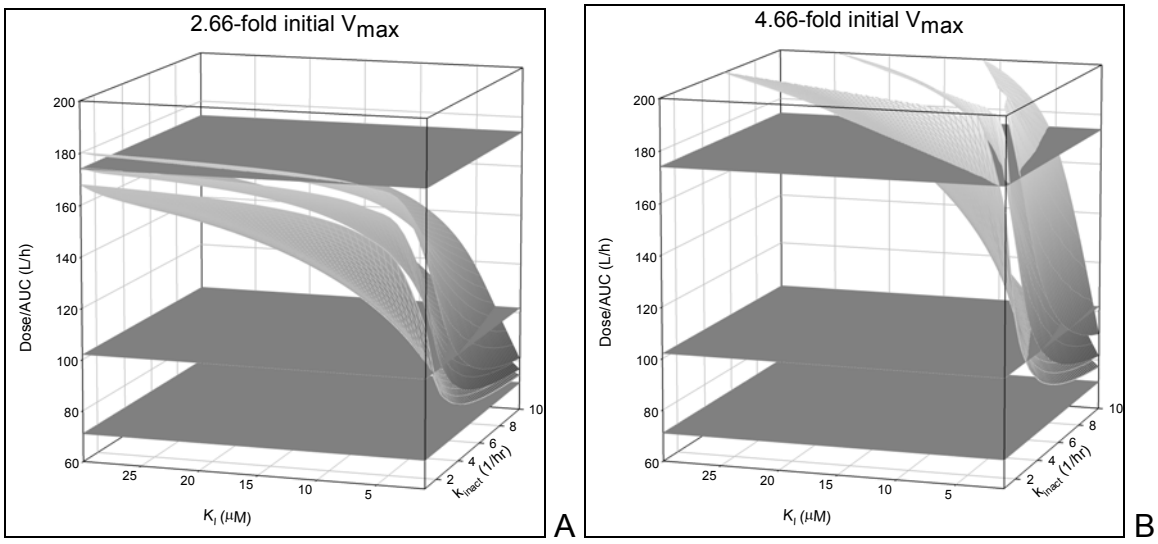

Figure 6-2. Changes in telithromycin apparent oral clearance (Dose/AUC) as a function of increasing values of CYP3A4 intrinsic clearance and time-dependent inhibition (K_I and K_{inact}) of the enzymatic pathway. A) 2.66-fold increase on the initial V_{max} value. B) 4.66-fold increase on the initial V_{max} value. The three horizontal planes show apparent oral clearance values of 174, 102 and 71 L/h, with the purpose of including the values observed from the ascending single-doses of 400, 800 and 1600 mg, respectively [89,119].

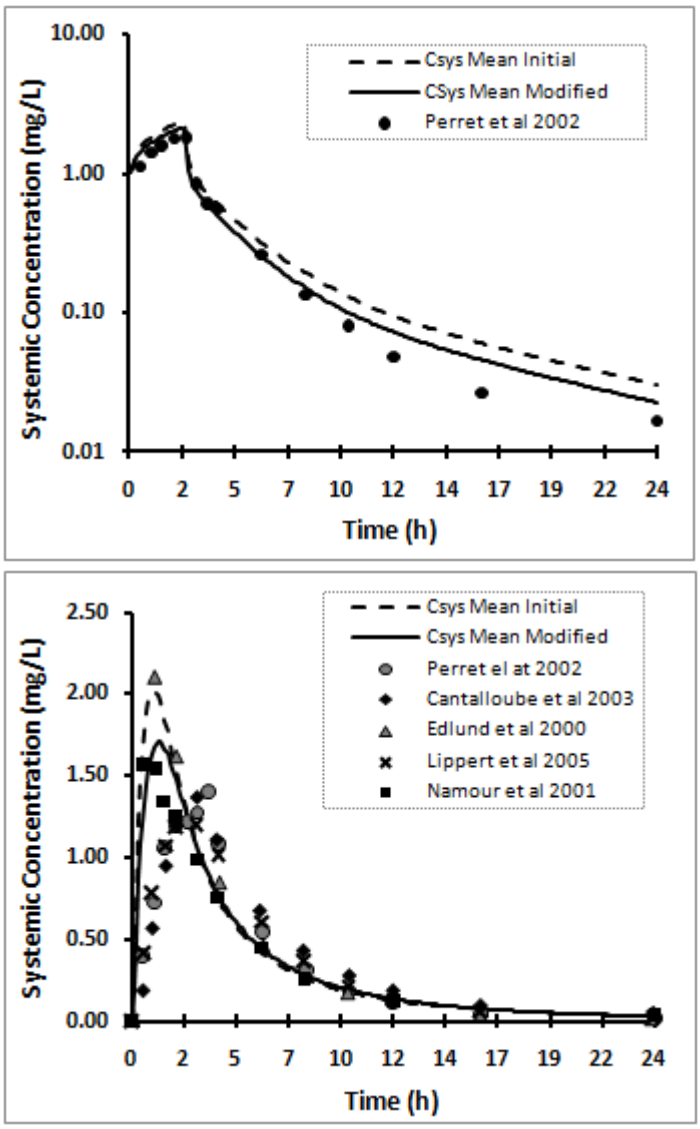

Figure 6-3. Predicted mean plasma concentration-time profile of telithromycin using the initial PBPK model (dashed line) or modified model (incorporating TDI of CYP3A4, solid line). A) After intravenous infusion (400 mg for 2.5h). B) After oral administration (800 mg SD). Symbols represent mean observed data from the literature as referenced in the graph legends.

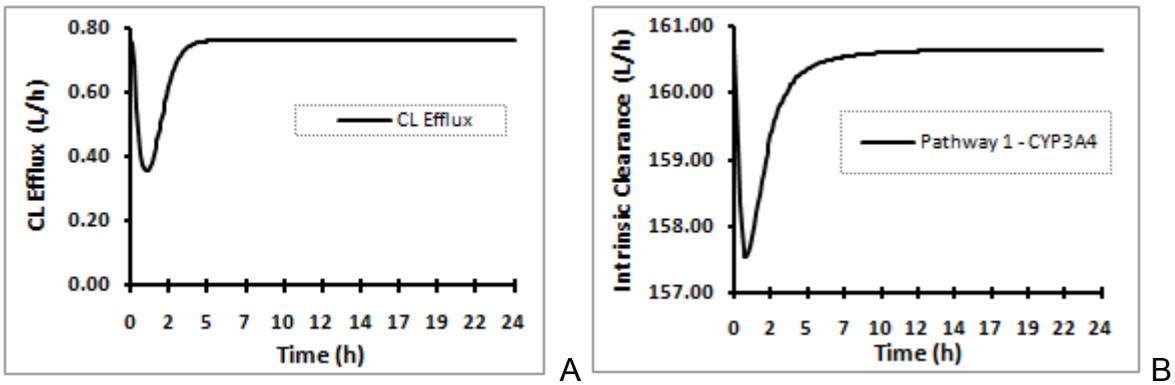

Figure 6-4. PBPK model predicted mean values of transport and enzymatic pathways of a single 400 mg dose of telithromycin over time. A) Intestinal efflux clearance by P-gp. B) Hepatic intrinsic clearance of CYP3A4.(K_m values incorporated in the model are 9.8 μM and 25 μM for P-gp and CYP3A4, respectively.

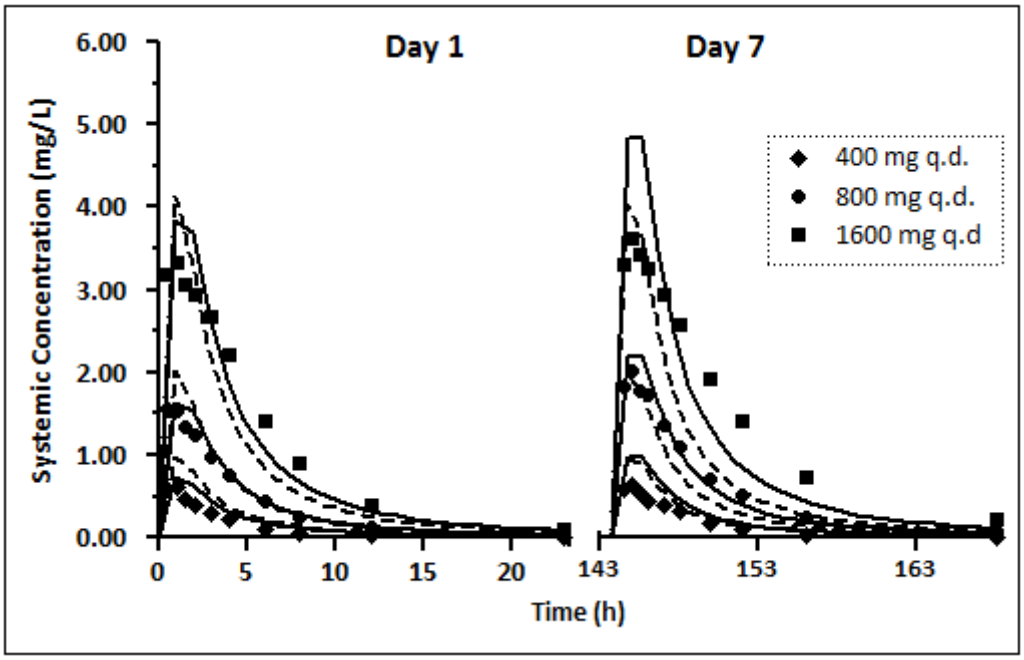

Figure 6-5. Prediction of mean concentration time-profile of telithromycin after ascending multiple oral doses (400, 800 and 1600 mg q.d.) in healthy subjects using initial model (dashed lines) and modified model incorporating time-dependent CYP3A4 inhibition (solid lines). Symbols represent mean observed data [89].

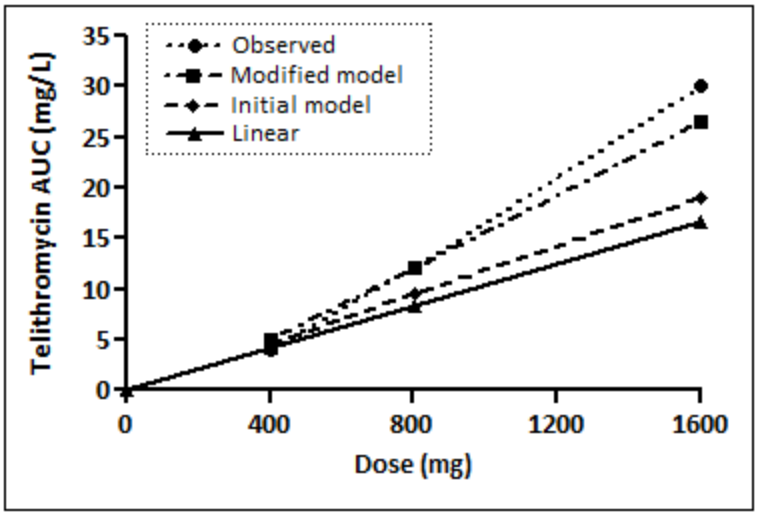

Figure 6-6. PBPK predicted by initial and modified TDI model and observed telithromycin nonlinear dose dependence after seven once-daily doses. The line of identity (solid line) would occur in the presence of linear dose dependence. Symbols represent mean observed [89] or predicted data.

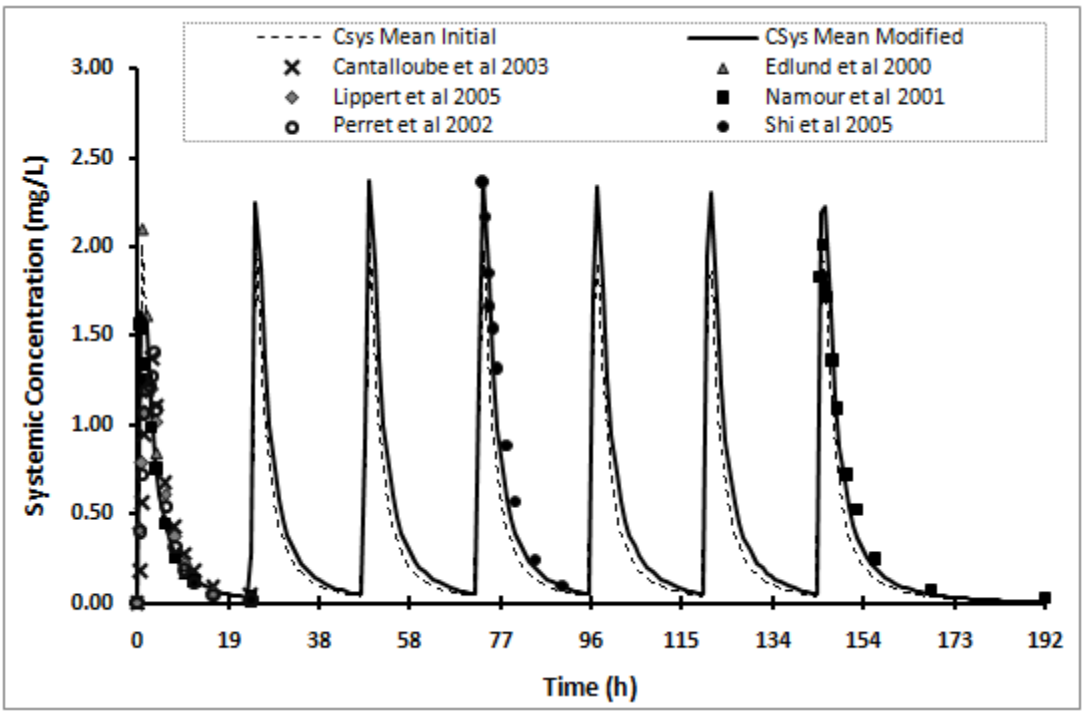

Figure 6-7. Predicted mean plasma profile of telithromycin after multiple oral doses (800 mg q.d.) in healthy subjects using initial and modified TDI model. Symbols represent mean observed data from six different trials.

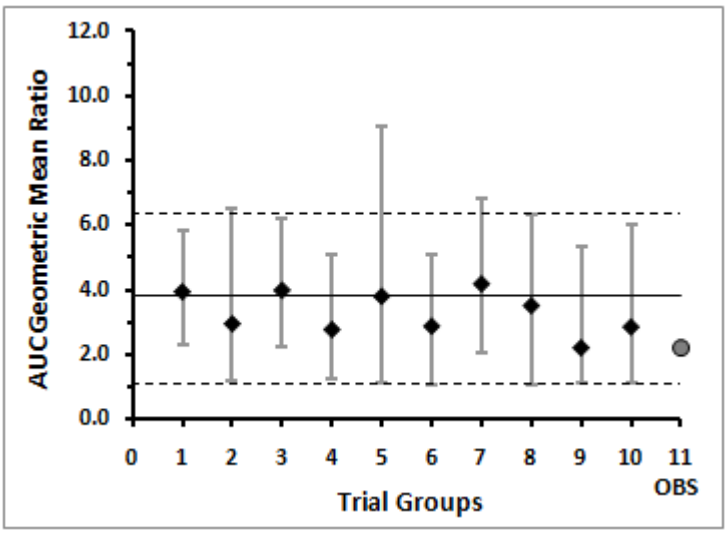

A

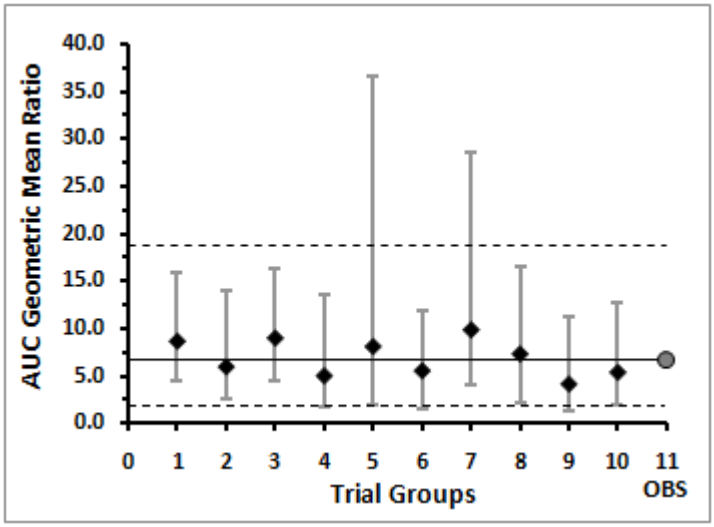

B

Figure 6-8. Geometric mean of AUC ratios (5th and 95th percentiles) of midazolam in the presence and absence of telithromycin (800 mg q.d for 6 days) in 10 different randomly selected groups of virtual subjects (n=12) (♦) and observed (n=12) (●) values. A) After intravenous administration of midazolam. B) After oral administration of midazolam. The solid line represents the AUC Geometric mean ratio of the virtual population (n=120); dashed lines represent the 5th and 95th percentiles of the virtual population.

Table 6-1. Predicted PK parameters of single (SD) and multiple once-daily doses (MD) of telithromycin using the modified model incorporating time-dependent inhibition of CYP3A4

PK Parameters	SD 400 mg		MD 400mg		SD 800 mg		MD 800 mg		SD 1600 mg		MD 1600 mg	
	[a] Obs	[b] Pred	[a] Obs	[b] Pred	[a] Obs	[b] Pred	[a] Obs	[b] Pred	[a] Obs	[b] Pred	[a] Obs	[b] Pred
C_{max} (mg/L)	0.80 (57)	0.77 (46)	0.83 (42)	1.04 (40)	1.90 (42)	1.76 (46)	2.27 (31)	2.36 (35)	4.07 (30)	4.29 (41)	4.48 (33)	5.18 (31)
AUC_{0-24h} (mg/L. h)	2.57 (40)	3.50 (62)	3.50 (31)	5.36 (51)	8.25 (31)	8.31 (58)	12.50 (43)	12.29 (43)	23.1 (34)	20.2 (48)	30.2 (22)	26.7 (39)
[c] t_{max} (h)	1.0 (0.5-4.0)	1.1 (0.6-2.5)	1.0 (0.5-4.0)	1.0 (1.0-2.9)	1.0 (0.5-4.0)	1.2 (0.6-2.8)	1.0 (0.5-3.0)	1.0 (1.0-2.9)	1.0 (0.5-4.0)	1.3 (0.6-2.7)	1.0 (0.5-3.0)	1.0 (1.0-2.9)
CL/F (L/h)	174 (49)	152	125 (53)	95	102 (31)	129 (54)	71 (29)	78 (47)	71	89 (53)	54	69 (39)
AUC/dose (mg/L. h)	5.1[d]	7.0	7.0[e]	10.7	8.4[d]	8.3	12.5[e]	12.3	12.4[d]	10.1	15.1[e]	13.4
R_{ac}	NA	NA	1.40	1.53	NA	NA	1.49	1.48	NA	NA	1.37	1.33
Ae_{0-24h} (% dose)	7.2 [d] (32)	12.1 (55)	9.6[e] (35)	16.3 (47)	12.7[d] (33)	14.3 (51)	17.7[e] (27)	19.2 (39)	18.4[d] (27)	17.59 (42)	24.4[e] (33)	21.3 (35)
$CL_{R\ 0-24h}$ (L/h)	12.2 (26)	14.5 (23)	11.2 (28)	14.5 (23)	12.3 (17)	14.5 (23)	12.5 (34)	14.5 (23)	13.3 (23)	14.5 (23)	13.1 (31)	14.5 (23)

Ae: accumulative amount of drug excreted in the urine after 24h; AUC_{0-24h} : area under the plasma concentration-time curve from time 0 to 24 h; AUC/dose: area under the plasma concentration-time curve normalized to the dose. C_{max}: maximum plasma concentration; CL/F: apparent oral clearance; CL_R: renal clearance; R_{ac}: accumulation ratio where AUC_{24}: area under the plasma concentration-time curve from 0 to 24 h and $AUC_{24,SS}$:AUC24 at steady state; t_{max}: time to C_{max}; NA: not applicable.

[a] Obs=Observed [89,119] values are means (% coefficient of variation) unless specified otherwise

[b] Pred= Predicted values are means (% coefficient of variation) from simulations using virtual population of 10 trials of healthy subjects.

[c] Values are medians (range).

[d] Values are significantly different among the other doses ($P < 0.001$)

[e] Values are significantly different among the other doses ($P < 0.001$)

.

Table 6-2. Drug-dependent parameters of telithromycin for the construction of PBPK model using SimCYP® (V10.10)

Parameter	Value	Methods/references
Molecular Weight (g/mol)	812.03	[88]
Log P	3.6	Predicted by Chemspider
pKa	5, 8.7	[88]
B/P	0.7	Parameter estimation[a]
*f*u	0.3	[88]
fu_{mic}	0.447	Predicted by SimCYP
*f*a	0.92	Predicted by SimCYP
ka (hr^{-1})	0.95	Predicted by SimCYP
P_{app} Caco-2 (10^{-6} cm/s)	21	[120]
J_{max} P-gp intestine (pmol/min)	5	[120]
K_m P-gp (μM)	9.8	[120]
V_{ss} (L/kg)	2.3	[121]
CL_{iv} (L/h)	57.7	[121]
CL_R (L/h)	13.2	[121]
CL_H (L/h)	37.5	[88]
CL_{add} (L/h)	6.9	[88]
Non-CYP CL_{int} (μL/min/mg protein)	39.5	Retrograde calculation
K_m CYP3A4(μM)	58	Assumed equal to Ki [118]
V_{max} CYP3A (pmol/min/pmol isoform)	35	Obtained by sensitivity analysis
J_{max} P-gp liver (pmol/min/million cells)	6	Retrograde calculation[b]
K_I CYP3A4 (μM)	6	Obtained by sensitivity analysis
k_{inact} CYP3A4 (hr^{-1})	10	Obtained by sensitivity analysis

[a] Using telithromycin mean plasma concentration from intravenous pharmacokinetic study in male healthy subjects [121].
[b] Retrograde calculation from biliary clearance of 6.9 L/hr.

Table 6-3. Observed vs. predicted apparent oral clearance (CL/F) after single (SD) and multiple (MD) ascending doses considering higher intrinsic clearance by CYP3A4 and time-dependent inhibition of this metabolic pathway (K_I and k_{inact} parameters).

Dose	[a] Observed CL/F (L/h)		[b] Predicted CL/F (L/h)					
			4x Vmax K_I 3 µM, k_{inact} 6 hr^{-1}		4.66x Vmax K_I 6 µM k_{inact} 10 hr^{-1}		5.33x Vmax K_I 3 µM k_{inact} 7 hr^{-1}	
	SD	MD	SD	MD	SD	MD	SD	MD
400 mg	174	125	155	89	178	98	177	90
800 mg	102	71	116	77	133	80	126	76
1600 mg	71	54	94	72	98	73	97	69

[a] Observed values [89,119].
[b] Values from simulations using healthy volunteers population representatives.

Table 6-4. Contribution of the intestinal efflux transporter P-gp on initial model predicted telithromycin pharmacokinetics after increasing single doses (SD)

[a] Predicted Parameter	SD 400 mg		SD 800 mg		SD 1600 mg	
	-P-gp	+P-gp	-P-gp	+P-gp	-P-gp	+P-gp
C_{max} (mg/L)	0.86	0.83	1.75	1.71	3.57	3.52
$AUC_{0\text{-}24h}$ (mg/L. h)	3.24	3.44	6.56	6.96	13.34	14.16
t_{max} (h)	1.05	1.05	1.05	1.05	1.05	1.05
*f*a (jejunum)	0.53	0.52	0.53	0.52	0.53	0.52
CL/F (L/h)	123	116	122	115	120	113

$AUC_{0\text{-}24h}$: area under the plasma concentration-time curve from time 0 to 24 h; C_{max}: maximum plasma concentration; *f*a: fraction absorbed in the jejune segment of small intestinal; CL/F: apparent oral clearance; t_{max}: time to C_{max}.

[a] Predicted from simulations using healthy volunteers population representatives. Study design attempted to match that reported [89].

Table 6-5. Predicted effect on midazolam exposure using the modified telithromycin model incorporating time-dependent CYP3A4 inhibition.

Midazolam PK Parameters	Single IV infusion of midazolam (2 mg, 0.5 h) + telithromycin (800mg q.d.)		Single oral dose of midazolam (6 mg) + telithromycin (800 mg q.d)	
	[a] Observed GMR	[b] Predicted GMR	[a] Observed GMR	[b] Predicted GMR
C_{max}	1.05	1.13	2.62	2.39
$AUC_{0-\infty}$	2.20	3.26	6.11	6.72
F_G	NA	NA	1.92	1.59
F_H	NA	NA	1.45	1.63

GMR: Values are expressed as geometric mean of the individual ratios of each parameter taking into account the parameters of midazolam alone as reference.
$AUC_{0-\infty}$: area under the plasma concentration-time curve from time 0 to infinity; C_{max}: maximum plasma concentration; F_G and F_H: intestinal and hepatic bioavailability, respectively.
[a] Observed from study#1056, NDA 21144 [119].
[b] Predicted from simulations using virtual population of 10 trials of healthy male subjects.
NA= Not applicable.

CHAPTER7
CONCLUSION

The overall objective of this thesis was to evaluate the usefulness and accuracy of two distinct tools in the assessment of pharmacokinetics and drug-drug interaction: Intravenous Microdialysis (IV MD) and Physiologically-based Pharmacokinetic (PBPK) modeling.

First, the feasibility and accuracy of intravenous microdialysis technique to determine plasma free concentrations of lipophilic and highly protein-bound drugs, using triamcinolone acetonide (TA) as a test compound, was evaluated. Initially, a simple and specific HPLC-PDA method was developed for simultaneously quantifying TA and its microdialysis calibrator, budesonide, in microdialysate and rat plasma samples. Validation results showed that the method is highly reproducible for both matrices and meets the requirements for the *in vitro* probe calibration studies and pharmacokinetic investigations. Subsequently, the practicability of using the microdialysis technique for TA was tested by a series of *in vitro* and *in vivo* microdialysis calibration studies. The overall results demonstrated that TA has the ability to freely and bidirectional cross the microdialysis probe membrane with recoveries around 55-65%; thus, TA is a suitable drug to be evaluated by microdialysis, despite its moderate lipophilicity and observed time-dependent recovery in IV MD calibration. An alternative method of MD probe calibration was then proposed and characterized to continuously monitor recovery during the time-frame of experiment, the retrodialysis by calibrator. Budesonide was verified as an appropriate calibrator to TA as the average ratios of the probe recoveries (Recovery Ratio TA: budesonide) were fairly constant under *in vitro* and *in vivo* scenarios, including over time *in vivo*. In the subsequent *in vivo* experimental evaluation

of the IV MD technique, the unbound plasma concentrations of TA under steady-state pharmacokinetics in anesthetized rodents was estimated and compared to the total concentrations, corrected for protein binding, obtained by conventional blood sampling. The unbound TA concentration in plasma obtained by conventional sampling was statistically similar to the unbound concentrations determined by intravenous microdialysis (α=0.05) technique using both methods of MD probe calibration, retrodialysis by drug and by calibrator. The accuracy of IV MD in our study led to the conclusion that IV MD sampling may be a feasible approach for free drug monitoring of lipophilic and highly protein-bound drugs.

Accordingly, IV MD technique may be a promising *in vivo* tool for continuous free drug monitoring in (pre)clinical settings due to its several advantages compared to traditional blood sampling, specially related to the reduction of the number of experimental animals used in drug research and facilitate clinical pharmacokinetic studies in the pediatric population. Additionally, IV MD may be a very valuable technique in the areas of therapeutic drug monitoring of highly-protein binding drugs, for example, antiretroviral agents which demonstrated elevated drug-drug interaction risks.

Second, the utility of PBPK modeling as an *in silico* tool to evaluate the drug-drug interaction potential inferred from the drug's nonlinear pharmacokinetics was demonstrated. Telithromycin, a substrate and inhibitor of the enzyme CYP3A4 with dose- and time-dependent PK nonlinearity was used as model drug. A telithromycin PBPK model, integrating available human PK , *in vitro* metabolic and *in silico* predicted enzymatic interaction parameters of time-dependent CYP3A4 inhibition, successful addressed the mechanisms of the drug nonlinearity and accurately predicted the clinical

observed drug-drug interaction magnitude with midazolam (a substrate for CYP3A4). Our results demonstrated the efficacy and predictive accuracy of PBPK modeling and simulation in informing the potential clinical DDI using available *in vivo* pharmacokinetic data, which is especially helpful when there is scarcity or uncertainty in metabolic and drug interaction data during early stage of drug development.

In conclusion, IV MD and PBPK modeling are useful and promising tools for evaluating pharmacokinetics and drug-drug interactions, thus aiding to guide successful drug development.

LIST OF REFERENCES

[1] Holmgaard R, Nielsen JB, Benfeldt E. Microdialysis sampling for investigations of bioavailability and bioequivalence of topically administered drugs: Current state and future perspectives. Skin Pharmacol and Physiol 2010; 23:225-243.

[2] Chaurasia CS, Muller M, Bashaw ED et al. AAPS-FDA Workshop White Paper: microdialysis principles, application, and regulatory perspectives. J Clin Pharmacol 2007; 47:589-603.

[3] Brunner M, Derendorf H. Clinical microdialysis: Current applications and potential use in drug development. TRAC 2006; 25:674-680.

[4] Zhao P, Zhang L, Lesko L, Huang S. Utility of physiologically- based pharmacokinetic modeling and simulation in drug development and challenges in regulatory reviews. Clin Pharm Therap 2010; 87:S72-S72.

[5] Zhao P, Zhang L, Grillo JA et al. Applications of physiologically based pharmacokinetic (PBPK) modeling and simulation during regulatory review. Clin Pharmac Therap 2011; 89:259-267.

[6] Tsai TH. Assaying protein unbound drugs using microdialysis techniques. J Chromatogr B Analyt Technol Biomed Life Sci 2003; 797:161-173.

[7] Plock N, Kloft C. Microdialysis--theoretical background and recent implementation in applied life-sciences. Eur J Pharm Sci 2005; 25:1-24.

[8] Stahl M, Bouw R, Jackson A, Pay V. Human microdialysis. Curr Pharm Biotechnol 2002; 3:165-178.

[9] Benfeldt E, Groth L. Feasibility of measuring lipophilic or protein-bound drugs in the dermis by in vivo microdialysis after topical or systemic drug administration. Acta Derm Venereol 1998; 78:274-278.

[10] Carneheim C, Stahle L. Microdialysis of lipophilic compounds: a methodological study. Pharmacol Toxicol 1991; 69:378-380.

[11] Rowland Yeo K, Jamei M, Yang J, Tucker GT, Rostami-Hodjegan A. Physiologically based mechanistic modelling to predict complex drug–drug interactions involving simultaneous competitive and time-dependent enzyme inhibition by parent compound and its metabolite in both liver and gut-The effect of diltiazem on the time-course of exposure to triazolam. Eur J Pharm Sci 2010; 39:298-309.

[12] Perdaems N, Blasco H, Vinson C et al. Predictions of metabolic drug-drug interactions using physiologically based modeling two cytochrome P450 3A4

substrates coadministered with ketoconazole or verapamil. Clin Pharmacokinet 2010; 49:239-258.

[13] Wienkers LC, Heath TG. Predicting in vivo drug interactions from in vitro drug discovery data. Nature 2005; 4:825-833.

[14] Grimm SW, Einolf HJ, Hall SD et al. The conduct of in vitro studies to address time-dependent inhibition of drug-metabolizing enzymes: A perspective of the Pharmaceutical Research and Manufacturers of America. Drug Metab Disposition 2009; 37:1355-1370.

[15] O'Connell MT, Tison F, Quinn NP, Patsalos PN. Clinical drug monitoring by microdialysis: application to levodopa therapy in Parkinson's disease. Br J Clin Pharmacol 1996; 42:765-769.

[16] Elshoff JP, Laer S. Development of an intravenous microdialysis method for pharmacokinetic investigations in humans. J Pharmacol Toxicol Methods 2005; 52:251-259.

[17] Barbour A, Schmidt S, Sabarinath SN et al. Soft-tissue penetration of ceftobiprole in healthy volunteers determined by in vivo microdialysis. Antimicrob Agents Chemother 2009; 53:2773-2776.

[18] Burkhardt O, Brunner M, Schmidt S, Grant M, Tang Y, Derendorf H. Penetration of ertapenem into skeletal muscle and subcutaneous adipose tissue in healthy volunteers measured by in vivo microdialysis. J Antimicrob Chemother 2006; 58:632-636.

[19] Engstrom M, Polito A, Reinstrup P et al. Intracerebral microdialysis in severe brain trauma: the importance of catheter location. J Neurosurg 2005; 102:460-469.

[20] Herkner H, Muller MR, Kreischitz N et al. Closed-chest microdialysis to measure antibiotic penetration into human lung tissue. Am J Respir Crit Care Med 2002; 165:273-276.

[21] Stolle LB, Arpi M, Holmberg-Jorgensen P, Riegels-Nielsen P, Keller J. Application of microdialysis to cancellous bone tissue for measurement of gentamicin levels. J Antimicrob Chemother 2004; 54:263-265.

[22] Stolle LB, Plock N, Joukhadar C et al. Pharmacokinetics of linezolid in bone tissue investigated by in vivo microdialysis. Scand J Infect Dis 2008; 40:24-29.

[23] Nowak G, Ungerstedt J, Wernerman J, Ungerstedt U, Ericzon BG. Clinical experience in continuous graft monitoring with microdialysis early after liver transplantation. Br J Surg 2002; 89:1169-1175.

[24] Isaksson B, D'souza MA, Jersenius U et al. Continuous assessment of intrahepatic metabolism by microdialysis during and after portal triad clamping. J Surg Res 2010.

[25] Davies MI, Cooper JD, Desmond SS, Lunte CE, Lunte SM. Analytical considerations for microdialysis sampling. Adv Drug Deliv Rev 2000; 45:169-188.

[26] de Lange EC, de Boer AG, Breimer DD. Methodological issues in microdialysis sampling for pharmacokinetic studies. Adv Drug Deliv Rev 2000; 45:125-148.

[27] Brunner M, Langer O. Microdialysis versus other techniques for the clinical assessment of in vivo tissue drug distribution. AAPS J 2006; 8:E263-71.

[28] Bungay PM, Morrison PF, Dedrick RL. Steady-state theory for quantitative microdialysis of solutes and water in vivo and in vitro. Life Sci 1990; 46:105-119.

[29] Lonnroth P, Jansson PA, Smith U. A microdialysis method allowing characterization of water intercellular space in humans. Am J Physiol 1987; 253:E228-E231.

[30] Le Quellec A, Dupin S, Genissel P, Saivin S, Marchand B, Houin G. Microdialysis probes calibration: gradient and tissue dependent changes in no net flux and reverse dialysis methods. J Pharmacol Toxicol Methods 1995; 33:11-16.

[31] Olson RJ, Justice JB. Quantitative microdialysis under transient conditions. Anal Chem 1993; 65:1017-1022.

[32] Wang Y, Wong SL, Sawchuk RJ. Microdialysis calibration using retrodialysis and zero-net flux: application to a study of the distribution of zidovudine to rabbit cerebrospinal fluid and thalamus. Pharm Res 1993; 10:1411-1419.

[33] Groth L, Jørgensen A. In vitro microdialysis of hydrophilic and lipophilic compounds. Anal Chim Acta 1997; 355:75-83.

[34] Chen KC, Hoistad M, Kehr J, Fuxe K, Nicholson C. Theory relating in vitro and in vivo microdialysis with one or two probes. J Neurochem 2002; 81:108-121.

[35] Stenken JA, Lunte CE, Southard MZ, Stahle L. Factors that influence microdialysis recovery. Comparison of experimental and theoretical microdialysis recoveries in rat liver. J Pharm Sci 1997; 86:958-966.

[36] Mazzeo AT, Alves OL, Gilman CB et al. Brain metabolic and hemodynamic effects of cyclosporin A after human severe traumatic brain injury: a microdialysis study. Acta Neurochir 2008; 150:1019-1031.

[37] Feuerstein D, Manning A, Hashemi P et al. Dynamic metabolic response to multiple spreading depolarizations in patients with acute brain injury: an online microdialysis study. J Cereb Blood Flow Metab 2010; 30:1343-1355.

[38] Richards DA, Tolias CM, Sgouros S, Bowery NG. Extracellular glutamine to glutamate ratio may predict outcome in the injured brain: a clinical microdialysis study in children. Pharmacol Res 2003; 48:101-109.

[39] Benfeldt E, Hansen SH, Volund A, Menne T, Shah VP. Bioequivalence of topical formulations in humans: Evaluation by dermal microdialysis sampling and the dermatopharmacokinetic method. J Invest Dermatol 2007; 127:170-178.

[40] Klonoff DC. Continuous glucose monitoring - Roadmap for 21st century diabetes therapy. Diabetes Care 2005; 28:1231-1239.

[41] Magkos F, Sidossis LS. Methodological approaches to the study of metabolism across individual tissues in man. Curr Opin Clin Nutr Metab Care 2005; 8:501-510.

[42] Cucullo L, Marchi N, Hossain M, Janigro D. A dynamic in vitro BBB model for the study of immune cell trafficking into the central nervous system. J Cereb Blood Flow Metab 2011; 31:767-777.

[43] Hage C, Mellbin L, Ryden L, Wernerman J. Glucose monitoring by means of an intravenous microdialysis catheter technique. Diabetes Technol Ther 2010; 12:291-295.

[44] Baumeister FA, Hack A, Busch R. Glucose-monitoring with continuous subcutaneous microdialysis in neonatal diabetes mellitus. Klin Padiatr 2006; 218:230-232.

[45] Goraca A. Minireview: microdialysis of the blood outflowing from the brain. Endocr Regul 2001; 35:229-236.

[46] Dasgupta A. Usefulness of monitoring free (unbound) concentrations of therapeutic drugs in patient management. Clin Chim Acta 2007; 377:1-13.

[47] Tsai TH, Chen YF. Pharmacokinetics of metronidazole in rat blood, brain and bile studied by microdialysis coupled to microbore liquid chromatography. J Chromatogr A 2003; 987:277-282.

[48] Cheng GW, Hsu KC, Lee CF, Wu HL, Huang YL. On-line microdialysis coupled with liquid chromatography for biomedical analysis. J Chromatogr Sci 2009; 47:624-630.

[49] Cheng GW, Wu HL, Huang YL. Automated on-line microdialysis sampling coupled with high-performance liquid chromatography for simultaneous determination of malondialdehyde and ofloxacin in whole blood. Talanta 2009; 79:1071-1075.

[50] Huang SP, Lin LC, Wu YT, Tsai TH. Pharmacokinetics of kadsurenone and its interaction with cyclosporin A in rats using a combined HPLC and microdialysis system. J Chromatogr B Analyt Technol Biomed Life Sci 2009; 877:247-252.

[51] Opezzo JA, Hocht C, Taira CA, Bramuglia GF. Pharmacokinetic study of methyldopa in aorta-coarctated rats using a microdialysis technique. Pharmacol Res 2001; 43:155-159.

[52] Telting-Diaz M, Scott DO, Lunte CE. Intravenous microdialysis sampling in awake, freely-moving rats. Anal Chem 1992; 64:806-810.

[53] Verbeeck RK. Blood microdialysis in pharmacokinetic and drug metabolism studies. Adv Drug Deliv Rev 2000; 45:217-228.

[54] Scott DO, Sorensen LR, Lunte CE. In vivo microdialysis sampling coupled to liquid chromatography for the study of acetaminophen metabolism. J Chromatogr 1990; 506:461-469.

[55] Tsai TH, Kao HY, Chen CF. Measurement and pharmacokinetic analysis of unbound ceftazidime in rat blood using microdialysis and microbore liquid chromatography. J Chromatogr B Biomed Sci Appl 2001; 750:93-98.

[56] Maia MB, Saivin S, Chatelut E, Malmary MF, Houin G. In vitro and in vivo protein binding of methotrexate assessed by microdialysis. Int J Clin Pharmacol Ther 1996; 34:335-341.

[57] Evrard PA, Cumps J, Verbeeck RK. Concentration-dependent plasma protein binding of flurbiprofen in the rat: an in vivo microdialysis study. Pharm Res 1996; 13:18-22.

[58] Yang H, Wang Q, Elmquist WF. The design and validation of a novel intravenous microdialysis probe: application to fluconazole pharmacokinetics in the freely-moving rat model. Pharm Res 1997; 14:1455-1460.

[59] Bouw MR, Hammarlund-Udenaes M. Methodological aspects of the use of a calibrator in in vivo microdialysis-further development of the retrodialysis method. Pharm Res 1998; 15:1673-1679.

[60] Larsson CI. The use of an "internal standard" for control of the recovery in microdialysis. Life Sci 1991; 49:PL73-8.

[61] Evrard PA, Deridder G, Verbeeck RK. Intravenous microdialysis in the mouse and the rat: development and pharmacokinetic application of a new probe. Pharm Res 1996; 13:12-17.

[62] Höcht C, Opezzo JW, Taira C. Validation of a new intraarterial microdialysis shunt probe for the estimation of pharmacokinetic parameters. J Pharm Biomed Anal 2003; 31:1109-1117.

[63] Paez X, Hernandez L. Plasma serotonin monitoring by blood microdialysis coupled to high-performance liquid chromatography with electrochemical detection in humans. J Chromatogr B Biomed Sci Appl 1998; 720:33-38.

[64] Castejon AM, Paez X, Hernandez L, Cubeddu LX. Use of intravenous microdialysis to monitor changes in serotonin release and metabolism induced by cisplatin in cancer patients: comparative effects of granisetron and ondansetron. J Pharmacol Exp Ther 1999; 291:960-966.

[65] Rabenstein K, McShane AJ, McKenna MJ, Dempsey E, Keaveny TV, Freaney R. An intravascular microdialysis sampling system suitable for application in continuous biochemical monitoring of glucose and lactate. Technol Health Care 1996; 4:67-76.

[66] Paez X, Hernandez L. Blood microdialysis in humans: a new method for monitoring plasma compounds. Life Sci 1997; 61:847-856.

[67] Stjernstrom H, Karlsson T, Ungerstedt U, Hillered L. Chemical monitoring of intensive care patients using intravenous microdialysis. Intensive Care Med 1993; 19:423-428.

[68] Rojas C, Nagaraja NV, Webb AI, Derendorf H. Microdialysis of triamcinolone acetonide in rat muscle. J Pharm Sci 2003; 92:394-397.

[69] Argenti D, Jensen BK, Hensel R et al. A mass balance study to evaluate the biotransformation and excretion of [14C]-triamcinolone acetonide following oral administration. J Clin Pharmacol 2000; 40:770-780.

[70] Rohatagi S, Hochhaus G, Mollmann H et al. Pharmacokinetic and pharmacodynamic evaluation of triamcinolone acetonide after intravenous, oral, and inhaled administration. J Clin Pharmacol 1995; 35:1187-1193.

[71] Sauernheimer C, Williams KM, Brune K, Geisslinger G. Application of microdialysis to the pharmacokinetics of analgesics: problems with reduction of dialysis efficiency in vivo. J Pharmacol Toxicol Methods 1994; 32:149-154.

[72] Pichini S, Papaseit E, Joya X et al. Pharmacokinetics and therapeutic drug monitoring of psychotropic drugs in pediatrics. Ther Drug Monit 2009; 31:283-318.

[73] Willmann S, Lippert J, Sevestre M, Solodenko J, Fois F. PK-Sim®: A physiologically based pharmacokinetic 'whole-body' model. Biosilico 2003; 1:121-124.

[74] Teorell T. Kinetics of distribution of substances administered to the body I The extravascular modes of administration. Arch Int Pharmacodyn Ther 1937; 57:205-225.

[75] Rowland M, Peck C, Tucker GT. Physiologically-based pharmacokinetics in drug development and regulatory science. Annu Rev Pharmacol Toxicol 2011; 51:45-73.

[76] Theil FP, Guentert TW, Haddad S, Poulin P. Utility of physiologically based pharmacokinetic models to drug development and rational drug discovery candidate selection. Toxicol Lett 2003; 138:29-49.

[77] Ginsberg G, Hattis D, Sonawane B. Incorporating pharmacokinetic differences between children and adults in assessing children's risks to environmental toxicants. Toxicol Appl Pharmacol 2004; 198:164-183.

[78] Edginton AN, Schmitt W, Willmann S. Development and evaluation of a generic physiologically based pharmacokinetic model for children. Clin Pharmacokinet 2006; 45:1013-1034.

[79] Johnson TN, Rostami-Hodjegan A. Resurgence in the use of physiologically based pharmacokinetic models in pediatric clinical pharmacology: parallel shift in incorporating the knowledge of biological elements and increased applicability to drug development and clinical practice. Pediatric Anesthesia 2011; 21:291-301.

[80] Johnson TN, Rostami-Hodjegan A, Tucker GT. Prediction of the clearance of eleven drugs and associated variability in neonates, infants and children. Clin Pharmacokinet 2006; 45:931-956.

[81] Johnson TN, Boussery K, Rowland-Yeo K, Tucker GT, Rostami-Hodjegan A. A semi-mechanistic model to predict the effects of liver cirrhosis on drug clearance. Clin Pharmacokinet 2010; 49:189-206.

[82] Fahmi OA, Hurst S, Plowchalk D et al. Comparison of different algorithms for predicting clinical drug-drug interactions, based on the use of CYP3A4 in vitro data: predictions of compounds as precipitants of interaction. Drug Metab Disposition 2009; 37:1658-1666.

[83] Jamei M, Marciniak S, Feng K, Barnett A, Tucker G, Rostami-Hodjegan A. The Simcyp (R) population-based ADME simulator. Expert Opin Drug Metab Toxicol 2009; 5:211-223.

[84] Jones HM, Gardner IB, Watson KJ. Modeling and PBPK simulation in drug discovery. AAPS J 2009; 11:155-166.

[85] Willmann S, Hoehn K, Edginton A et al. Development of a physiology-based whole-body population model for assessing the influence of individual variability on the pharmacokinetics of drugs. J Pharmacok Pharmacod 2007; 34:401-431.

[86] Jamei M, Dickinson GL, Rostami-Hodjegan A. A framework for assessing inter-individual variability in pharmacokinetics using virtual human populations and integrating general knowledge of physical chemistry, biology, anatomy, physiology and genetics: A tale of 'bottom-up' vs 'top-down' recognition of covariates. Drug Metab Pharmacok 2009; 24:53-75.

[87] Zhang L, Reynolds KS, Zhao P, Huang S. Drug interactions evaluation: An integrated part of risk assessment of therapeutics. Toxicol Appl Pharmacol 2010; 243:134-145.

[88] Shi J, Montay G, Bhargava VO. Clinical pharmacokinetics of telithromycin, the first ketolide antibacterial. Clin Pharmacokinet 2005; 44:915-934.

[89] Namour F, Wessels DH, Pascual MH, Reynolds D, Sultan E, Lenfant B. Pharmacokinetics of the new ketolide telithromycin (HMR 3647) administered in ascending single and multiple doses. Antimicrob Agents Chemother 2001; 45:170-175.

[90] Derendorf H, Rohdewald P, Hochhaus G, Mollmann H. HPLC determination of glucocorticoid alcohols, their phosphates and hydrocortisone in aqueous solutions and biological fluids. J Pharm Biomed Anal 1986; 4:197-206.

[91] Doppenschmitt SA, Scheidel B, Harrison F, Surmann JP. Simultaneous determination of triamcinolone acetonide and hydrocortisone in human plasma by high-performance liquid chromatography. J Chromatogr B Biomed Appl 1996; 682:79-88.

[92] Mollmann H, Rohdewald P, Schmidt EW, Salomon V, Derendorf H. Pharmacokinetics of triamcinolone acetonide and its phosphate ester. Eur J Clin Pharmacol 1985; 29:85-89.

[93] Qu J, Qu Y, Straubinger RM. Ultra-sensitive quantification of corticosteroids in plasma samples using selective solid-phase extraction and reversed-phase capillary high-performance liquid chromatography/tandem mass spectrometry. Anal Chem 2007; 79:3786-3793.

[94] Zhang S, Thorsheim HR, Penugonda S, Pillai VC, Smith QR, Mehvar R. Liquid chromatography-tandem mass spectrometry for the determination of methylprednisolone in rat plasma and liver after intravenous administration of its liver-targeted dextran prodrug. J of Chromatogr B 2009; 877:927-932.

[95] Yang H, Wang Q, Elmquist WF. Fluconazole distribution to the brain: a crossover study in freely-moving rats using in vivo microdialysis. Pharm Res 1996; 13:1570-1575.

[96] Scott DO, Sorenson LR, Steele KL, Puckett DL, Lunte CE. In vivo microdialysis sampling for pharmacokinetic investigations. Pharm Res 1991; 8:389-392.

[97] Yang R, Tan X, Kennedy R.J. J, Thomas A, Landis M, Qureshi N. Hemorrhagic shock in the rat: comparison of carotid and femoral cannulation. 2008; 144:124-126.

[98] Canadian Council of Animal Care. Guide to the care and use of experimental animals. 1993.

[99] Araujo BV, Silva CF, Haas SE, Dalla Costa T. Microdialysis as a tool to determine free kidney levels of voriconazole in rodents: A model to study the technique feasibility for a moderately lipophilic drug. J Pharm Biomed Anal 2008; 47:876-881.

[100] Traunmueller F, Steiner I, Zeitlinger M, Joukhadar C. Development of a high-performance liquid chromatographymethod for the determination of caspofungin with amperometric detection and its application to in vitro microdialysis experiments. J Chromatogr B 2006; 843:142-146.

[101] Yokel RA, Allen DD, Burgio DE, McNamara PJ. Antipyrine as a dialyzable reference to correct differences in efficiency among and within sampling devices during in vivo microdialysis. J Pharmacol Toxicol Methods 1992; 27:135-142.

[102] Sjoberg P, Olofsson IM, Lundqvist T. Validation of different microdialysis methods for the determination of unbound steady-state concentrations of theophylline in blood and brain tissue. Pharm Res 1992; 9:1592-1598.

[103] Marchand S, Frasca D, Dahyot-Fizelier C, Breheret C, Mimoz O, Couet W. Lung microdialysis study of levofloxacin in rats following intravenous infusion at steady state. Antimicrob Agents Chemother 2008; 52:3074-3077.

[104] Brunner M, Joukhadar C, Schmid R, Erovic B, Eichler HG, Muller M. Validation of urea as an endogenous reference compound for the in vivo calibration of microdialysis probes. Life Sci 2000; 67:977-984.

[105] Ettinger SN, Poellmann CC, Wisniewski NA et al. Urea as a recovery marker for quantitative assessment of tumor interstitial solutes with microdialysis. Cancer Res 2001; 61:7964-7970.

[106] Liu P, Fuhrherr R, Webb AI, Obermann B, Derendorf H. Tissue penetration of cefpodoxime into the skeletal muscle and lung in rats. Eur J Pharm Sci 2005; 25:439-444.

[107] Muller M. Science, medicine, and the future: Microdialysis. BMJ 2002; 324:588-591.

[108] Schwalbe O, Buerger C, Plock N, Joukhadar C, Kloft C. Urea as an endogenous surrogate in human microdialysis to determine relative recovery of drugs: analytics and applications. J Pharm Biomed Anal 2006; 41:233-239.

[109] Aventis Pharmaceuticals Ltd. Nasacort HFA (triamcinolone acetonide). NDA number 020784. 2007.

[110] Stahle L. On mathematical models of microdialysis: geometry, steady-state models, recovery and probe radius. Adv Drug Deliv Rev 2000; 45:149-167.

[111] Kripalani KJ, Cohen AI, Weliky I, Schreiber EC. Metabolism of triamcinolone acetonide-21-phosphate in dogs, monkeys, and rats. J Pharm Sci 1975; 64:1351-1359.

[112] Rojas C, Nagaraja NV, Derendorf H. In vitro recovery of triamcinolone acetonide in microdialysis. Pharmazie 2000; 55:659-662.

[113] Derendorf H, Hochhaus G, Rohatagi S et al. Pharmacokinetics of triamcinolone acetonide after intravenous, oral, and inhaled administration. J Clin Pharmacol 1995; 35:302-305.

[114] Huang S, Strong JM, Zhang L et al. New era in drug interaction evaluation: US Food and Drug Administration update on CYP enzymes, transporters, and the guidance process. J Clin Pharmacol 2008; 48:662-670.

[115] Food and Drug Administration of the United States, Center for Drug Evaluation and Research (CDER), Center for Biologics Evaluation and Research (CBER). Draft guidance for industry: drug interaction studies -study design, data analysis, and implications for dosing and labeling. 2006

[116] Zhang L, Zhang Y, Zhao P, Huang S. Predicting drug-drug interactions: An FDA perspective. AAPS J 2009; 11:300-306.

[117] Drusano G. Pharmacodynamic and pharmacokinetic considerations in antimicrobial selection: focus on telithromycin. Clin Microb Infection 2001; 7:24-29.

[118] Sanofi-Aventis Canada Inc. Product monograph- KETEK® (telithromycin film-coated tablets, 400 mg) Anti-bacterial agent. 2009.

[119] Aventis Pharmaceuticals Ltd. Ketek (telithromycin tablets). Drug approval package. 2004.

[120] Pachot JI, Botham RP, Haegele KD, Hwang K. Experimental estimation of the role of P-Glycoprotein in the pharmacokinetic behaviour of telithromycin, a novel ketolide, in comparison with roxithromycin and other macrolides using the Caco-2 cell model. J Pharmacy Pharm Sci 2003; 6:1-12.

[121] Perret C, Lenfant B, Weinling E et al. Pharmacokinetics and absolute oral bioavailability of an 800-mg oral dose of telithromycin in healthy young and elderly volunteers. Chemotherapy 2002; 48:217-223.

[122] Bhargava V, Lenfant B, Perret C, Pascual MH, Sultan E, Montay G. Lack of effect of food on the bioavailability of a new ketolide antibacterial, telithromycin. Scand J Infect Dis 2002; 34:823-826.

[123] Venkatakrishnan K, von Moltke LL, Obach RS, Greenblatt DJ. Drug metabolism and drug interactions: Application and clinical value of in vitro models. Curr Drug Metab 2003; 4:423-459.

[124] Lee JH, Lee MG. Dose-dependent pharmacokinetics of telithromycin after intravenous and oral administration to rats: Contribution of intestinal first-pass effect to low bioavailability. J Pharmacy Pharm Sci 2007; 10:37-50.

[125] Rodgers T, Leahy D, Rowland M. Physiologically-based pharmacokinetic modeling 1: Predicting the tissue distribution of moderate-to-strong bases. J Pharm Sci 2005; 94:1259-1276.

[126] Rodgers T, Rowland M. Physiologically-based pharmacokinetic modelling 2: Predicting the tissue distribution of acids, very weak bases, neutrals and zwitterions. J Pharm Sci 2006; 95:1238-1257.

[127] Rodgers T, Rowland M. Mechanistic approaches to volume of distribution predictions: Understanding the processes. Pharm Res 2007; 24:918-933.

[128] Jamei M, Turner D, Yang J et al. Population-Based mechanistic prediction of oral drug absorption. AAAPS J 2009; 11:225-237.

[129] Rostami-Hodjegan A, Tucker GT. Simulation and prediction of in vivo drug metabolism in human populations from in vitro data. Nature Rev Drug Discovery 2007; 6:140-148.

[130] Yeo KR, Jamei M, Yang J, Tucker GT, Rostami-Hodjegan A. Physiologically based mechanistic modelling to predict complex drug-drug interactions involving simultaneous competitive and time-dependent enzyme inhibition by parent compound and its metabolite in both liver and gut-The effect of diltiazem on the time-course of exposure to triazolam. Eur J Pharm Sci 2010; 39:298-309.

[131] Pang SK, Rowland M. Hepatic Clearance of Drugs .3. Additional experimental-evidence supporting well-stirred model, using metabolite (Megx) generated from lidocaine under varying hepatic blood-flow rates and linear conditions in perfused rat-liver in situ preparation. J Pharmacokinet Biopharm 1977; 5:681-699.

[132] Johnson TN, Tucker GT, Tanner MS, Rostami-Hodjegan A. Changes in liver volume from birth to adulthood: A meta-analysis. Liver Transplantation 2005; 11:1481-1493.

[133] Mayhew BS, Jones DR, Hall SD. An in vitro model for predicting in vivo inhibition of cytochrome P450 3A4 by metabolic intermediate complex formation. Drug Metab Disposition 2000; 28:1031-1037.

[134] Rowland Yeo K, Walsky RL, Jamei M, Rostami-Hodjegan A, Tucker GT. Prediction of time-dependent CYP3A4 drug–drug interactions by physiologically based pharmacokinetic modeling: Impact of inactivation parameters and enzyme turnover. Eur J Pharm Sci 2011; *in press*.

[135] Yang J, Liao M, Shou M et al. Cytochrome P450 turnover: Regulation of synthesis and degradation, methods for determining rates, and implications for the prediction of drug interactions. Curr Drug Metab 2008; 9:384-393.

[136] Cantalloube C, Bhargava V, Sultan E, Vacheron F, Batista I, Montay G. Pharmacokinetics of the ketolide telithromycin after single and repeated doses in patients with hepatic impairment. Int J Antimicrob Agents 2003; 22:112-121.

[137] Edlund C, Alvan G, Barkholt L, Vacheron F, Nord CE. Pharmacokinetics and comparative effects of telithromycin (HMR 3647) and clarithromycin on the oropharyngeal and intestinal microflora. J Antimicrob Chemother 2000; 46:741-749.

[138] Lippert C, Gbenado S, Qiu CF, Lavin B, Kovacs SJ. The bioequivalence of telithromycin administered orally as crushed tablets versus tablets swallowed whole. J Clin Pharmacol 2005; 45:1025-1031.

[139] Parrott N, Lukacova V, Fraczkiewicz G, Bolger MB. Predicting pharmacokinetics of drugs using physiologically based modeling-application to food effects. AAPS J 2009; 11:45-53.

[140] Shi J, Montay G, Leroy B, Bhargava VO. Effects of itraconazole or grapefruit juice on the pharmacokinetics of telithromycin. Pharmacotherapy 2005; 25:42-51.

[141] Hinton LK, Galetin A, Houston JB. Multiple inhibition mechanisms and prediction of drug-drug interactions: Status of metabolism and transporter models as exemplified by gemfibrozil-drug interactions. Pharm Res 2008; 25:1063-1074.

[142] Kanamitsu S, Ito K, Green CE, Tyson CA, Shimada N, Sugiyama Y. Prediction of in vivo interaction between triazolam and erythromycin based on in vitro studies using human liver microsomes and recombinant human CYP3A4. Pharm Res 2000; 17:419-426.

[143] Kato M, Shitara Y, Sato H et al. The quantitative prediction of CYP-mediated drug interaction by physiologically based pharmacokinetic modeling. Pharm Res 2008; 25:1891-1901.

[144] Zhao P, Ragueneau-Majlessi I, Zhang L et al. Quantitative evaluation of pharmacokinetic inhibition of CYP3A substrates by ketoconazole: A simulation study. J Clin Pharmacol 2009; 49:351-359.

[145] Gibson CR, Bergman A, Lu P, Kesisoglou F, Denney WS, Mulrooney E. Prediction of Phase I single-dose pharmacokinetics using recombinant cytochromes P450 and physiologically based modelling. Xenobiotica 2009; 39:637-648.

[146] Lukacova V, Woltosz WS, Bolger MB. Prediction of modified release pharmacokinetics and pharmacodynamics from in vitro, immediate release, and intravenous data. AAPS J 2009; 11:323-334.

[147] Howgate EM, Rowland-Yeo K, Proctor NJ, Tucker GT, Rostami-Hodjegan A. Incorporation of inter-individual variability into the prediction of in vivo drug clearance from in vitro data. Drug Metab Rev 2005; 37:99.

[148] Fowler S, Zhang H. In vitro evaluation of reversible and irreversible cytochrome P450 inhibition: Current status on methodologies and their utility for predicting drug-drug interactions. AAPS J 2008; 10:410-424.

[149] Obach RS. Predicting drug-drug interactions from in vitro drug metabolism data: challenges and recent advances. Curr Opin Drug Discov Devel 2009; 12:81-89.

[150] Tucker GT, Houston JB, Huang SM. Optimizing drug development: strategies to assess drug metabolism/transporter interaction potential - towards a consensus. Br J Clin Pharmacol 2001; 52:107-117.

[151] Aventis Pharmaceuticals Ltd. Ketek (telithromycin) Briefing document for the FDA Anti-Infective Drug Products Advisory Committee Meeting. 2003.

[152] Sindrup SH, Brosen K, Gram LF. Pharmacokinetics of the selective serotonin reuptake inhibitor paroxetine - nonlinearity and relation to the sparteine oxidation polymorphism. Clin Pharm Ther 1992; 51:288-295.

[153] Bertelsen KM, Venkatakrishnan K, Von Moltke LL, Obach RS, Greenblatt DJ. Apparent mechanism-based inhibition of human CYP2D6 in vitro by paroxetine:

Comparison with fluoxetine and quinidine. Drug Metab Disposition 2003; 31:289-293.

[154] Quinney SK, Zhang X, Lucksiri A, Gorski JC, Li L, Hall SD. physiologically based pharmacokinetic model of mechanism-based inhibition of CYP3A by clarithromycin. Drug Metab Disposition 2010; 38:241-248.

[155] Venkatakrishnan K, Obach RS. In vitro-in vivo extrapolation of CYP2D6 inactivation by paroxetine: Prediction of nonstationary pharmacokinetics and drug interaction magnitude. Drug Metab Disposition 2005; 33:845-852.

BIOGRAPHICAL SKETCH

Manuela de Lima Toccafondo Vieira was born in 1976, in Belo Horizonte, Brazil. She earned her bachelor's degree in pharmacy with graduate diploma in Industry from the Federal University of Minas Gerais, Brazil in 1999. Manuela earned a diploma in homeopathy pharmacy from the Association of Homeopathic Pharmacists of Brazil in 2000. She practiced as a pharmacist from 1999 to 2004. In 2006, she graduated with a Master of Science degree in pharmaceutical sciences from the College of Pharmacy of the Federal University of Minas Gerais. In August 2007, she joined the PhD program in the Department of Pharmaceutics, College of Pharmacy of the University of Florida, working under the supervision of Dr Hartmut Derendorf. Manuela received her Doctor of Philosophy degree in pharmaceutical sciences in August 2011.